A STUDY OF THE UNIFIED POWER QUALITY CONDITIONER (UPQC) FOR IMPROVED RADIAL DISTRIBUTION NETWORK

By

Josiah Okpanachi HARUNA, B.Eng. (ABU) 2007

MSC/ENG/3473/09-10

A THESIS SUBMITTED TO THE SCHOOL OF POSTGRADUATE STUDIES,

AHMADU BELLO UNIVERSITY, ZARIA

IN PARTIAL FULFILLMENT OF THE REQUIREMENTS FOR THE AWARD OF A MASTER OF SCIENCE (M.Sc.) DEGREE IN ELECTRICAL ENGINEERING

DEPARTMENT OF ELECTRICAL AND COMPUTER ENGINEERING, FACULTY OF ENGINEERING, AHMADU BELLO UNIVERSITY, ZARIA

NIGERIA

JULY, 2013

DECLARATION

I declare that the work in this Thesis entitled A STUDY OF THE UNIFIED POWER QUALITY CONDITIONER FOR IMPROVED RADIAL DISTRIBUTION NETWORK has been carried out by me in the Department of Electrical and Computer Engineering. The information derived from the literature has been duly acknowledged in the text and a list of references provided. No part of this thesis was previously presented for another degree or diploma at this or any other Institution.

Josiah O. HARUNA

_____ _____

Signature Date

CERTIFICATION

This thesis entitled A STUDY OF THE UNIFIED POWER QUALITY CONDITONER FOR IMPROVED RADIAL DISTRIBUTION NETWORK by Josiah Okpanachi HARUNA meets the regulations governing the award of the degree of Masters of Science (M.Sc.) Electrical Engineering of the Ahmadu Bello University, and is approved for its contribution to knowledge and literary presentation

Prof. J. O. Ojo		
(Chairman Supervisory Committee)	Signature	Date
Dr. B. Jimoh		
(Member Supervisory Committee)	Signature	Date
Dr. M. B. Muazu		
(Head of Department)	Signature	Date
Prof. A. A. Joshua		
(Dean, School of Postgraduate Studies)	Signature	Date

ACKNOWLEDGEMENT

I thank God who through His son Jesus Christ, has reached to me and lifted me up from the impossible depth to which I had fallen and who progressively over this years is making a place for me.

For a work like this, there would be several people to say thank you to. There would be those who made obvious and tangible contributions to its success and those who in no less measure simply prayed in their hearts hoped and desired ones success, may God bless you.

I will like to thank Prof. J.O. Ojo my major supervisor for everything: For showing me the path to becoming a good researcher, for the guidance and financial help. Dr. Jimoh my minor supervisor stood by me all through the way. May God bless you for all the concern shown, advices given and financial support you rendered to me.

I will like to thank my parents: Mr. and Mrs. Moses Haruna, my siblings, the families of Mr. and Mrs. Afam Eruchalu, Mr. and Mrs. Israel Nnodum, Mr. and Mrs. Yahaya, Mr. and Mrs. Toryila and the Church of Christ. I am grateful that I don't have to meet any minimum standards to get your love and support.

I thank the Head of Department, Department of Electrical and Computer Engineering Dr. M.B. Muazu, for his leadership and for showing concern in the course of my research work. I am also grateful to Dr. S.M. Sani, for his contributions to my success, Dr. J.Y. Oricha for all the advice he gave me in the course of my studies, Engr. Taiwo for providing me space to work. Thanks to Dr. O. Akinsami and Dr. S. Garba (the Departmental Post Graduate Coordinators) for their untiring efforts to seeing to the completion of our studies. Engr. Gbenga for being there for me and indeed all staff of the department of Electrical and Computer Engineering both academic and non-academic, you have all contributed in no small way to molding me into the man that I am.

I will like to thank my colleagues and friends for their support. The MSc. Electrical Engineering (Power Systems Option) class of 2009/2010: Manga, Mamud, Latifat, Attah, Momoh, Barak, Shereef, Ismail. It was painful to have lost Kelvin Makonju in the course of our studies but I am grateful to God to have met and known every one of you. Kolo Yetu and Stephen Yabo, there is no way to quantify the help you rendered to me during the course of my studies, God bless you. David Laburta and the entire Laburta family, thank you for the many options you made available to me. The Staff and Pupils of Bold Step International Schools I am glad to have being part of you. Thanks to the family of Ayodele Ake, to Elijah, Ugochi, Justin, Ochai, Mallam, Innocent, and the entire Post Graduate Fellowship (PGF), Fellowship of Christian Student (FCS) ABU Zaria.

ABSTRACT

This work assesses the feasibility and performance of an enhanced Unified Power Quality Conditioner (UPQC). A UPQC configuration has been developed which incorporates Photo voltaic (PV) cells and Battery Energy Storage System (BESS) in the DC link of the UPQC. The BESS is connected using a bi-directional DC-DC converter. The system operates in two modes namely: Interconnected and Islanding. This arrangement enabled the reliable and efficient compensation of interruption, and the amelioration of the effects of loss of supply. A pre-defined power management strategy has been determined in which the combination of the PV/BESS takes care of a maximum of 1.4940MW of load active power demand during interruption and loss of supply. This value is such as to ensure active power balance in the system. A detailed model of the system has been developed in the two modes of operation. Data for the hourly demand on the 11kV Gaskiya feeder of the Power Holding Company of Nigeria (PHCN) Zaria and that for the hourly solar insolation in Zaria (Latitude 11.067 and Longitude 7.7) have been obtained. A thorough evaluation of the feasibility and performance of the system on the 11kV Gaskiya feeder is presented using the developed models, m-files and the embedded function of MATLAB/Simulink. Results show that at a solar insolation level of S = 0.07 representing the least insolation, S = 0.45 representing the most prevalent solar insolation other than the least and S = 0.85 representing the highest insolation, there is real time collaboration, based on the determined power management strategy, between the batteries and PV cells in meeting system demand. In the islanding mode, a part of load active power (1.4940MW) demand is met by the combination of the PV cells and batteries. Thus, interruption and loss of supply is mitigated by the system. Also, the capabilities of the UPQC to regulate load voltage and supply power factor remains uncompromised.

TABLE OF CONTENTS

Title Page

Declaration……...ii

Certification……iii

Acknowledgement.……iv

Abstract……....v

Table of Contents……vi

List of Tables.……..x

List of Figures...……xi

List of Appendices……xvi

Abbreviations and Symbols……xvii

CHAPTER ONE: INTRODUCTION……..1

1.1 Overview……...1

1.2 Significance of the Study……5

1.3 Aims and Objectives of the Study……..6

1.4 Limitation of the Study ……...6

1.5 Thesis Outline……...7

CHAPTER TWO: LITERATURE REIVIEW.....8

2.1 Introduction……..8

2.2 Review of Fundamental Concepts…….....8

2.2.1 Definition of Major Power Quality Events……8

2.2.2 Some Effects of Poor Power Quality……10

2.2.3 Electricity Distribution Network…….....11

2.2.4 The Unified Power Quality Conditioner (UPQC)……14

2.2.5 DC-DC Converters……....29

2.3 Review of Similar Works……...32

2.3.1 Classification Based on Supply System……33

2.3.2 Classification Based on Configuration……34

2.3.3 UPQC for Grid Integration of Renewable Energy Sources……..35

2.4 Statement of Problem..……..38

2.5 Conclusion……..38

CHAPTER THREE: MATERIALS AND METHODS……...39

3.1 Introduction……39

3.2 PHCN Data for 11kV Gaskiya Feeder Zaria……..39

3.3 NASA Solar Insolation Data for Zaria……42

3.4 MATLAB/Simulink……...42

3.5 Methodology……...45

3.5.1 Modes of Operation……..45

3.6 Conclusion……..49

CHAPTER FOUR: MODEL DERIVATIONS AND DESIGN CONSIDERATIONS…….51

4.1 Introduction……51

4.2 Model Derivations in a-b-c: Interconnected Mode…….51

4.2.1 Model of the Distribution System…….51

4.2.2 Model of Rectifier…….52

4.2.3 Model of Inverter……..54

4.2.4 Model of the DC-DC Converters…….55

4.2.5 Model of the DC Link……...56

4.2.6 Non-Linear Model of PV……..57

4.2.7 Dynamic Model of Battery……...58

4.2.8 Model of the Whole System…….59

4.3 Model of the System in q-d-o: Interconnected Mode…….59

4.4 Model of the System in Complex Form: Interconnected Mode…….60

4.5 Model of the System in Islanding Mode……...61

4.5.1 Possibility A……..62

4.5.2 Possibility B……..63

4.6 Design Consideration…….64

4.6.1 Distribution Network……64

4.6.2 Switching Devices ON Resistance……65

4.6.3 Inverter LC Filter……..65

4.6.4 DC-DC Converter Inductor Filter…….66

4.6.5 Active Power Balance……...67

4.6.6 Simulation Equations……72

4.7 Conclusion……..74

CHAPTER FIVE: RESULTS AND ANALYSIS……..75

5.1 Introduction……75

5.2 Steady State Analysis……75

5.2.1 UPQC on Distribution Network…….……...77

5.2.2 UPQC with Limitations……90

5.2.3 UPQC with PV and Battery Energy Storage System.……92

5.2.4 Loss of Supply Compensation……104

5.3 Open Loop Large Signal Simulation……..111

5.3.1 UPQC without Limitations……112

5.4 Conclusion ……...117

CHAPTER SIX: CONCLUSION AND RECOMMENDATIONS. …….118

6.1 Summary……...……...…118

6.2 Conclusion.……..…….....118

6.3 Recommendations for Further Work …...……118

LIST OF TABLES

Table 2.1 Some Power Switching Devices and their Characteristics……17

Table 2.2 Truth Table of a Boost DC-DC Converter…….30

Table 3.1 Data of the Hourly Demand on the 11kV Gaskiya Feeder……41

Table 3.2 Frequency Table for Solar Insolation in Zaria……...42

Table 4.1 System Parameters……72

Table 5.1 Parameters of PV System.……95

LIST OF FIGURES

Figure 1.1 Block Diagram of the Distribution Line Equipped with UPQC and PV/BESS…….4

Figure 2.1 Pictorial Views of Major Power Quality Problems on Distribution Level……..10

Figure 2.2 Schematic of Radial Distribution System Showing Consumers Connected to the Same Point of Common Coupling (PCC)……13

Figure 2.3 Schematic of a Radial Distribution System Showing the UPQC deployed at the premises of one Consumer…….14

Figure 2.4 General Block Diagram Representation of the UPQC System……15

Figure 2.5 A Three Phase Inverter……..16

Figure 2.6 Single Phase Inverter Showing Switch Realization…….18

Figure 2.7 Simple Switching Function……..19

Figure 2.8 One Phase of a Three Phase Inverter……19

Figure 2.9 SPWM Illustration……22

Figure 2.10 Switching Function in One Switching Period……23

Figure 2.11 Fundamental Component of the Average Switching Function……..24

Figure 2.12 q-d-o Transformation Shown by Trigonometric Relationship……...27

Figure 2.13 Circuit Configuration of a Boost DC-DC Converter……..30

Figure 2.14 Generation of Duty Ration for DC-DC Converter…….31

Figure 2.15 Classification of Universal Power Quality Conditioner UPQC…….32

Figure 2.16 Left Shunt Inverter Configuration of the UPQC……35

Figure 2.17 Right Shunt Inverter Configuration of the UPQC……..35

Figure 3.1 MATLAB M-File Editor Interface……...44

Figure 3.2 Simulink Interface for Simulation……44

Figure 3.3 Detailed Configuration of the UPQC with PV/BESS Deployed on a Distribution System……46

Figure 3.4 Line Diagram of the UPQC with Details of Switches……..47

Figure 3.5 Islanding Mode: A Possible Implementation……...48

Figure 3.6 Islanding Mode: A Second Possible Implementation……..49

Figure 4.1 Distribution Network showing the Influence of the UPQC…….52

Figure 4.2 Rectifier Connected to the Distribution Network……..53

Figure 4.3 Inverter Connected to the Distribution Network……..54

Figure 4.4 Boost DC-DC Converter at the Output of the PV Cells……...55

Figure 4.5 Boost DC-DC Converter at the Output of the Battery Bank……56

Figure 4.6 DC Link Circuits……..57

Figure 4.7 Battery Structure……...58

Figure 4.8 DC-DC Converter showing Details of Interconnections with other parts of the System……66

Figure 5.1 Flow Chart for UPQC with no Limitation……78

Figure 5.2 Voltage Injected by Series Inverter to Regulate Load Voltage……79

Figure 5.3 Series Inverter Current at Different Load Power…….80

Figure 5.4 Series Inverter Modulation Index with Variation in Supply Voltage at Different Load Power…….81

Figure 5.5 Supply Current at three Different Apparent Power pf = 0.8……82

Figure 5.6 Current Drawn by Shunt Inverter at Different Load Power……..83

Figure 5.7 Shunt Inverter Modulation Index…….85

Figure 5.8 Flow Chart for Power Flow Studies…….87

Figure 5.9 Average Power Flow through the System……88

Figure 5.10 Reactive Power Flow through the System……..89

Figure 5.11 Critical Value of DC Link Capacitor Voltage……91

Figure 5.12 Optimum Voltages at Maximum Power in Different Insolation Level……..94

Figure 5.13 Flow Chart for UPQC with PV and BESS…….....96

Figure 5.14 Voltage Injected by Series Inverter with Variation of Load at Different Supply Voltages (S = 0.85)……97

Figure 5.15 Peal Supply Current with Variation of Load at Different Supply Voltages (S = 0.85)……...98

Figure 5.16 Series Converter Modulation Index with Variation of Load at Different Supply Voltages (S = 0.85)……99

Figure 5.17 Shunt Inverter Modulation Index with Variation of Load at Different Supply Voltages (S = 0.85)……..100

Figure 5.18 Battery Current with Variation of Load at Different Supply Voltages (S = 0.85)...101

Figure 5.19 Battery Current with Variation of Load at Different Supply Voltages (S = 0.45)...103

Figure 5.20 Battery Current with Variation of Load at Different Supply Voltages (S = 0.07)...104

Figure 5.21 Battery Current vs Load Real Power in Islanding Mode Possibility A (S = 0.85)..106

Figure 5.22 Battery Current vs Load Real Power in Islanding Mode Possibility A (S = 0.45)..107

Figure 5.23 Battery Current vs Load Real Power in Islanding Mode Possibility A (S = 0.07)..108

Figure 5.24 Battery Current vs Load Real Power in Islanding Mode Possibility B (S = 0.85)...109

Figure 5.25 Battery Current vs Load Real Power in Islanding Mode Possibility B (S = 0.45)...110

Figure 5.26 Battery Current vs Load Real Power in Islanding Mode Possibility B (S = 0.07)...111

Figure 5.27 Simulation Results for Voltage Sag Condition……112

Figure 5.28 Generation of SPWM Pulses for Converter Switches (Voltage Sag Condition)…..113

Figure 5.29 Simulation Results for Normal Operation……114

Figure 5.30 Generation of SPWM (Normal Operation)……..115

Figure 5.31 Simulation Results for Voltage Swell Condition…….116

Figure 5.32 Generation of SPWM (Voltage Swell)…….117

LIST OF APPENDICES

APPENDIX A: SYSTEM MODEL IN ABC REFERENCE FRAME……124

APPENDIX B: MODEL OF SYSTEM IN QDO REFERENCE FRAME…….136

APPENDIX C: MODEL EQUATIONS IN COMPLEX FORM……144

APPENDIX D: DC-DC CONVERTER PARMETER DETERMINATION……..147

APPENDIX E: NASA HOURLY SOLAR INSOLATION IN ZARIA……..151

APPENDIX F: PROGRAM LISTING……152

APPENDIX G: SIMULINK MODEL FOR SIMULATION STUDIES…….……159

APPENDIX H: SCANNED COPY OF PHCN ZARIA HOURLY DEMAND ON 11kV GASKIYA FEEDER. …….160

ABBREVIATIONS AND SYMBOLS

APF	Active Power Filter
BESS	Battery Energy Storage System
dc	Direct Current
EU	European Union
IEEE	International Institute of Electrical and Electronic Engineers
LC	Inductor Capacitor Filter
LPF	Low Pass Filter
NASA	National Aeronautics and Space Administration
PCC	Point of Common Coupling
pf	Power Factor
PHCN	Power Holding Company of Nigeria
PV	Photo voltaic
rms	Root Mean Square
UPQC	Unified Power Quality Conditioner
VSC	Voltage Source Converter
VSI	Voltage Source Inverter
VSR	Voltage Source Rectifier
SPWM	Sinusoidal Pulse Width Modulation
KVL	Kirchhoff's Voltage Law
KCL	Kirchhoff's Current Law
SP2W	Single Phase Two Wire
3P3W	Three Phase Three Wire
3P4W	Three Phase Four Wire

POWER CONVENTION USED

Real Power = +P (Power Supplied)

Real Power = -P (Real Power Absorbed)

Reactive Power = +Q (Reactive Power Absorbed)

Reactive Power = -Q (Reactive Power Supplied)

CHAPTER ONE

INTRODUCTION

1.1 Overview

IEEE standard 1159 defines power quality as the concept of powering and grounding sensitive equipment in a manner that is suitable for the operation of the equipment (ieeexplore.ieee.org). This definition derives from the understanding that majority of the power quality issues arise as a result of poor and/or improper grounding of equipment.

In general, the term power quality can be defined as the physical characteristics of the electrical supply provided under normal operating condition that do not disturb or disrupt the user processes (Khadkikar, 2008). Any deviations from these physical characteristics are termed power quality events. Power Quality has become an issue of serious concern at the electric power distribution level. According to Khadikar (2008), this is largely due to:

(i) The changing nature of loads on the distribution networks

(ii) The increased awareness of consumers of their rights to low cost electricity of high reliability and constancy in supply.

(iii) The growing interest in the utilization of renewable energy resources for electric power generation.

Most modern electrical appliances for example industrial drives, electronic ballast fluorescent lights, switching power supplies and so forth are becoming increasingly power electronics based. Whereas these loads possess certain advantages like, enhanced controllability, high power density and so forth, they also bring with them disadvantages which were not there in the early

power distribution systems. Some of these disadvantages include increased sensitivity to supply voltage, harmonics and reactive power requirements. These inherent characteristics of power electronic based loads have helped to raise awareness of power quality issues.

With the deregulation of the electric power sector in most parts of the world, there is a growing interest in the utilization of renewable energy resources (mostly solar and wind) for electric power generation. Individuals and companies can now harness available renewable energy resources in their localities to compliment utility supply thereby reducing long term cost of electricity consumption and indeed in some countries sell excess generated energy to the utility. The integration of renewable energies and their accommodation in the existing electricity networks is often a complex issue and is making the electric power distribution networks more susceptible to power quality problems (Khadkikar, 2008).

Power quality concerns are not only on the side of the consumers alone. There are power quality issues on the side of the utilities too. The utilities are concerned for instance about current total harmonic distortion of the consumers load. Current trends in mitigating some of the major power quality problems are towards multitasking devices which are capable of simultaneously mitigating several power quality problems on the networks (Khadem *et al.,* 2010). Of this category, the Unified Power Quality Conditioner (UPQC) is one of the most versatile. The UPQC can be used to mitigate simultaneously a vast majority of the power quality problems both at the utility side and at the consumer end (Khadkikar, 2008; Davari *et al.,* 2009; Khadem *et al.,* 2010).

The UPQC, however, cannot supply large active power to customers steadily due to the limitation of energy storage (Davari *et al.,* 2009). The UPQC cannot, therefore, compensate for

voltage interruptions and loss of supply which is necessary for systems that experience long duration of interruption and loss of supply. The inability of the UPQC to supply large active power for a long time as noted is as a result of the lack of a constant source of dc supply at the dc link. Efforts have been made by some researchers to solve this problem. Such efforts however, perhaps due to the experiences of these researchers with their respective power utilities, have been in two major directions:

(i) Some have used PV array directly in the dc link (Marcelo *et al.*, 2006; Khadem *et al.*, 2010). However, such systems have the disadvantage that interruption/loss of supply compensation is only possible when there is sufficient solar insolation (Khadem *et al.*, 2010). Also ensuring power balance in such a system involves the implementation of complex control schemes (due to the non-deterministic nature of solar resource). Moreover, the solar PV array may not be operated at Maximum Power Point (MPP) leading to wastages in several aspects.

(ii) Others have used the PV array with some form of energy storage system thereby making possible Maximum Power Point Tracking (MPPT) (Davari *et al.*, 2009) but the power flow is unidirectional that is; the PV is used to charge the Battery Energy Storage System (BESS) and then the BESS supplies system needs with the disadvantage that excessive solar insolation is wasted.

The current effort has developed a system configuration which in addition to all the power quality compensation capabilities of the UPQC, possesses:

(i) The capability of real time collaboration between the PV cell and energy system in addressing system demands thereby ensuring efficient utilization of available renewable energy resources.

(ii) The capability of ameliorating the effects of loss of supply at whatever period when they occur.

This work evaluates through a thorough analysis and simulation studies, the feasibility and performance of a combination of the UPQC and photovoltaic (PV)/Battery Energy Storage System (BESS) when installed on a radial distribution network. The BESS is connected to the system via a bi-directional dc-dc converter to enable bi-directional flow of power. The developed configuration ameliorates the effect of interruptions and loss of supply without compromising other functions of the UPQC. Also, it also made it possible to store excess solar energy when it is available while simultaneously possessing the capability of augmenting the output power of the PV panels at periods of low solar energy or high load demand. This has brought about the efficient utilization of available alternative source of energy. The block diagram is shown in Figure 1.1

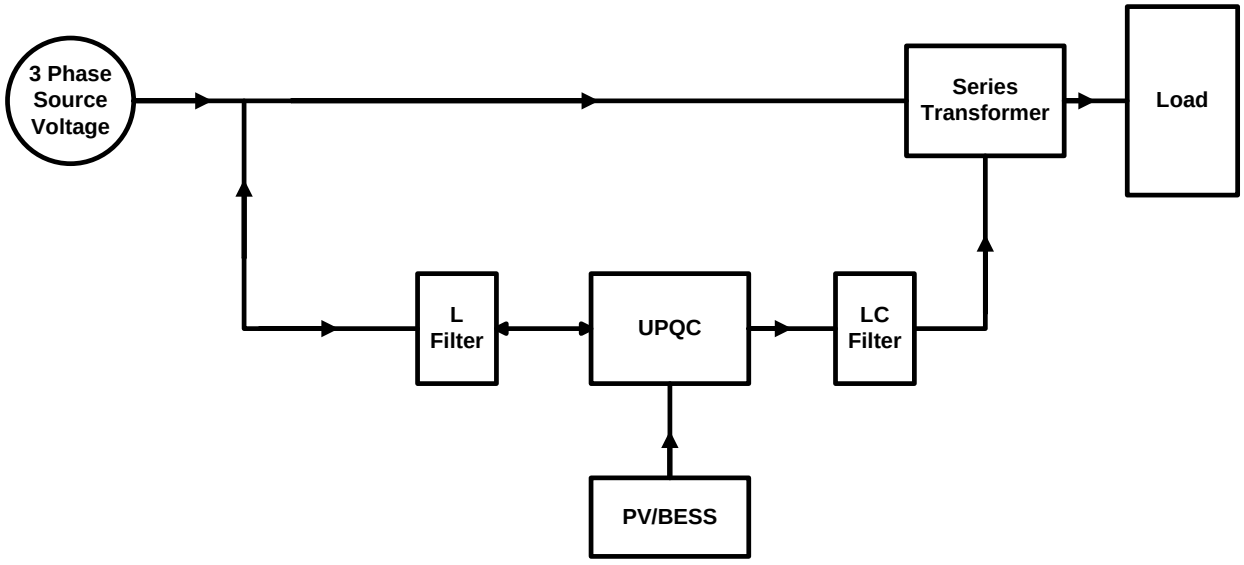


Figure 1.1 Block Diagram of the Distribution Line Equipped with UPQC and PV/BESS.

1.2 Significance of the Study

There is in most developing countries of the world a concerted effort at closing the gap between electrical power generation and its demand. As an immediate solution to the problem, gas turbine (GT) power plants are being set up in most places. The preference for GT stations is because of their relatively lower gestation period. As this generating stations come on stream, ailing industries are resurrected. These industries draw a lot of reactive power which makes the desired effect of the efforts of governments not to be evident to the ordinary consumer of electricity. Reactive power even though not used for any useful work, flows in the system. Moreover, because of the consumer nature of most developing economies, there is an increasing penetration of power electronics based load on the distribution network. These loads are non-linear in nature, hence generating a lot of harmonics which in a broad sense add to the reactive power demand in a network. Therefore, in order for the result of the efforts of government at increasing generation to become evident for all, there is a need not only for additional capacity in transmission but also for some sought of load conditioning. The proposed system offers such functionalities.

One effect of power quality events is economic losses as a result of equipment down time, damaged production processes and so forth. To forestall such losses it is important that sensitive load on the distribution network be protected from voltage disturbance.

The electricity supply sector in most countries of the world including Nigeria has been deregulated. It is therefore important to give consumers the flexibility in choosing their generation source and the amount of energy they need from a particular supplier and in fact offer everyone interested in generation of electricity the opportunity to participate. The proposed system can be extended such that individual consumers can install their own PV generation for their use and with the right environment hopefully to sell to the utilities.

1.3 Aim and Objectives of the Study

The aim of this work is to carry out the feasibility and performance analysis of the combination of the UPQC and PV/BESS on a realistic distribution network.

The research objectives are stated as follows:

(i) To develop a general mathematical model of the developed system configuration.

(ii) To carry out an in-depth analytical study of the system so as to determine the behavior of the system under different operating conditions.

(iii) To realize a system which is capable of efficiently compensating for long duration interruption and load reactive power requirements.

(iv) To realize a system with the capacity to ameliorate the effects of loss of supply.

1.4 Limitation of the Study

The following limitations where encountered in this work

i. Whereas, data for the chosen feeder was obtained, experimental validation was not completely possible since the UPQC is not installed on this feeder or any other network in the entire country.

ii. NASA solar data were used rather than NIMET. It doesn't appear as though it would introduce a significant error. However, with the absence of usable local solar data, the extent of deviation could not be determined.

1.5 Thesis Outline

The remaining part of this thesis is organized as follows:

CHAPTER TWO presents a detailed literature review for the research. The review is divided into two viz. review of fundamental concepts and review of similar works. The necessity of the present work is highlighted within the context of reviewed works.

CHAPTER THREE presents the materials used and method adopted. Data and software tools have been used for the work. A detailed circuit configuration is given and mode switching operations (i.e. between interconnected and islanding modes) briefly discussed

CHAPTER FOUR shows the derivation of the system model in the two mode of operation. The model is derived in the physical reference frame, transformed to the q-d reference frame and then the complex form is derived. The necessity of this process is explained in the chapter. Also, certain design considerations necessary for the determination of the parameters of the system are presented.

CHAPTER FIVE shows the result of the steady state analysis. Various plots of different analysis carried out are presented and discussed. A simulation study of certain aspects of the system is also included.

CHAPTER SIX reports the important conclusions of the thesis work. Recommendations are also made for future work. At the end of the thesis, cited references and appendices are provided.

CHAPTER TWO

LITERATURE REVIEW

2.1 Introduction

This chapter is aimed at developing the necessary background knowledge of the study system. It presents a review of pertinent concepts and a review of previous works done similar to the study area. A description of the various component sub-systems of the study system, their principle of operation, the constraints of circuit configuration and some methods of control, has been provided. The peculiarity of a radial distribution network within the context of disturbances on the network is also shown. The arbitrary reference frame transformation has also been described along with how to determine a particular reference frame. Finally, a critical and systematic review of different articles similar to the study is provided.

2.2 Overview of Fundamental Concepts

This section presents some basics definitions and concepts. It also outlines the underlying concepts relevant to the understanding of the study system.

2.2.1 Definition of major power quality events

The following are the major power quality problems at the distribution level (Alexander, *et al.* 2007; Khadkikar, 2008):

(i) Voltage Sag: it is a brief decrease of the rms (root mean square) line voltage of 10 to 90 percent of the nominal line voltage. The duration of the sag is 0.01 seconds to 1 minute. Voltage sag can be caused by system fault, increased load demand, transitional event such as large motor starting etc.

(ii) Voltage Swell: it is the converse to the sag. It is a brief increase in the rms line voltage of 110 to 180 percent of the nominal line voltage for duration of 0.01 seconds to 1 minute. Voltage swells can be caused by system fault, switching off of large rated loads.

(iii) Transients: it is an undesirable momentary deviation of the supply voltage or current which can be impulsive or oscillatory in nature. An impulsive transient is a sudden non power frequency change in voltage or current which is unidirectional in nature. These transients are mainly caused by lightning strike, switching of inductive loads. An oscillatory transient is a brief bidirectional variation in voltage, current or both on a power line.

(iv) Voltage flicker: a very rapid change in the supply voltage.

(v) Waveform Distortion: it is a steady state deviation in the voltage or current waveform from an ideal sine wave at fundamental supply frequency characterized by the spectral content of the deviation. This distortion can be classified as dc offset, harmonics, notching and noise.

(vi) Harmonics: harmonics are sinusoidal voltage or currents having frequencies that are integral multiples of fundamental supply voltage frequency. Harmonic distortion is caused by the non-linear characteristics of the devices and loads on the power system.

(vii) Interruption: an interruption is defined as a reduction in line voltage or current to less than 10 percent of the nominal not exceeding 60 seconds in length.

Other power quality events include unbalance, frequency deviation. Figure 2.1(Alexander, *et al.*, 2007) shows a pictorial view of major power quality events.

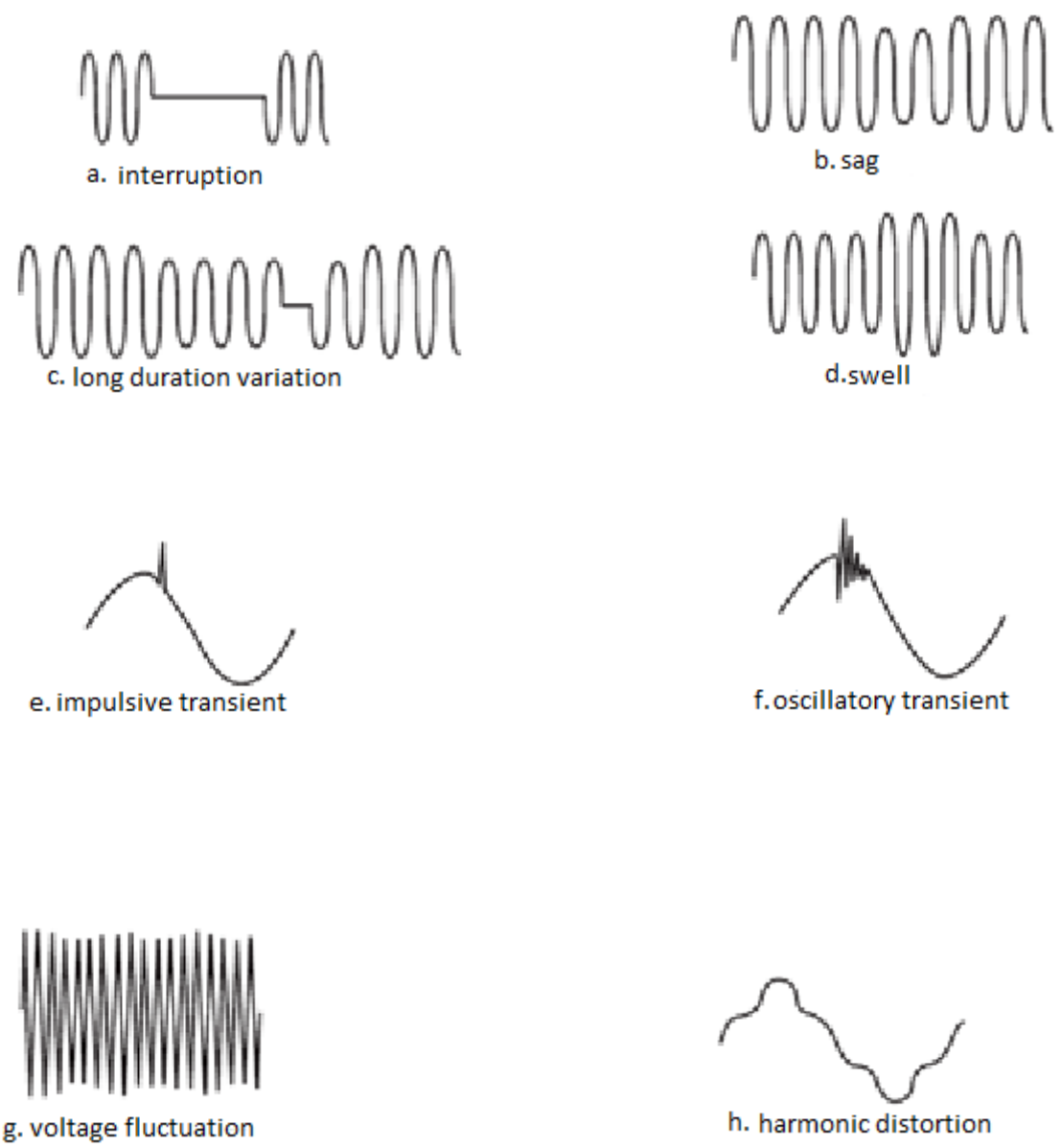


Figure 2.1 Pictorial Views of Major Power Quality Problems on Distribution Level (Alexander, *et al.*, 2007)

2.2.2 Some Effects of Poor Power Quality

The annual cost of wastage caused by poor power quality for EU-25 exceeds €150billion where industry accounts for 90% of this wastage. Of this percentage, dips and short interruptions accounts for almost 60% of the overall cost to industry and 57% for the total sample (Khadem, *et*

al., 2010). In Nigeria such data of the effect of power quality events is not available. However, from the information from Europe, it could be concluded that power quality events have also cost the country severely over the years.

The following are some effects of poor power quality (Alexander, *et al.,* 2007):

(i) Metering: it can affect the accuracy of utility metering

(ii) Protection relays: can cause protective relays to malfunction

(iii) Downtime: It can result in equipment downtime and/or damages resulting in loss of productivity.

(v) Cost: It can result in costs due to the preceding effect and wastages as a result of equipment malfunction during production.

(vi) Electromagnetic compatibility: It can result in problems with electromagnetic compatibility and noise

2.2.3 Electricity Distribution Network

The components of a typical electrical power system includes: generation, transmission, distribution systems and loads. The distribution system is mainly responsible for the conveyance of generated electric power to the consumer by means of lower voltage (compared to transmission systems) networks. Distribution systems can be divided into primary and secondary distribution systems. The primary distribution networks supply medium and large scale consumers while the secondary distribution networks supply mostly residential consumers (Debapriya, 2006).

In Nigeria, the primary distribution network is a 33kV or 11kV, 3phase 3wire system. The distribution system operates radially which has certain advantages, for example: less short circuit current and better protective coordination. However, there are certain disadvantages, the most popular being that a fault at any point on the line will affect all consumers downstream of the fault point (Debapriya, 2006).

The changing nature of loads on the present day distribution systems has yielded loads which are very sensitive to such faults which might occur. Many of these loads incorporate processes which are power electronic based because of the advantages it offers; for example, more power per weight. However, the loads are non-linear and they in turn pollute the distribution network (injecting harmonic currents) which in a broad sense adds to the reactive power requirement of these loads.

Such pollution originating from one consumer premise in a radial system may constitutes a cause of power quality problems at the premises of other consumers connected to the same point of common coupling (PCC). Consider Figure 2.2 which shows the schematic of a typical radial system.

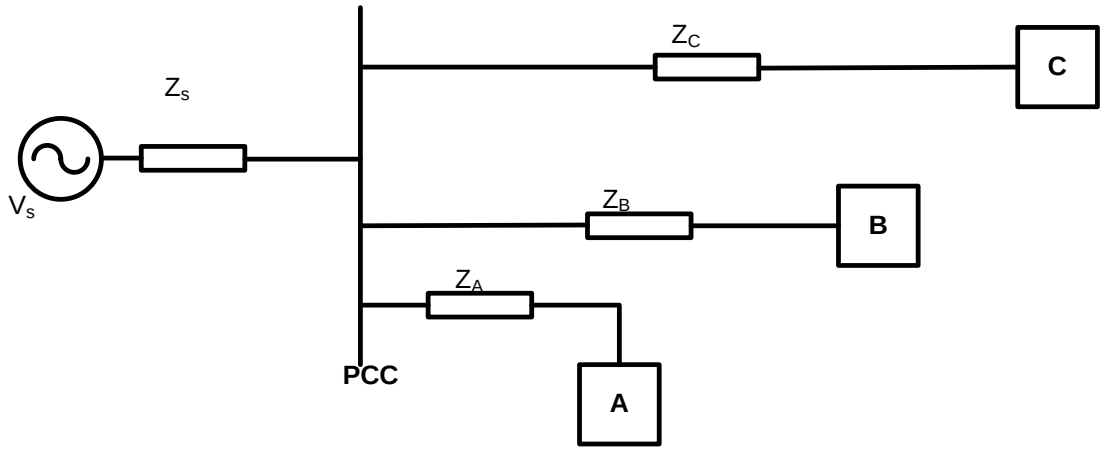


Figure 2.2 Schematic of Radial Distribution System Showing Consumers Connected to the Same Point of Common Coupling (PCC).

If consumer A for instance injects a current which is rich in harmonics because of non-linear loads, consumer B and C will see a voltage from the utility which is distorted even if the actual supply from the utility is pure. However, the voltage disturbances can also be the result of the utility's operation and other environmental factors.

This establishes the need for individual consumers to deploy power quality mitigating devices at their premises as shown in Figure 2.3 where for instance, consumer C has deployed the UPQC at its premises. This not only protects them from such disturbances which can disturb and disrupt their processes with the attendant huge cost implication but also protects the utility from consumer side power quality issues and free the consumer from paying heavy fines normally imposed by the utility for such user side disturbances.

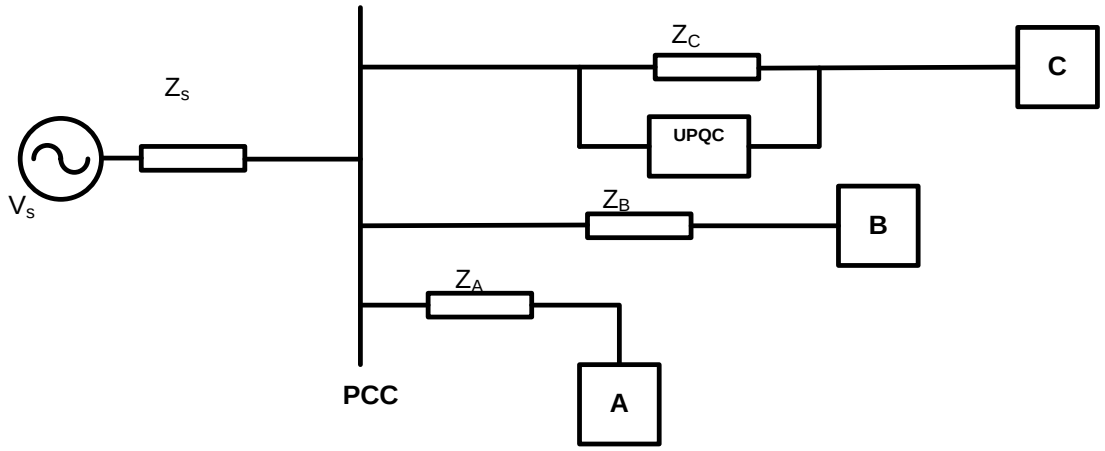


Figure 2.3 Schematic of a Radial Distribution System Showing the UPQC Deployed at the Premises of one Consumer

2.2.4 The Unified Power Quality Conditioner (UPQC).

The UPQC comprises of two Active Power Filters (APFs) connected back to back with a common dc link between them (Khadkikar, 2008). A block diagram of the UPQC is shown in Figure 2.4. The series APF (so called because it is connected in series with the line) is a three phase voltage source inverter while the shunt APF (connected across the load) is a three phase boost rectifier. Both converters are pulse width modulated (PMW) controlled. The PWM scheme is used to achieve the following objective: For the series converter, to regulate the load voltage and for the shunt inverter, to supply reactive power, regulate the supply power factor (p.f) and maintain the dc link voltage constant at its rated value.

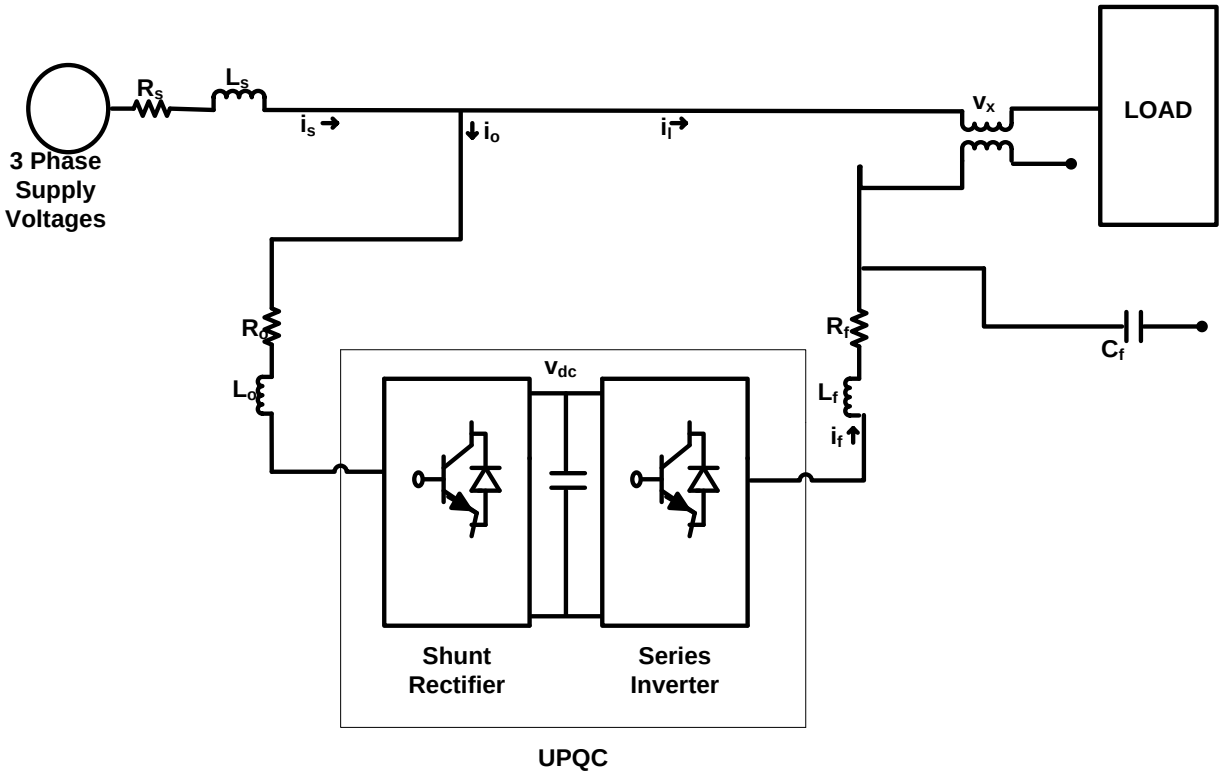


Figure 2.4 General Block Diagram Representation of the UPQC System.

Voltage Source Inverters (VSIs):

Basically, power electronic converters are an arrangement of switching devices and a determined switching procedure or sequence within the constraints of circuit configuration to achieve the objective of power conversion. Converters are used to convert either DC power to DC, DC to AC, AC to DC or AC to AC. DC to DC converter is discussed in Section 2.2.5. AC to DC converters are called rectifiers while a DC to AC converter is called an inverter. Figure 2.5 shows a realization of a three phase inverter (Mohammad, 2005). It comprises of an arrangement of six switching devices which are controlled to provide a variable frequency voltage source. The control of the output voltage of an inverter is achieved by (Sheetal, 2009):

(a) External control of ac output voltage

(b) External control of dc input voltage

(c) Internal control of the inverter.

The external controls require the use of peripheral components whereas the internal control does not require external components hence it is used most often (Sheetal, 2009). An inverter is described as a voltage source inverter also known as voltage fed inverter or a current source inverter depending on whether the input voltage or current remains constant. An inverter is described as a variable dc link converter if the input voltage is controllable (Sheetal, 2009).

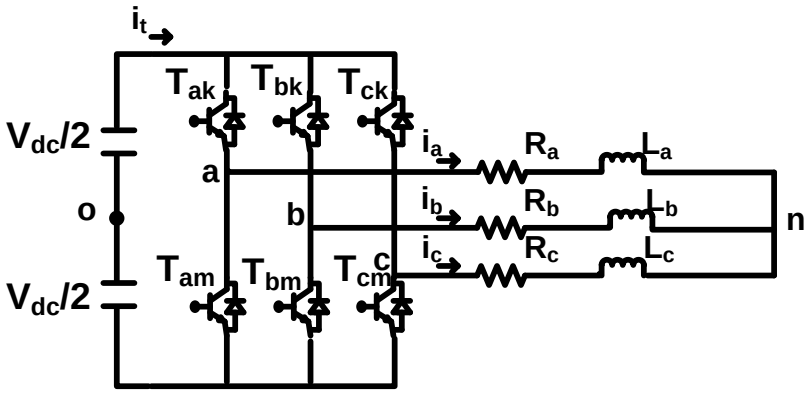


Figure 2.5: Three Phase Inverter

Switches and switching realization: There is various power switching semiconductor device families, differing in their characteristics and capabilities (or limitations). However, the principal device families of concern in the power switching semi-conductor range are the diodes, transistors and thyristors (Barry, 2012). Table 2.1shows some members of this families and their characteristics which inform their suitability or otherwise for a particular application.

As stated earlier, the three phase inverter shown in Figure 2.5 comprises of an arrangement of six switching devices. The arrangement and choice of these switching devices is such as to realize the required power conversion, satisfy Kirchhoff's Laws (KVL and KCL) for the circuit

and for quadrant operation. Realization of switch depends on the polarity of voltage the device must block in the OFF state and the polarity of the current the device must conduct during the conduction state.

Table 2.1: Some Power Switching Devices and their Characteristics (Mohammad, 2005)

Type	V/I Rating	Upper Frequency	ON Resistance
General Purpose Diode	5kV/5kA	1kHz	0.16mΩ
High Speed Diode	3kV/1kA	10kHz	1mΩ
ScHoTTKY Diode	40V/60A	20kHz	10mΩ
BJT(Single)	400V-630V/40A-250A	25kHz-35kHz	4mΩ-31mΩ
Thyristors	2800V-6500V/1500-5000A	60kHz	0.45mΩ-0.72mΩ

In this respect, there are four basic quadrant of operation of switches. Most applications require switches that can operate in a combination of quadrants. Consider Figure 2.6 which shows a single phase inverter in which the generic switch has been used. When switch is turned ON, it should conduct positive current and when turned OFF it should block positive voltage . However, turning OFF demands that a path is provided through for to discharge. , therefore, must be able to conduct that negative current. The reverse of this occurs when is turned ON and it conducts positive current, . On turning it OFF, the current will have to discharge through which must be able to handle the negative current. DC- AC converters, therefore, require switches which can handle both positive and negative currents but only block positive voltages (i.e. switches that operate in the first and second quadrant). This is realized using a transistor and an anti-parallel diode as shown insert in Figure 2.6.

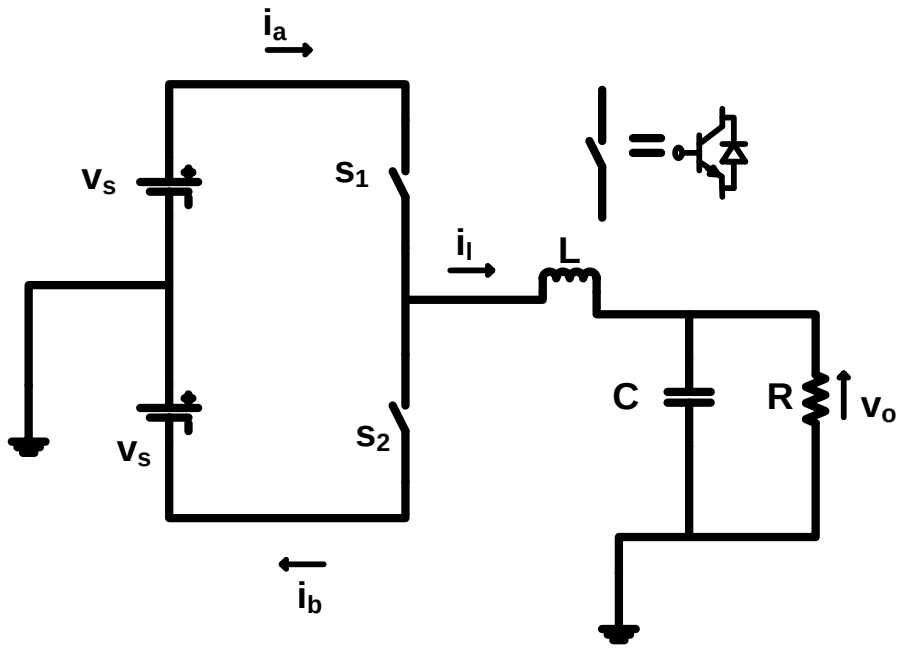


Figure 2.6: Single Phase Inverter Showing Switch Realization.

Switching function: Power converters normally interface sources with loads. The desired output of the converters for any application depends on the needs of such application. In the case of the inverter for instance, a voltage output of a certain magnitude, phase angle and frequency (which can be fixed or varied) might be required. This output is obtained by the switching ON and OFF of the switches in the converter according to a repetitive pattern. So, a train of pulses of amplitude one (1) is applied to the switching device. This train of pulses is referred to as the switching function. When the switching function is 1, the switch is turned ON and when it is zero, it is turned OFF. The desired output characteristics of the converter (magnitude, phase angle and frequency) are obtained by the pattern of these repetitive groups of pulses which are manipulated using some form of modulation. Figure 2.7 shows a simple un-modulated switching function.

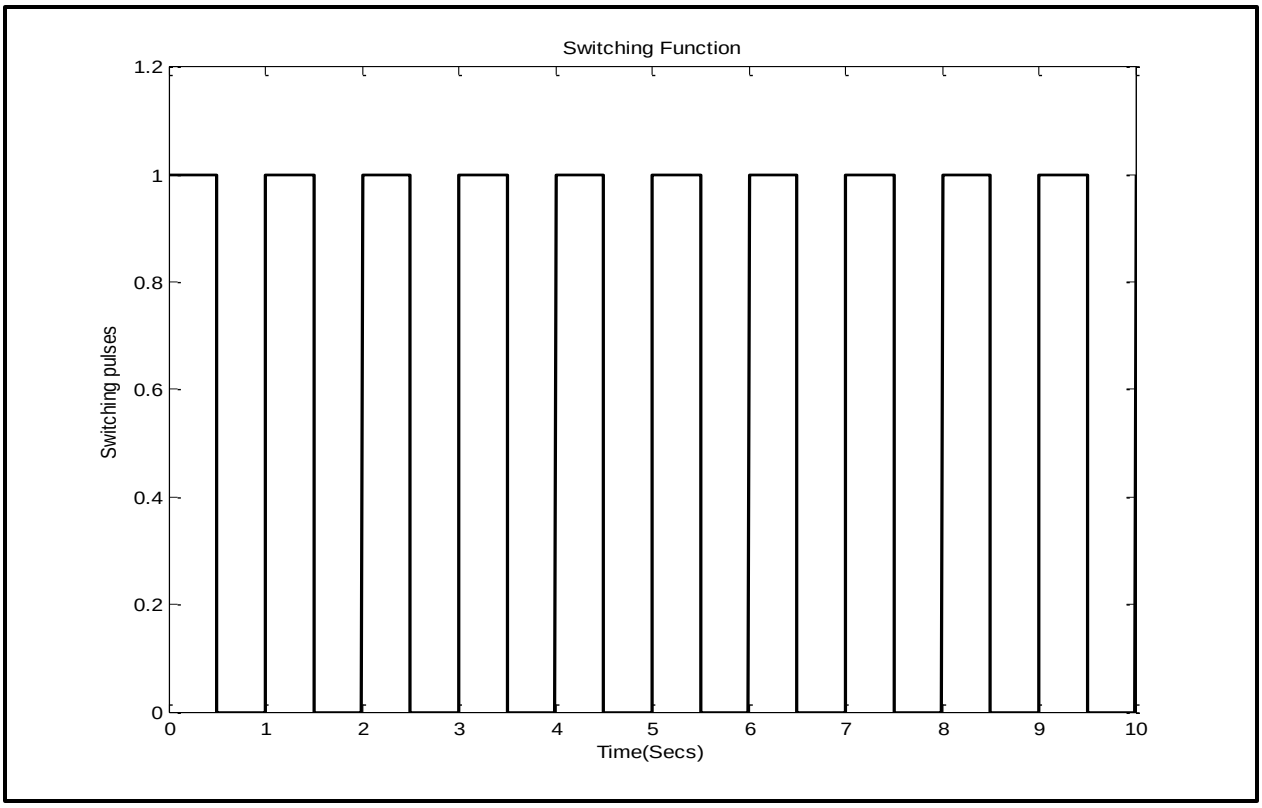


Figure 2.7: Simple Switching Function

Principle of operation: The principle of operation of the inverter is explained with Figure 2.8 which shows one-phase of the three-phase system of Figure 2.5.

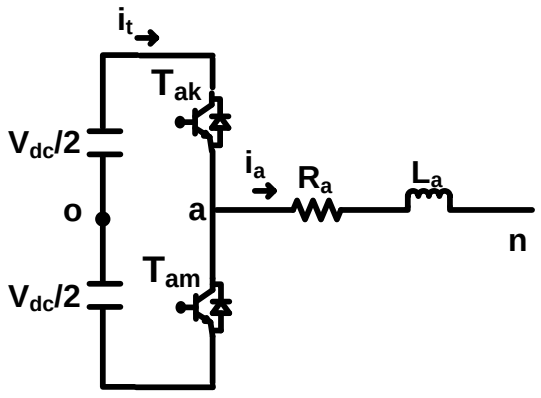


Figure 2.8: One-Phase of a Three-Phase Inverter.

Let be the switching function for and the switching function for . When , is turned ON and when , is turned OFF. Similarly, when , is turned ON and when , is turned OFF. Kirchhoff's Laws places two constraints on the system which are:

(a) KVL: and cannot be turned ON at the same time as this will short circuit the source.

(b) KCL: One of the switching devices must turn ON at all times to provide a path for current to flow.

Hence, when , and when , . and are complimentary and from digital electronics

(2.1)

From Figure 2.8,

(2.2)

Now,

When

— (2.3)

And when

— (2.4)

Multiplying equation 2.3 by and equation 2.4 by and adding the two outcomes, equation 2.5 is obtained.

— (2.5)

Substituting equation 2.1 into equation 2.5;

— (2.6)

This result in;

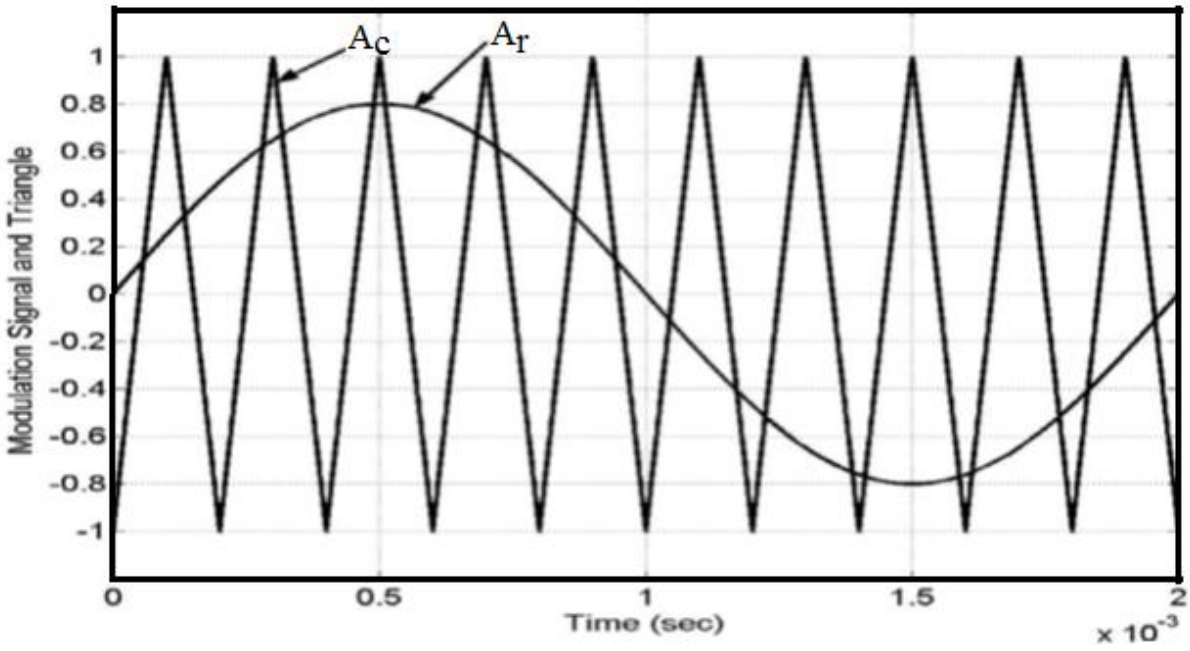
— (2.7)

Equation (2.7) gives the output voltage of the inverter in terms of the switching function. It is obvious how the switching function of the inverter can be used to produce an output voltage suited for a particular application. The switching functions are modulated by several techniques including PWM.

Pulse Width Modulation (PWM) control: PWM scheme involves varying the duty ratio (defined as the ratio of the ON time to the switching period) of constant amplitude pulses for each period. The duty ratio of these pulses is varied to obtain output voltage control. There are different PWM techniques differing essentially in the harmonic content of the output voltage. One of the most popularly used techniques in the industry is the sinusoidal PWM (SPWM) technique illustrated in Figure 2.9 (Sheetal, 2010).

In the SPWM technique, a high frequency triangular carrier wave A_c is compared with a sinusoidal reference signal, A_r. A_r is related to the magnitude, phase angle and frequency of desired voltage. The switching instance of the switches is determined by the intersection of A_c with A_r. From Figure 2.9, the switch is ON when $A_r > A_c$ and OFF when $A_r < A_c$.

(a.)



(b.)

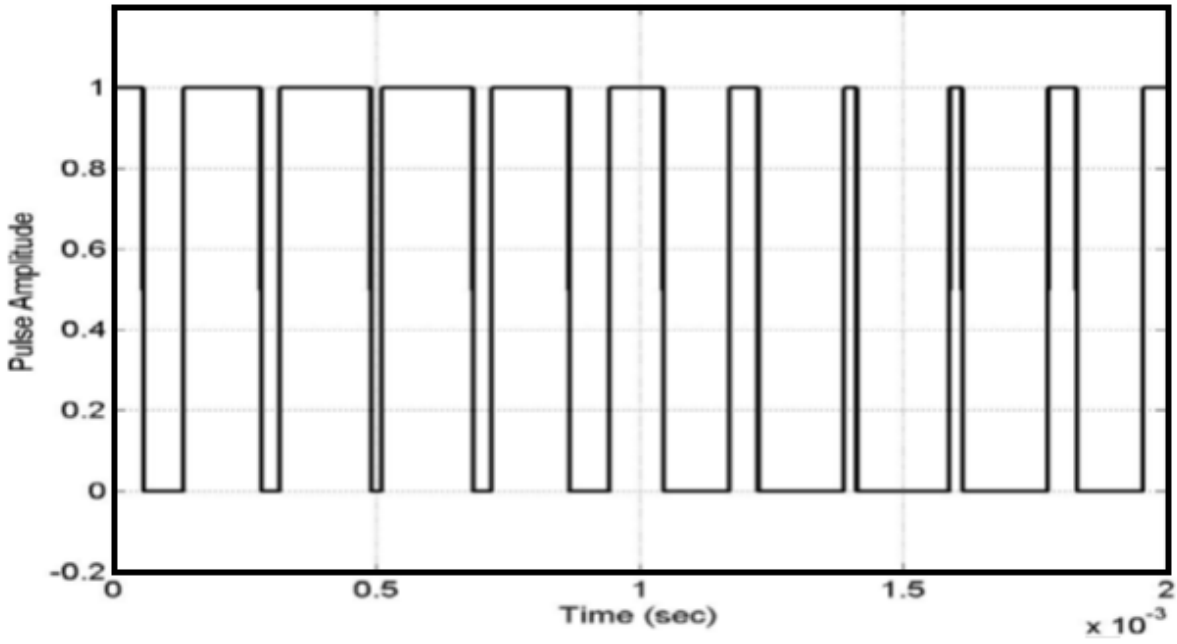


Figure 2.9 SPWM Illustration (a) Comparison of Sine and Triangle Wave (b) Switching Pulses

If Figure 2.9 (b) shows the switching pattern for , for instance, the PWM patterns for and are identical to that of with the appropriate phase shifts. It is assumed that the switching points within one switching period are symmetrical (Seyed, 1996), the fundamental angular frequency of the inverter is while the angular frequency of the switching function is . Let be the average of within one period corresponding to the switching frequency. Then from Figure 2.10, the switching function can be expressed in terms of Fourier series as

(2.8)

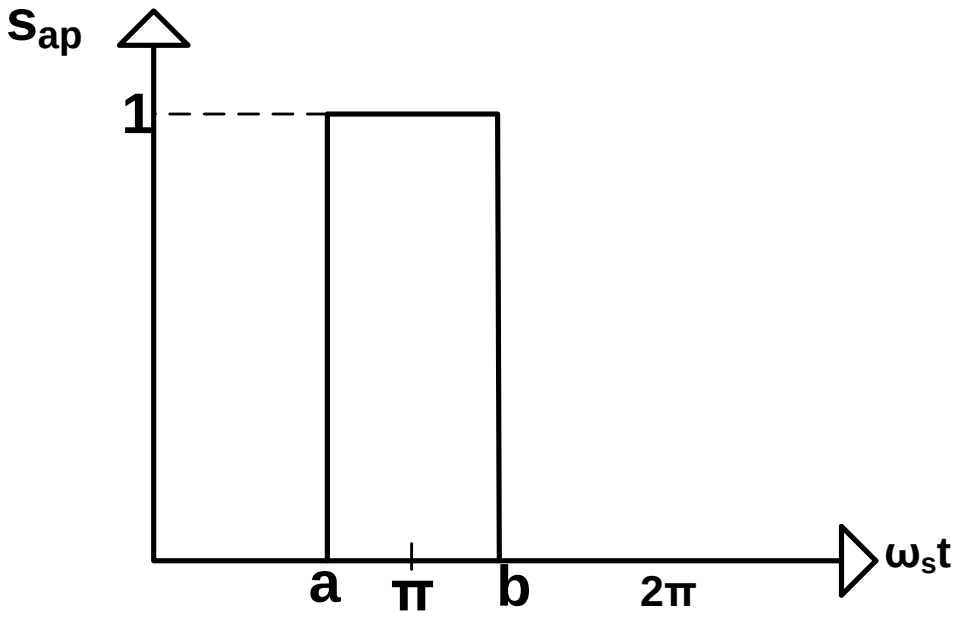


Figure 2.10 Switching Function in One Switching Period

— Therefore:

— (2.9)

– — (2.10)

The hardware implementation of the carrier based PWM is difficult to implement because of the difficulty in calculating the intersection points. A commonly accepted alternative is to sample the modulation signal at the positive and/or negative peaks of the triangular career waveform and then keeping the sample constant over the switching period (Malijana, *et al.*, 2010). Figure 2.11 (Seyed, 1996) shows the variation of within one period corresponding to system fundamental frequency.

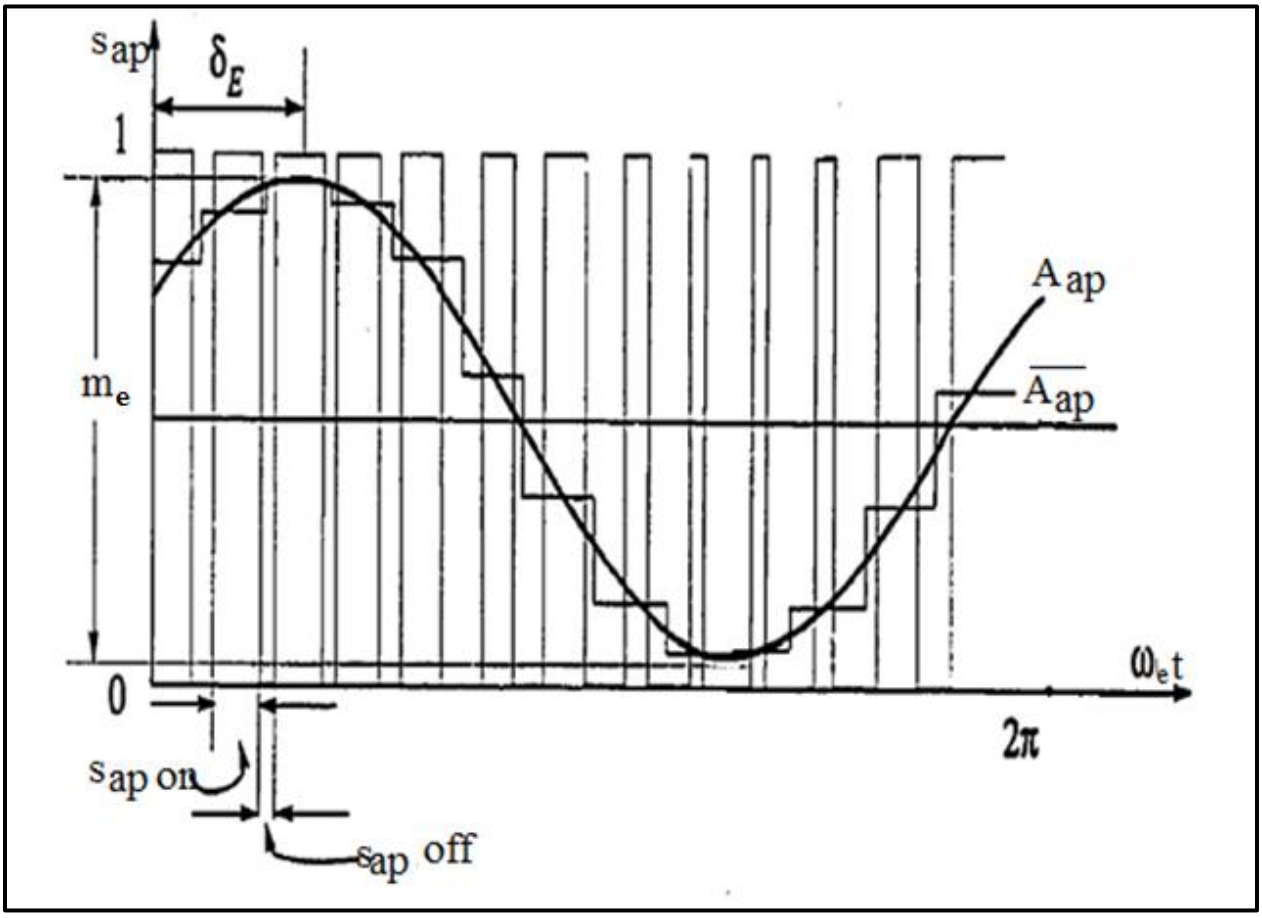


Figure 2.11 Fundamental Component of the Average Switching Function (Seyed, 1996).

The fundamental component of in Figure 2.11 is (Seyed, 1996)

— – (2.11)

Let (2.12)

Then – (2.13)

(2.14)

The fundamental component model of the inverter is:

– (2.15)

Reference frame transformation: Pulse Width Modulation requires the comparison of some reference signal with a carrier signal to generate the pulses. This is shown in Figure 2.9. There are several methods used (mostly in combination) for the extraction of the reference signals. The method used depends largely on the application and can be broadly categorized into:

(i) Frequency domain method

(ii) Time domain method

(iii) Heuristic techniques, for example, Artificial Neural Network (ANN), Fuzzy Logic and so forth

(iv) PC based methods, and so forth.

Frequency domain method is based on the determination of Fast Fourier Transform (FFT) coefficient. It involves large computation time and hence hardly used since response time is very crucial in the control of Active Power Filters. The time domain method include: instantaneous reactive power theory, synchronous reference frame method, symmetrical component theory and so forth. These methods always require some form of transformation which makes for easy analysis and even simpler practical implementation.

Reference frame transformation, is a change of variable that transforms the variables in a reference frame to variables in another reference frame with the hope that in the new reference frame the complexity of the equations is reduced and solutions can be obtained with far less rigor.

For example, R.H. Park formulated a change of variable which replaced the variables (voltages, currents and flux linkages) associated with the stator windings of a synchronous machine by variables fixed in the rotor (Paul, *et al.,* 2002). This transformation eliminated all time-varying inductances from the voltage equation of the synchronous machine.

An arbitrary reference frame is defined in which all known real transformation can be obtained by assigning the appropriate speed of rotation to the arbitrary reference frame (Paul, *et al.*, 2002). The change of variables for a physical system to the arbitrary reference frame for a 3-phase system is expressed as:

(2.16)

So that

;

are the three-phase variables of the circuit elements and are the transformed variables in the arbitrary reference frame. Figure 2.12 gives an illustration of the transformation.

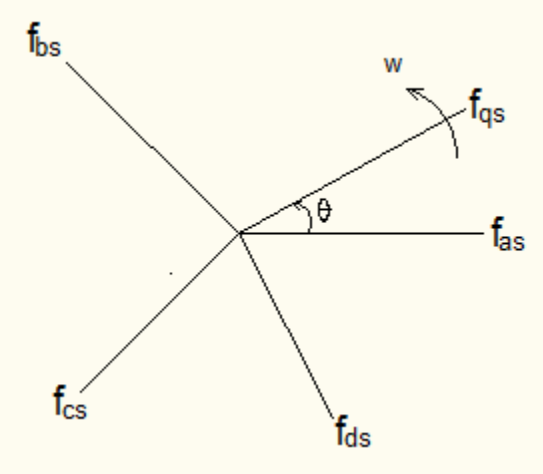


Figure 2.12: q-d-o Transformation shown by Trigonometric Relationship.

— —
— — (2.17)
– – –

From equation (2.17),

— —
— — (2.18)

(2.19)

ω, is the angular velocity of the arbitrary reference frame. Various transformations can be obtained by assigning the value of ω. In this work, ω, is assigned the value (the frequency of , and). The advantage of this transformation is that time-varying sinusoidal functions become dc (constant) functions and at steady state, the differential equations become algebraic equations whose solutions are more readily obtained. For instance, given the three phase voltages below:

—

—

.

The arbitrary reference frame voltages are obtained from equation 2.16 as:

=

— —

– — — —

– – – —

(The full derivation with relevant trigonometric identities is provided in appendix B)

.

are therefore constant values in the q-d-o reference frame. If the initial condition is chosen to be the same both for the a-b-c and q-d-o reference frames,

And

2.2.5 DC-DC Converters

A dc-dc converter converts directly from dc to dc. The need to convert from dc to dc arises in many applications either because a fixed dc voltage needs to be converted to a variable dc source or vice versa, that is, a variable dc source to a fixed dc voltage. The various types of dc converters include the buck converter where the output voltage is less than the input voltage, the boost converter where the output voltage is greater than the input voltage and the buck-boost converter that combine the functionalities of both the buck and the boost converter (Mohammad, 2005).

The boost dc converter has been used in this work because of the need to provide a constant dc voltage at the input of the inverter which is higher than the output voltage of the PV array and the battery. The circuit configuration is shown in Figure 2.13.

Principle of operation:

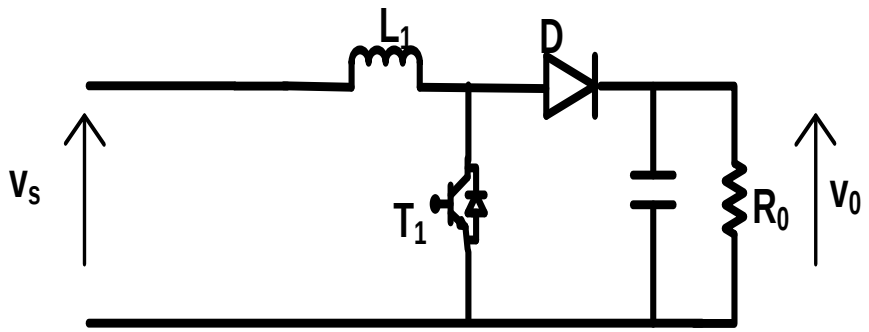


Figure 2.13 Circuit Configuration of a Boost DC-DC Converter.

S_1 and S_D are switching functions for device T_1 and D respectively. Table 2.2 shows all the possible state combinations of the switching device S_1 and S_D:

Table 2.2: Truth Table of a Boost dc-dc Converter.

Mode	S_1	S_D
1	0	0
2	1	0
3	0	1
4	1	1

When a switch is OFF its state is 0 and when it is ON its state is 1.

However, due to the constraints of KVL and KCL as in the case of the inverter, only modes 2 and 3 can be used. The switches T_1 and D are thus complimentary and

(2.20)

The control of the output voltage is achieved by varying the duty ratio, k, of the switching function S_1 using PWM. The duty ratio is the ratio of the ON time (t_{on}) of the switch to the total time or switching period, T.

—, (2.21)

And (2.22)

In this case a dc reference signal is compared with a saw tooth career signal to generate the switching pulses as shown in Figure 2.14.

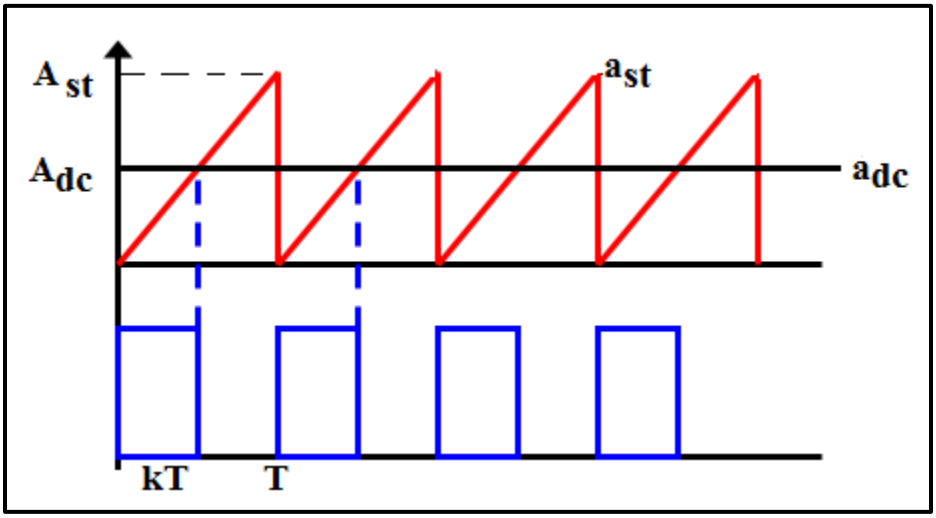


Figure 2.14 Generation of Duty Ratio for DC-DC Converter

The frequency of the carrier signal is equal to the switching frequency. If is the peak value of the carrier signal and is peak value of the reference signal, the equation of the carrier signal is given as

— (2.23)

And at the switching instance, t = kT, the carrier signal must be equal to the reference signal

— (2.24)

And hence, — (2.25)

Showing that k is changed by varying the value of the dc reference signal.

2.3 Review of Similar Works

Fujita *et al.,* (1998) have classified the UPQC into two types: General UPQC for power distribution system and industrial power system. The other is a specific UPQC for a supply voltage flicker/imbalance-sensitive load. They based their classification on the position of the shunt inverter relative to the series inverter. The right shunt inverter was called the general UPQC while the left shunt inverter was called the specific UPQC. Subsequent researchers, however, have not followed this manner of classification; due largely to the ability to now implement advance and complex control methods. The UPQC is now classified along the lines of configuration, supply system, converter topology, control method and so forth (Khadkikar, 2008). A thorough review of relevant works is done in this section. For the purpose of the current work, reviewed work are presented under the classification shown in Figure 2.15

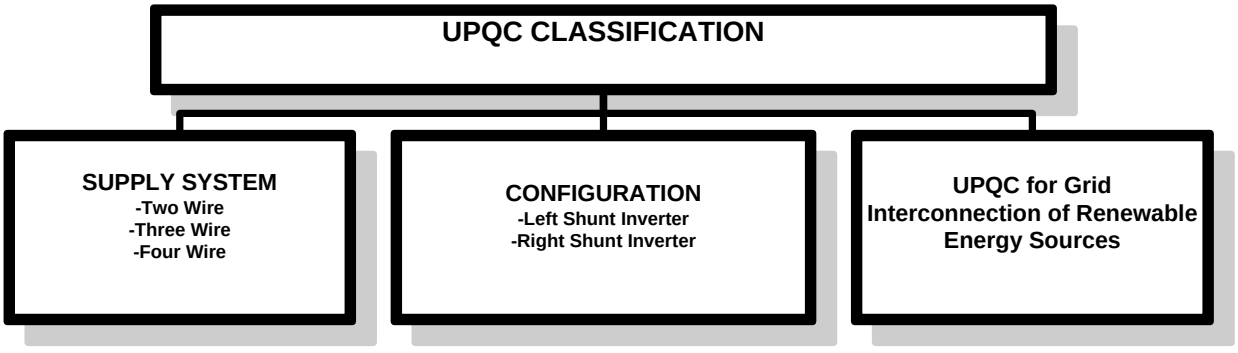


Figure 2.15 Classification of Universal Power Quality Conditioner (UPQC)

2.3.1 Classification Based on Supply System

Based on the supply system, the UPQC can be classified as single phase two wire (SP2W), three phase three wire (3P3W) or three phase four wire (3P4W). Majority of the researches done are based on the three phase three wire (3P3W) UPQC.

Khadkikar, *et al.,* (2011) worked on a single phase UPQC. Their emphasis was on the development of a simple control algorithm for the system which they termed Unit Vector Template Generation (UVTG). This algorithm involved generating the reference signals for both the shunt and series inverter of the UPQC using Phase Locked Loop (PLL) and proportional-integral (PI) controller. The developed algorithm required less computation time and it was easy to implement for practical hardware solution. However, it required a huge investment on the design of filters. Moreover, the suitability for a three phase system was not demonstrated.

Paduchuri, *et al.,* (2012) proposed a UPQC system for a three phase four wire (3P4W) system using a three-phase three wire (3P3W) UPQC. This system can be achieved either with a split capacitor at the dc link or by using a fourth inverter leg on the shunt inverter. Using the split capacitor has the disadvantage that it could lead to some oscillations due to some intrinsic differences between two otherwise similar capacitors. In their system they used the second option perhaps to avoid such oscillations but this had the tendency to increase size and cost and complicate the control some more. However, the cost of providing extra neutral wire by the utilities is reduced.

Metin *et al.,* (2009) worked on a three-phase three-wire 3P3W UPQC to compensate harmonics voltage disturbances and reactive power. Using synchronous reference frame for the series inverter and instantaneous reactive power theory for the shunt inverter, they were able to achieve

their objectives with fewer measurements of control variables. They had to rely however on two reference variable determination methods both of which involved complex transformations

Woo *et al.,* (2010) proposed a new method for the UPQC-Q scheme that involves minimum active power injection. The UPQC –Q scheme involves using the series inverter to regulate the load bus voltage as usual. However, the series inverter in the UPQC-Q scheme did this by injecting voltage in quadrature with the source current. The idea was to minimize real losses in the UPQC since only quadrature voltage is used. However, with this scheme there was the issue of the rating concern for the series inverter as the difference between the source voltage and rated load voltage increased whether for sag or swell. To minimize this problem, they proposed a control method that enabled the series inverter to inject a minimum active power thereby using the same rated series inverter to compensate higher difference between source and rated load voltages. With this system however, there was still the issue of the difference in voltage angle between supply voltage and load voltage introduced by the injected series inverter voltage and the determination of the exact angle of the series inverter to ensure minimum active power injection.

2.3.2 Classification Based on Configuration

Figure 2.16 and 2.17 show the block diagram of the left shunt and right shunt configuration respectively. The right shunt inverter is the most commonly used due to zero power injection/ absorption mode (Khadkikar, 2008). It is also desirable especially in a highly distorted environment as the shunt inverter is used to compensate load side disturbances so that the current in the series inverter is sinusoidal (but again this depends on the control algorithm). The left shunt inverter is however used in special cases where for instance the concern is not so much

load current harmonics. This configuration was used by Fujita *et al.*, (1998) to avoid conflict between the inverter and an existing passive filter.

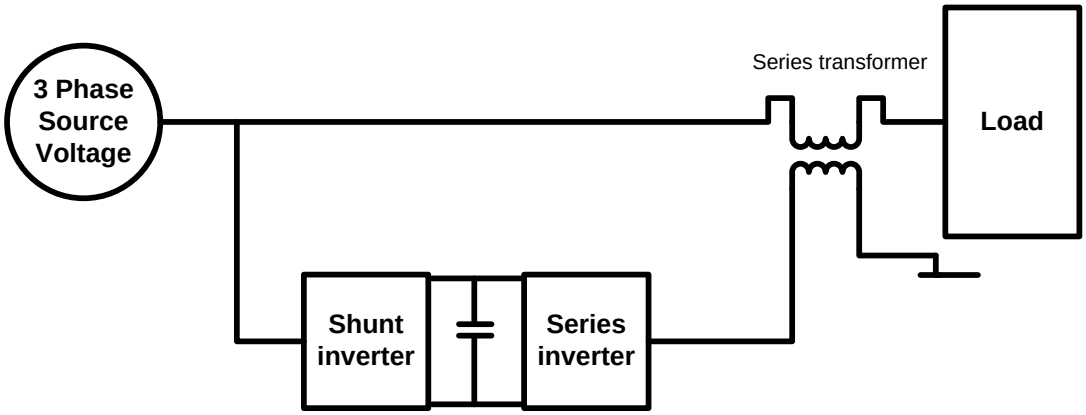


Figure 2.16 Left Shunt Inverter Configuration of the UPQC.

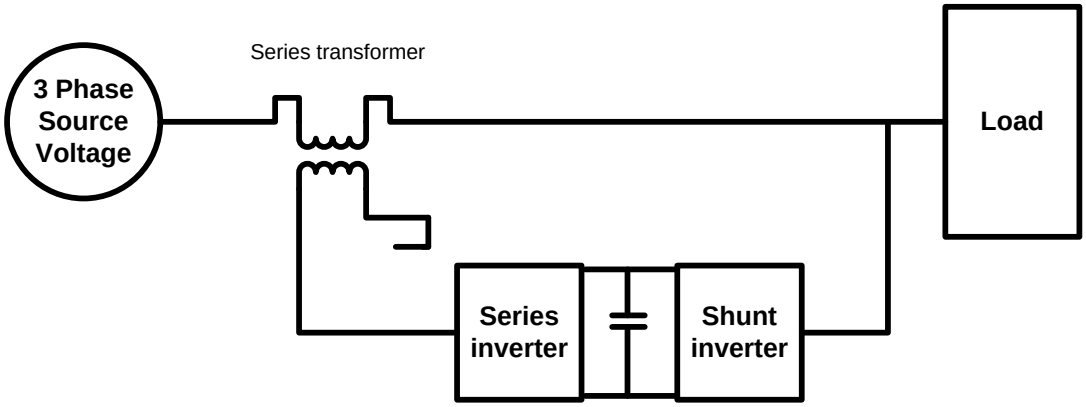


Figure 2.17 Right Shunt Inverter Configuration of the UPQC.

2.3.3 UPQC for Grid Integration of Renewable Energy Resources

Extended use of fossil fuels reserve in the current manner is not sustainable. The needs for supplementary or even alternative source that ideally will be non-depletable energy source have since been recognized (Considine, 1977). Nigeria as a country has an abundance of solar

radiation which can be readily deployed as a source of renewable energy for power generation. It has been confirmed that Nigeria receives 5.08 10^{12} kWh of energy per day from the sun. This translated to 2.54 10^{6} MWh of electrical energy given 5% efficiency of solar energy appliances and just 1% of the country's surface area (Sambo, 2005). Renewable energy sources can be used either as standalone installations or interconnected with the grid. It has been estimated that the greatest application of solar PV energy will be its usage in the interconnected system (Hosseinpour, et al., 2009).

Jayanti *et al.,* (2006) worked on the rating requirements of the UPQC for voltage ride through capability. They studied a fixed speed induction generator (FSIG) wind generation (WG) in the context of fault occurring in the grid. For wind generators connected directly to the grid, it require shutting down the wind generators when a fault, say voltage dip, occurs in an interconnecting bus to avoid system collapse. With their work using the UPQC to serve as an interface, fault ride through capabilities of the Wind Generation system was enhanced. They concentrated their efforts only on determining what would be the minimum rating of the UPQC to provide this capability.

Byung-Moon Han, *et al.,* (2006) proposed a new configuration for the UPQC comprising a dc/dc converter and super capacitors. The super capacitors were used as energy storage devices enabling the UPQC to compensate for voltage interruption on the system. By appropriately sizing the super capacitor banks, the system was able to compensate for voltage interruption lasting for a maximum of 2 seconds which they determined arbitrarily perhaps to reduce the size or number of super capacitors required. Therefore, if the interruption last beyond this time, the system losses the ability to compensate as the energy stored in the super capacitor banks would have been used up. If it must compensate for longer period, the capacitor bank must be increased

in size and this is the compromise that must be reached. Moreover, the dc/dc converter design was quite complex. They were able to achieve bi-directional flow of power through the dc/dc converter. They, however, used five modules and a transformer which led to leakages and reduction of both efficiency and effectiveness.

Marcelo *et al.,* (2006) used the UPQC as an interfacing device to connect a PV system to the grid. They did not make use of dc-dc converter hence increasing conversion efficiency. They also used Maximum Power Point Tracking (MPPT) to determine the dc link voltage. However, when there is no sunlight, the dc link voltage is fixed. Hence, the system worked by taking all the power available from the PV system and augmenting with the utility. If PV output is more than load requirements for instance, excess power is fed to the grid. When there is no insolation then all load requirement is supplied from the utility. They did not however reckon with issues like interruption and loss of supply, as they only tried to improve the efficiency of the PV conversion by utilizing fewer converters.

Davari *et al.,* (2009) used the UPQC with PV and battery storage with a multi input and single output system in an attempt to harness available diverse renewable energy sources. The system was used in a sequence such that the solar PV cells charged the battery when there was available solar insolation and the battery supported the dc link at periods when there is no solar insolation. The system suffered from inefficient utilization of available solar insolation at periods of high insolation or low system demand

Hosseinpour *et al.,* (2009) like Marcelo *et al.,* worked on a UPQC model that interfaces solar PV cells with the grid. Their system worked in the two modes namely, interconnected: where the utility and PV supplies load requirements or islanding: where a part of the load requirement is

supplied by the PV cells alone. They did not use any storage means which meant that the system could only compensate when there was sufficient solar insolation.

2.4 Statement of Problem

The reviewed literatures have shown considerable efforts in the direction of improving the power quality compensating capabilities of the UPQC. There has been efforts to (i) enhance the power handling capacity of the constituent converters through the implementation of various control algorithms (ii) minimize losses by ensuring minimum real power injection by the series inverter (iii) utilize alternative energy sources (mostly solar) at the dc link to enable the UPQC to compensate for interruption. However, the issue of efficient and reliable utilization of available solar insolation to compensate for interruption and loss of supply using a simple system configuration has not been addressed. In the light of this, there is need for a scheme that ensures real time collaboration between the solar PV cells and the battery energy storage system. This system should be able to in addition to compensating interruption meet a part of load requirement at times of loss of supply. The system should do all of these while retaining the reported UPQC power quality compensating capabilities. It is to this end that the present research work is undertaken.

2.5 Conclusion

In this chapter, the theoretical background of the study system has been presented. The presentation is made in terms of the constituent sub-component systems: the principle of operation and relevant mathematical theories. Also, a summary of reviewed works similar to the area of study is presented. Reviewed literature where categorized based mainly on the physical configuration of the UPQC and the discussion presented according to this categorization.

CHAPTER THREE

MATERIALS AND METHODS

3.1 Introduction

This chapter provides a detailed description of the material used for the research and methodology adopted. Materials used include:

(i) Power Holding Company of Nigeria (PHCN) data for the 11kV Gaskiya Feeder, Zaria.

(ii) National Aeronautics and Space Administration (NASA) solar insolation data for Zaria (Latitude 11.06 and Longitude 7.7)

(iii) MATLAB/Simulink software.

The methodology adopted has been presented in section 3.5

3.2 PHCN Data for 11kV Gaskiya Feeder, Zaria

The 11kV Gaskiya feeder is a radial distribution network feeding Government Reserve Area (G.R.A) and Zaria industrial area. Data was obtained from a current transformer connected to the line. It measures the total current drawn by connected loads. From these values, the total apparent power variation over a period of time is determined. The data obtained was for a five working days period. Since the work is not about forecasting load behavior, the obtained data can be viewed as representative of the behavior of the loads on the network within a typical week. Moreover, majority of the loads on the network are industrial loads which are not operated during the weekends. Table 3.1 shows the PHCN data for the 11kV Gaskiya feeder for a week in December 2012 as obtained from PHCN. A scanned copy of the original document has been

included in Appendix H. The first column on the table shows the particular days the data was collected. From the table it can be seen that data was collected beginning on the 8th of December to the 12th of December. The first row shows the time of the day. For each day, data was collected from 00 hours to 23 hours. The elements within the table shows the value of the current measured for each time at different times covering the 24 hours in a day.

Table 3.1 Data of the Hourly Demand on the 11kV PHCN Gaskiya Zaria Feeder December 2012

	0.00	1.00	2.00	3.00	4.00	5.00	6.00	7.00	8.00	9.00	10.00	11.00	12.00	13.00	14.00	15.00	16.00	17.00	18.0	19.0	20.0	21.00	22.00	23.00
08	Ls	110	100	100	100	120	150	160	150	160	150	150	150	150	140	140	140	150	150	160	160	140	140	120
09	120	120	100	100	110	140	150	100	F	F	Ls	Ls	Ls	150	150	150	150	150	150	150	160	160	140	140
10	110	120	100	100	100	130	150	150	130	150	150	150	150	150	140	140	140	140	Ls	Ls	Ls	Ls	Ls	Ls
11	Ls	Ls	Ls	Ls	Ls	Ls	Ls	160	150	150	150	150	150	150	150	150	Ls	Ls	Ls	Ls	Ls	150	130	130
12	120	Ls	Ls	Ls	Ls	Ls	Ls	Ls	160	160	160	150	Ls	Ls	Ls	B	Ls	Ls	Ls	Ls	170	160	150	130

Key

Ls – Load Shedding Due to Limitation in the Injection Substation.

F – Fault.

3.3 NASA Solar Insolation Data for Zaria

The NASA data are satellite derived and they span a 22 years period. The data used is a monthly average taken at specific times of the day with a three hourly interval. The NASA data was used because of the inability to obtain useful solar insolation data from the Nigerian Metrological Agency (NIMET). Data obtained from the NIMET office in the Nigerian College of Aviation Technology (NCAT) Zaria were unusable due to some inconsistencies. For example, there were in the NIMET data times when sunshine was recorded for zero hours in a day. Moreover, the instrument used was not the conventional instrument for measuring solar insolation. Comparison of the NASA data used with surface measurement taken at the Baseline Surface Radiation Network (BSRN) shows a Root Mean Square Error of 15.37% (NASA, 2013). The obtained data are thus sufficient for the purpose of the study as an actual measurement might not give a considerable departure from what has been obtained. The obtained data were grouped according to Table 3.2 and the class mark used as representative of the group in the analysis. Raw data included in Appendix E.

Table 3.2 Frequency Table for Solar Insolation in Zaria

Solar insolation	Frequency	Class Mark
0.00-0.14	24	0.07
0.15-0.34	0	0.245
0.35-0.54	15	0.445
0.55-0.74	12	0.645
0.75-0.94	9	0.845
0.95-1.14	0	1.045

3.4 MATLAB/Simulink

Power electronics systems, usually, are multimode systems (Ned, 1995). The circuit topology of power electronics systems change with changes in mode. Hence, closed form solutions of the

state of power electronic systems as a function of time are usually not possible. Computer simulations have made it possible to model such systems and observe their responses to certain conditions. There are two basic types of tools for simulation (Ned, 1995), Circuit Oriented Simulators and Equation Solvers.

MATLAB does function as an equation solver. MATLAB is extensible and highly integrated. MATLAB can be used for computation, programming, visualization and simulation. Simulink is the companion tool of MATLAB used for simulation. In MATLAB, a system can be represented by its model equations (differential equations or/and algebraic) in its different mode of operation and a solution obtained. MATLAB provides the capability of obtaining solution in various visual forms. MATLAB/Simulink version 9 m-file editor and the accompanying Simulink has been used in the present work because it provides all the capability needed for the work. Figure 3.1 shows the MATLAB editor interface for version 9 while Figure 3.2 shows a Simulink model for simulation using the embedded MATLAB function.

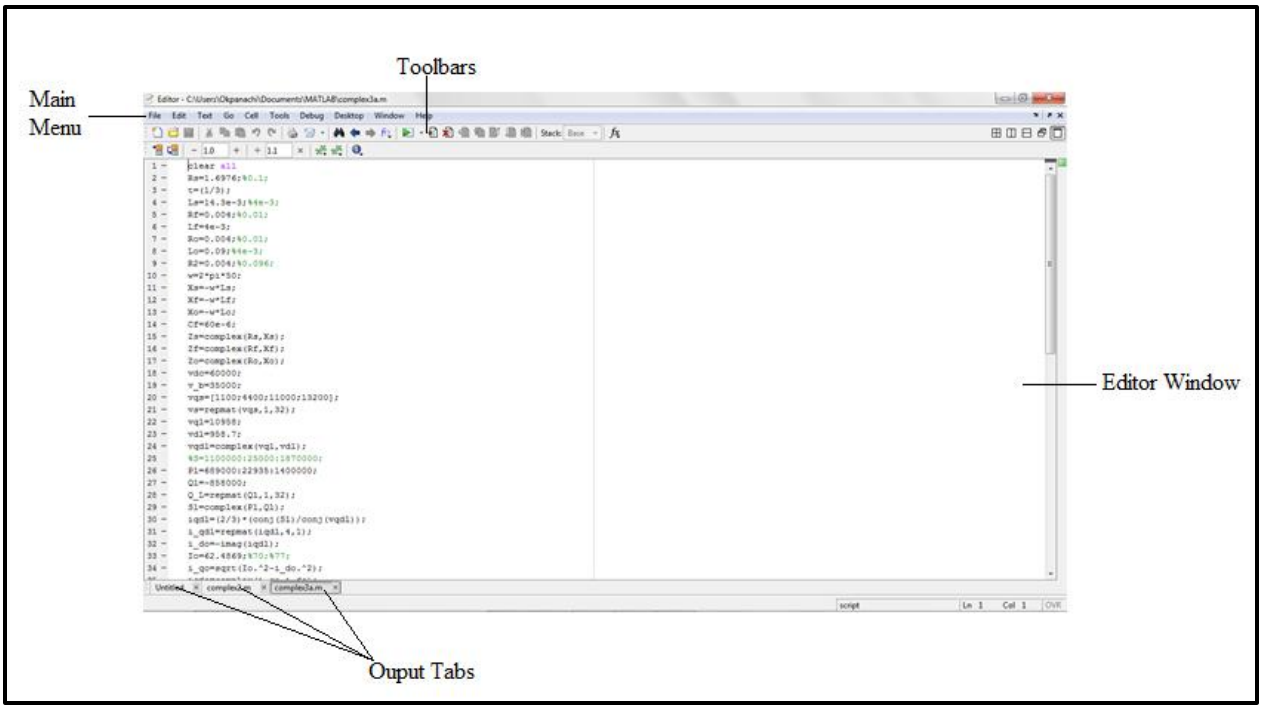


Figure 3.1: MATLAB M- File Editor Interface (Version 9)

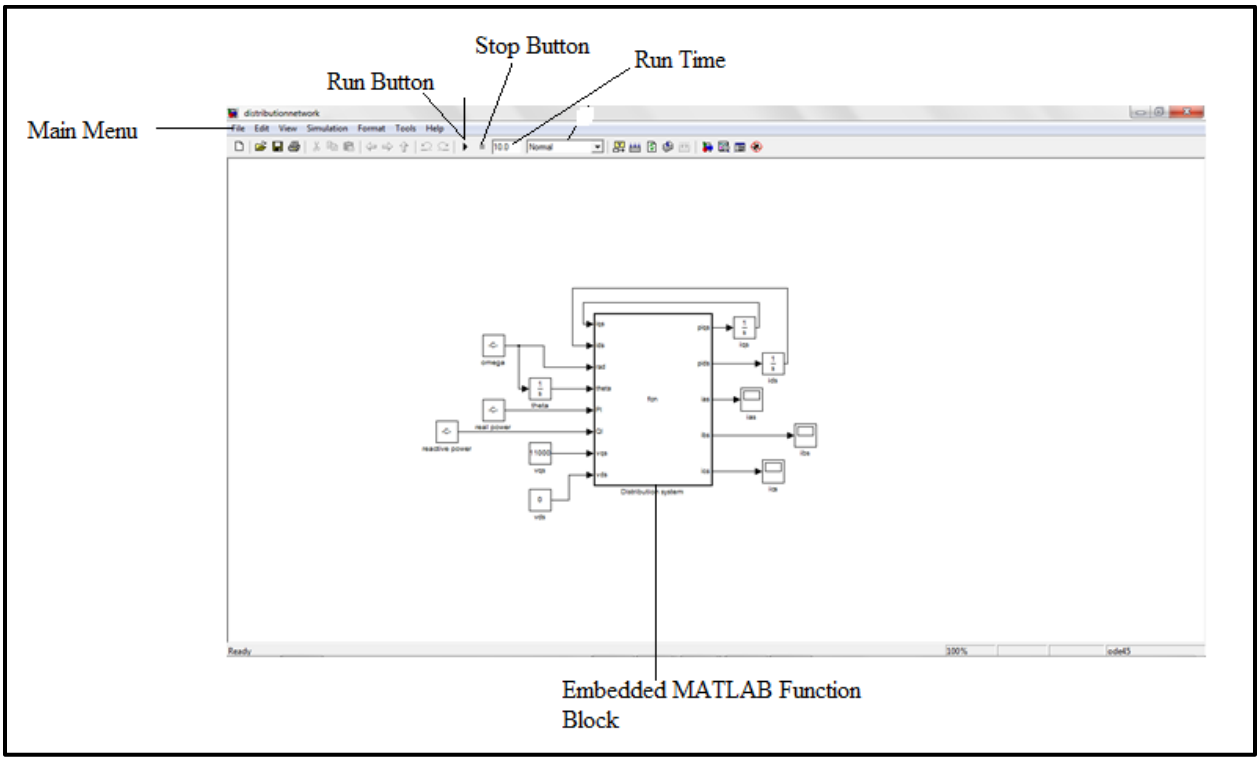


Figure 3.2: Simulink Interface for Simulation

3.5 Methodology

The following steps have been followed for the research:

(i) A general mathematical dynamic model of the UPQC and PV-BESS in the two modes of operation, that is, interconnected and islanding modes was developed

(ii) The steady state model of the system for voltage sag, voltage swell, interruption/loss of supply and reactive power compensation was developed

(iii) Comparison of the performance of the system with the PV-BESS connected with the performance without the PV-BESS to observe the power quality enhancement derived by connecting the PV-BESS.

(iv)Validation of system performance using data of the load demand pattern on 11kV Gaskiya primary distribution feeder in Zaria and that of the solar insolation in Zaria was carried out.

3.5.1 Modes of Operation

The system operates in two modes

i. Interconnected mode: when the PV/BESS supplies power to load and source shown in Figure 3.3

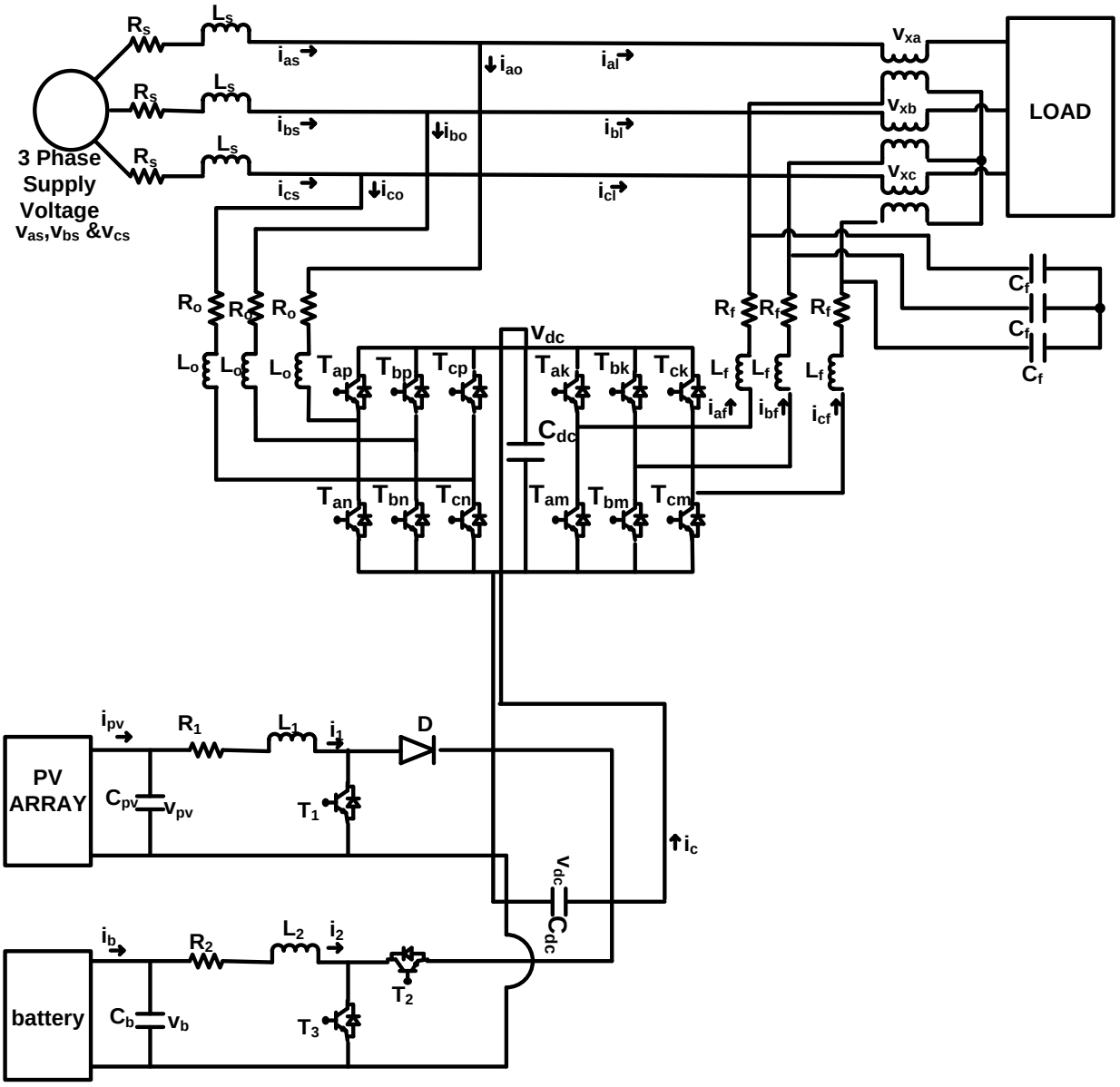


Figure 3.3 Detailed Configuration of the UPQC with PV/BESS Deployed on a Distribution System.

Figure 3.4 shows the details of switches on the system which has been excluded from Figure 3.3 for lack of space. It is the operation of these switches that result into any one of the two possibilities in the islanding mode

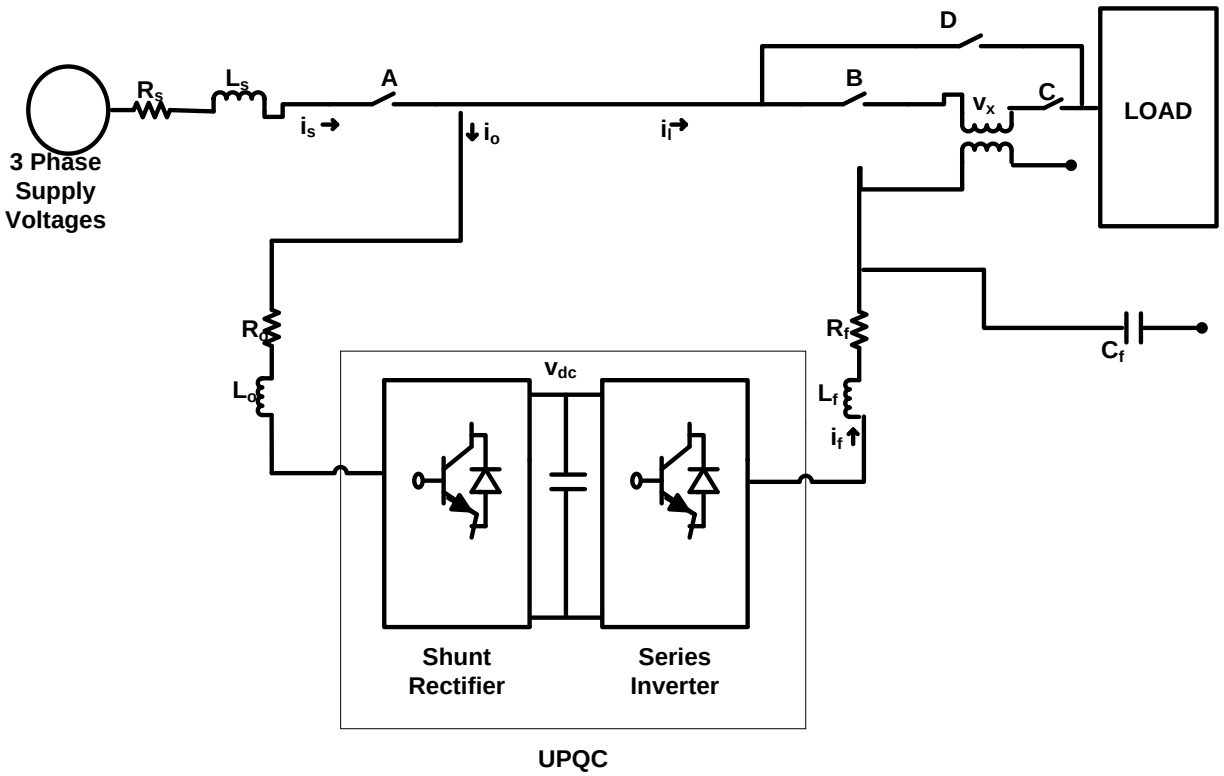


Figure 3.4: Line Diagram of the UPQC with details of Switches.

In the interconnected mode, all the switches are closed except switch D which is opened. The first possibility in the islanding mode shown in Figure 3.5 is obtained by opening switch A, B and C and closing switch D only. The second possibility shown in Figure 3.6 is obtained by opening switches A and D, closing C and shutting B.

ii. Islanding mode: where the source voltage is interrupted and the PV/BESS provides the load power separately. As shown in Figure 3.4 there are two possibilities in this mode. In possibility A, shown in detail in Figure 3.5, power is conveyed to the load through the shunt converter. In possibility B, shown in detail in Figure 3.6, power is conveyed to the load through the series inverter.

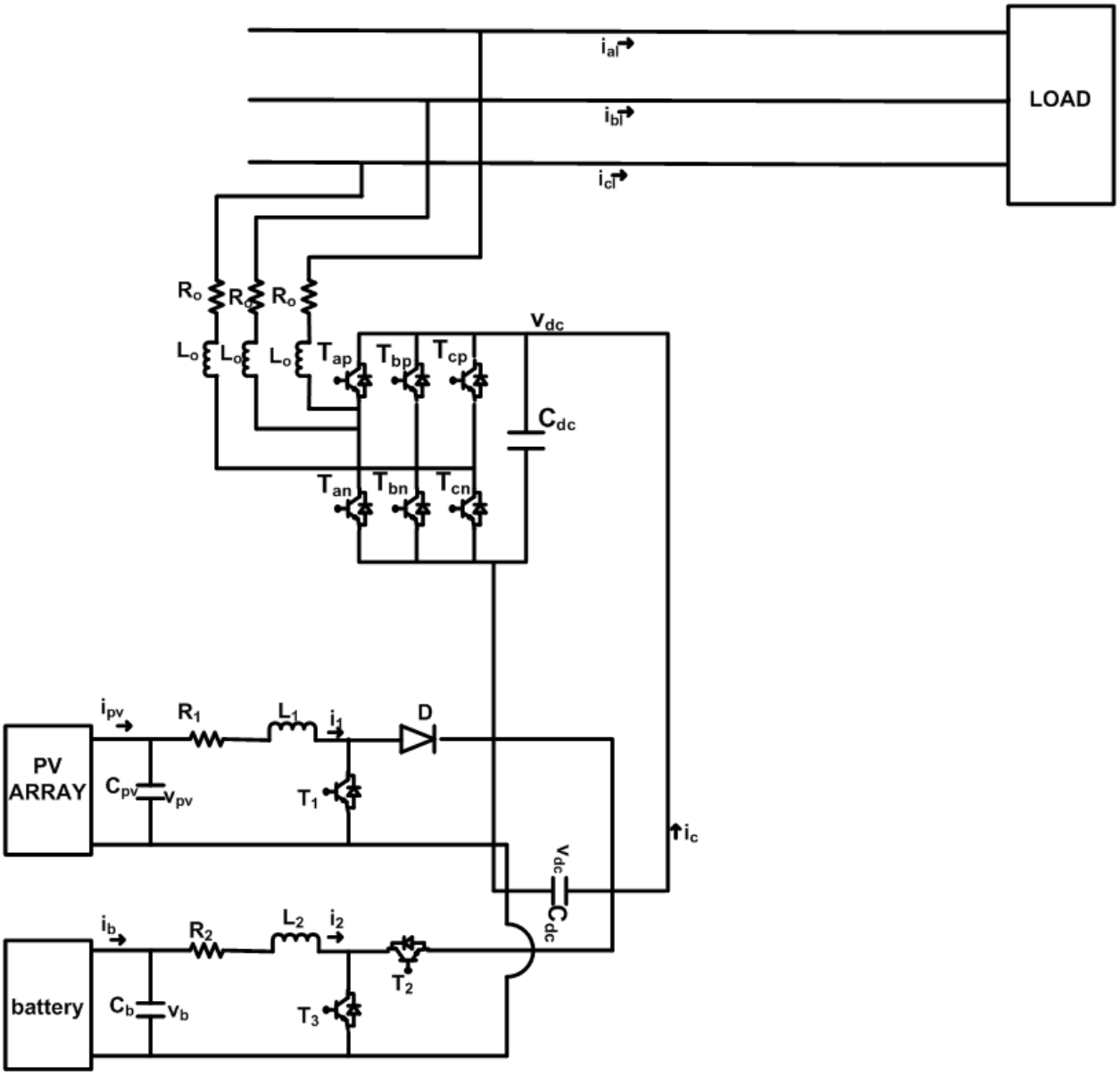


Figure 3.5 Islanding Mode: A Possible Implementation

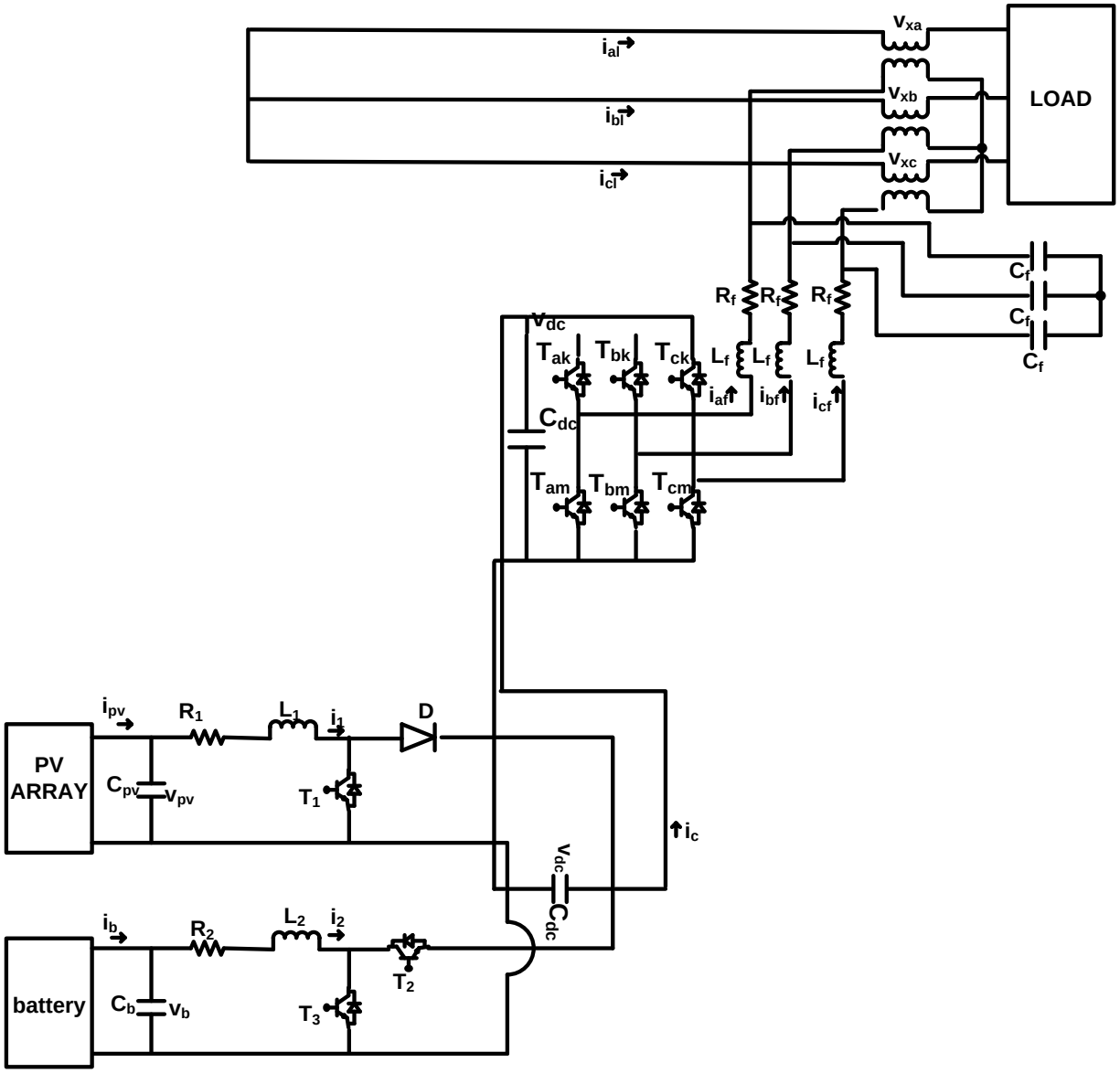


Figure 3.6 Islanding Mode: A Second Possible Implementation

3.6 Conclusion

The materials used and method adopted for this research has been presented in this chapter. MATLAB/Simulink is shown to be sufficient for the purpose of the analysis carried out in this work. The chapter also shows and describes the data used for the work. The manner in which the

data has been collected was described and a discussion of the adequacy of the data for observing the expected behavior of the system is given.

CHAPTER FOUR

MODEL DERIVATIONS AND DESIGN CONSIDERATIONS

4.1 Introduction

In this chapter, the derivation of the system model is done. First, in the physical reference frame and then transformed to the q-d-o reference frame using reference frame transformation described in Section 2.2.4. The transformed equations are then converted to their complex forms. These steps are aimed at reducing the rigor in analyzing the system which is otherwise very involving and cumbersome and also to aid understanding of the design considerations. The converter switching function which was described in Section 2.2.4 has been used for the four converters in the system, to obtain the converter models. This method has the advantage that it is readily amenable to various modulation techniques.

4.2 Model Derivations in a-b-c: Interconnected Mode

The model derivations are presented sub-component by sub-component to aid understanding of the process. In Section 4.2.8, the entire system model is put together and subsequently the transformation is done. Note: in the derivations that follow that, —.

4.2.1 Model of the Distribution system

The circuit diagram of the three phase distribution network showing the influence of the UPQC is provided in Figure 4.1

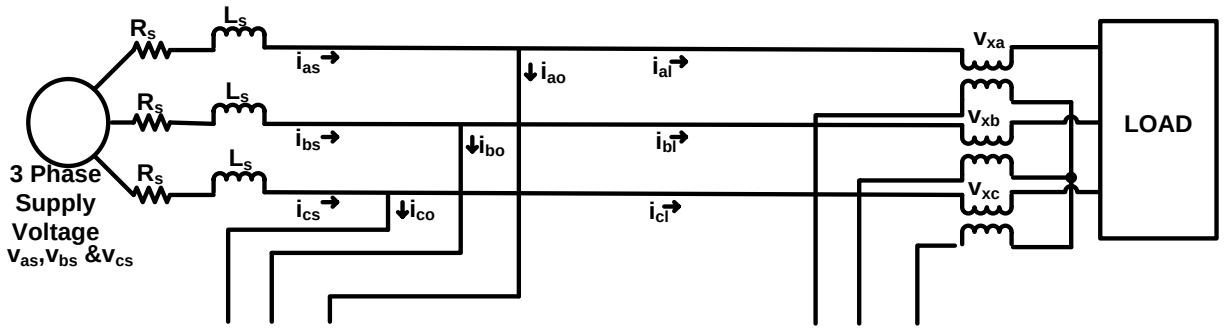


Figure 4.1 Distribution Network Showing the Influence of the UPQC.

From Figure 4.1, using KVL and KCL:

(4.1)

(4.2)

(4.3)

(4.4)

(4.5)

(4.6)

Where, are the supply voltages. are the supply currents, are voltages injected by the series inverter, are load currents, are load voltages and are currents drawn by the rectifier.

4.2.2 Model of Rectifier

Figure 4.2 shows the rectifier connected to the distribution network

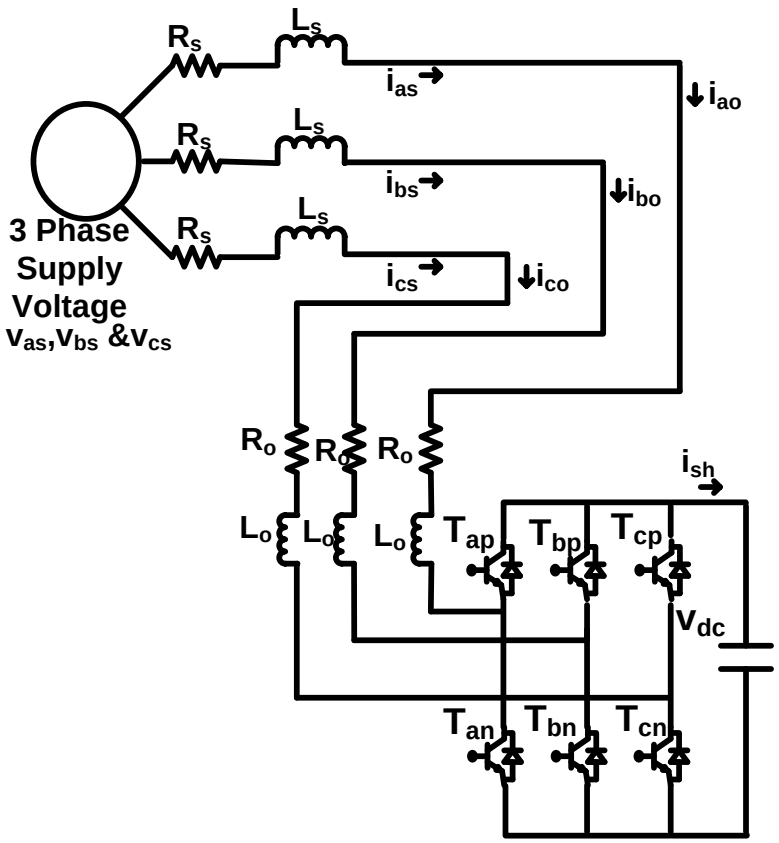


Figure 4.2 Rectifier Connected to the Distribution Network.

From Figure 4.2,

Let be the switching functions for respectively and be the switching function for respectively.

Applying KVL, KCL and averaging technique

— (4.7)

— (4.8)

— (4.9)

(4.10)

4.2.3 Model of Inverter

Figure 4.3 shows the inverter connected to the distribution network through the series transformer

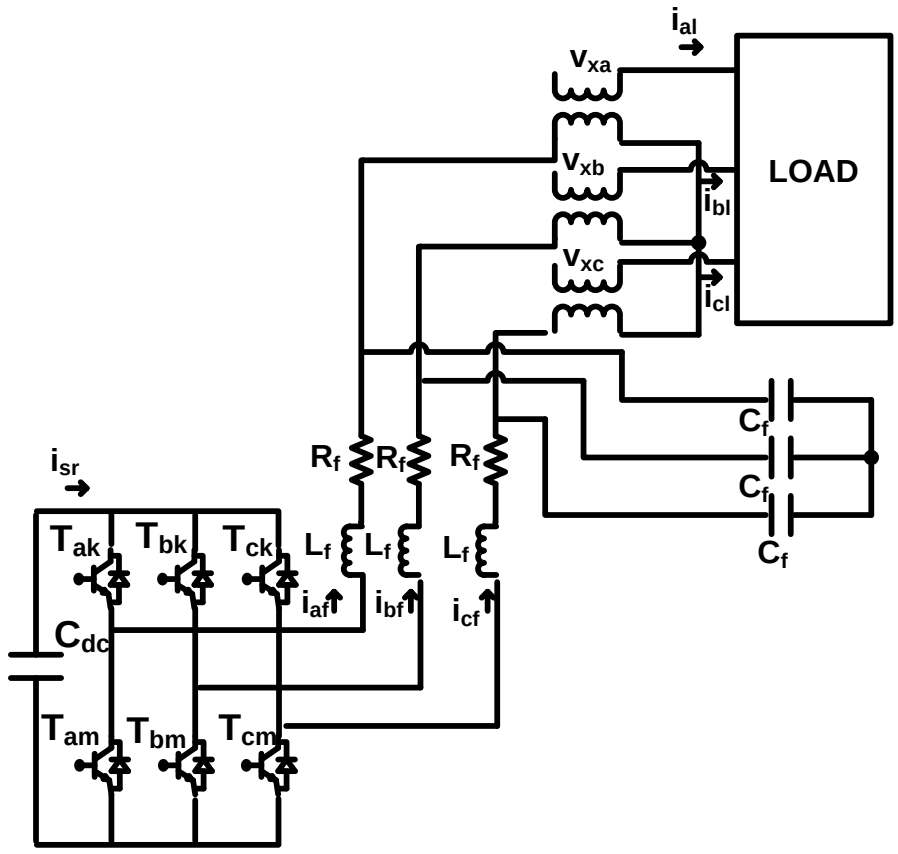


Figure 4.3 Inverter Connected to the Distribution Network

From Figure 4.3, Let be the switching functions for respectively and be the switching function for respectively and the turns ratio of the series transformer. From KVL, KCL and averaging technique

— – (4.11)

— – (4.12)

— – (4.13)

(4.14)

Filter capacitor equations:

— (4.15)

— (4.16)

— (4.17)

4.2.4 Model of the DC-DC Converters

There are two dc-dc converters in the system. One connected to the output of the PV panel and the other to the battery bank. Figure 4.4 shows the dc-dc converter connected to the PV panel while Figure 4.5 shows the dc-dc converter connected to the battery output.

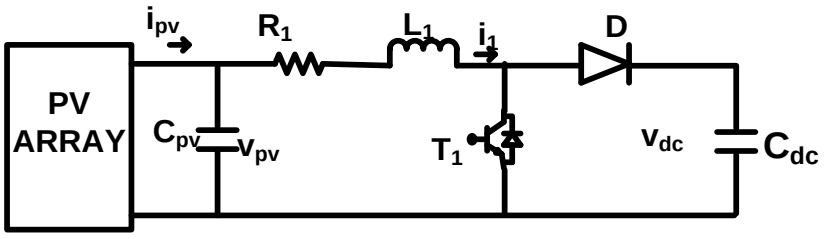


Figure 4.4 Boost DC-DC Converter at the Output of the PV Cells.

Let s_1 be the switching function for T_1 and S_D the switching function for D.

(4.18)

(4.19)

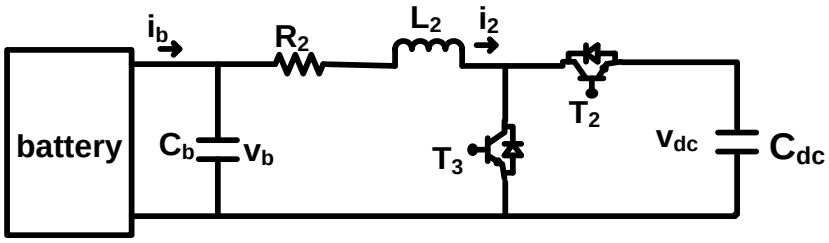


Figure 4.5 Boost DC-DC Converter at the Output of the Battery Bank

From Figure 4.5, let s_2 be the switching function for T_2 and s_3 the switching function for T_3.

(4.20)

(4.21)

4.2.5 Model of the DC Link

The DC link circuit is shown in Figure 4.6. It interconnects the rectifier, inverter and the combination of the PV and BESS.

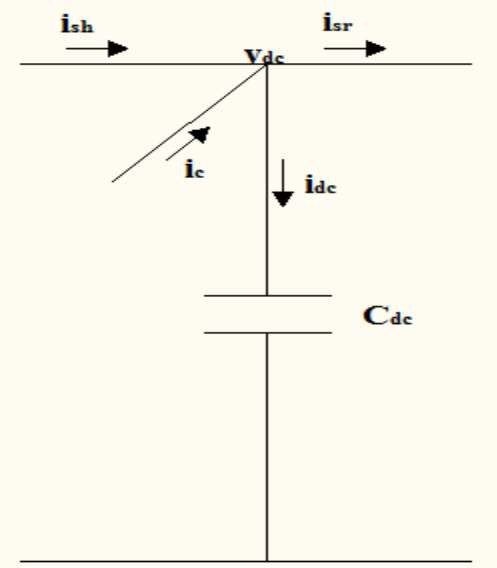


Figure 4.6 DC link Circuits.

From Figure 4.6,

Applying KCL,

(4.22)

Substituting equations (4.10) and (4.14) into (4.22)

(4.23)

(4.24)

4.2.6 Non- Linear Model of PV

The non-linear models of PV are given as (Hossien, 2012):

——— (4.25)

— (4.26)

4.2.7 Dynamic Model of Battery

Figure 4.7 shows the structure of the battery. The dynamic model is given by equation (4.27) to (4.29) (Hossien, 2012).

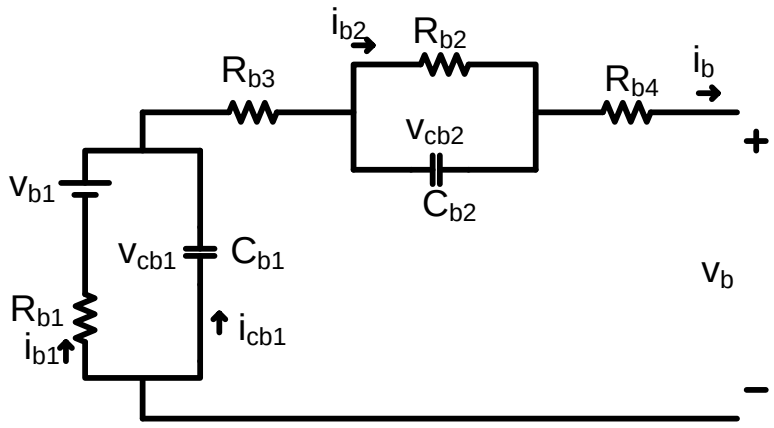


Figure 4.7 Battery Structure

(4.27)

(4.28)

(4.29)

4.2.8 Model of the Whole System

The model of the entire system is given by equations 4.1 to 4.29. The detailed derivations of these models are shown in Appendix A. Subsequently, in the next section, the model is transformed into the q-d-o reference frame.

4.3 Model of the System in q-d-o: Interconnected Mode

Defining: and assuming a three phase balance system, equations (4.1) to (4.17) and (4.22) are transformed using reference frame transformation to give:

(4.29)

(4.30)

(4.31)

(4.32)

(4.33)

(4.34)

(4.35)

(4.36)

(4.37)

(4.38)

(4.39)

The full derivation is shown in Appendix B.

4.4 Model of the System in Complex Forms: Interconnected Mode

The steady state equations are obtained from equations (4.29) to (4.39) by setting where is a constant. However, because of the number of equations involved, obtaining a solution is still a very cumbersome process. The complex forms of the equations are therefore derived for the steady state analysis in Section 5.2. They are as follows:

(4.40)

(4.41)

(4.42)

(4.43)

(4.44)

(4.45)

Where the following definitions have been made:

Details of the derivations are provided in Appendix C.

Additionally, since the Power demand of the load is known,

(4.46)

Also, in order to achieve the objective of making the source to supply only the active power requirement of the load (i.e.),

(4.47)

4.5 Model of the System in Islanding Mode

The islanding mode refers to the situation where the source is interrupted and a part of the load power requirement is supplied by the PV and energy storage alone. There are two possible configurations for this mode. The two configurations are referred to here as possibility A and possibility B respectively.

4.5.1 Possibility A

This possibility in the islanding mode is shown in Figure 3.5

Model in a-b-c:

Applying KVL, KCL and averaging technique,

— (4.48)

— (4.49)

— (4.50)

(4.51)

(4.52)

(4.53)

(4.54)

(4.55)

(4.56)

Model in q-d-o:

— (4.57)

— (4.58)

– (4.59)

(4.60)

4.5.2 Possibility B:

Possibility B in the Islanding mode, is shown in Figure 3.6

Model in a-b-c:

— – (4.61)

— – (4.62)

— – (4.63)

— (4.64)

— (4.65)

— (4.66)

(4.67)

(4.68)

(4.69)

(4.70)

(4.71)

(4.72)

Model in q-d-o:

(4.73)

(4.74)

(4.75)

(4.76)

(4.77)

4.6 Design Considerations

The studied system is designed for the 11kV PHCN Gaskiya feeder. Knowledge of the load profile of this feeder under normal operating conditions bas been obtained as given in Table 3.1.

4.6.1 Distribution Network

Route length of the conductor is .

Cross sectional area

Resistivity of Aluminum

It is known that:

(4.78)

Taking the impedance of the conductor to be lumped at the middle

Assuming an X/R ratio of 5 then

4.6.2 Switching Devices ON Resistance

From Table 2.1 taking the least resistance for the switching device,

4.6.3 Inverter LC Filter

There is a need for a Low Pass Filter (LPF) at the output of the series inverter to suppress the harmonics generated by the switching actions of the inverter

For an ideal voltage source at the cut- off frequency (Bijoyprakash, 2012):

(4.79)

The filter output to input voltage harmonics must be less than 3% (Bijoyprakash, 2012):

Hence or

(4.80)

Choosing

Then

4.6.4 DC-DC Converter Inductor Filter

For the PV solar panel system and the connected dc-dc converter, the voltage at maximum power has been used. For each solar insolation used, the voltage at maximum power is determined from the plot of the optimum voltage for given solar radiations. The voltage for optimum power is then used to calculate the current using equation 4.25. The duty ratio of the connected dc-dc converter is thereby fixed at three discrete values determined by the input optimal voltages for the chosen solar insolation and the design voltage of the dc link. Figure 4.8 gives a detail view of events at the output of the dc-dc converter.

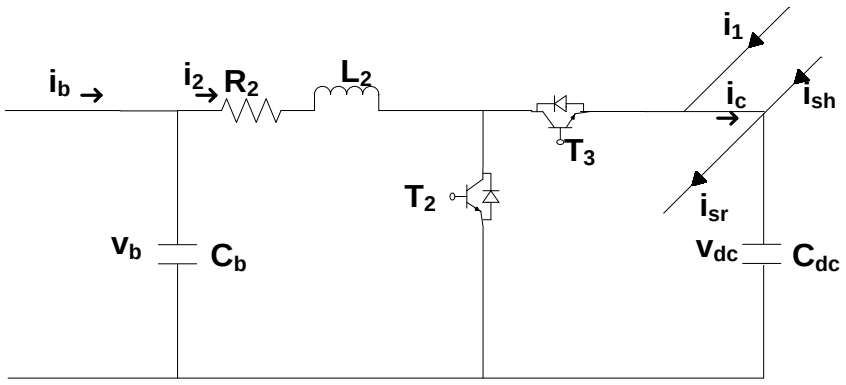


Figure 4.8 DC-DC Converter Showing Details of Interconnection with Other Parts of the System

(4.81)

. Also,

(4.82)

The capacitor can be obtained from the equation below (Muhammad, 2005):

(4.83)

is the frequency of the switching pulses.

(4.84)

(4.85)

Note:

4.6.5 Active Power Balance

The active power balance can be stated as:

(4.86)

Where P_s is the supply active power, P_l is the active power demand of the load and $P_{PV/BESS}$ is the power from the PV cells and batteries

That is for any operating condition (whether sag, swell or normal condition) and at any instance of time, the algebraic sum of the active power from the supply and the active power of the load and the power from the PV/BESS is equal to zero. Hence the PV/BESS sub system can only be

designed with a capacity to supply the balance of power between the supply and the load. The immediate consequence of this design criterion is that when there is loss of power supply, the PV/BESS system might only be able to supply only a part of the load requirement. Alternatively, since the PV system is modular, it can be designed such that its available power is adjustable between the two modes of operation which are, islanding and interconnected mode. This however, would lead to a lot of waste as there would be available redundant power during the interconnected mode which is contrary to the philosophy of the research. Hence the entire system has been designed so that the PV/BESS system only carters for a part of the load power requirement in the islanding mode.

The load apparent power varies from 1.1MVA to 1.87MVA

For a load reactive power of 0.858MVAR lagging

(4.87)

Therefore, real power of the load will vary from 0.688MW to 1.66MW

At normal operation (i.e.) and for maximum load (i.e.)

Now for , if the supply current is maintained at a rated maximum of 100A (for a load value of 1.4MW), then the available power from the supply will be 0.166MW. The real power maximum deficit to be supplied by the PV/BESS is 1.66MW-0.166MW=1.4940MW.

Of this requirement, let the PV supply 60% while the balance goes to the battery.

That is,

P_{PV} = 0.8964MW

And P_B = 0.5976MW.

Where P_{PV} is the Power from the PV and P_B is the Power from the batteries.

To supply this power for a dc link voltage of 60kV, and

(4.88)

Taking a nominal PV system operating voltage of 30kV

For this condition,

are calculated from equation 4.41 as:

And from equation 4.42 as:

To find the values of first the values of are obtained then

For and maximum load power condition which has been used so far in the calculation, are obtained from equation 4.40 as:

While are gotten from equation 4.44 as:

Hence, are calculated from equation 4.43 as 0.1122 and 0.0036 respectively.

These values will now help to determine . Recall:

– (4.89)

– (4.90)

Therefore,

Equation (4.82) is for the duty ratio of the battery dc-dc converter. The same equation for the PV cells dc-dc converter is as given:

_____ (4.91)

At full load, for , battery power is maximum and equal to 0.5976MW. From which can be calculated using equation 4.92

(4.92)

The equivalent of equation (4.81) for the dc-dc converter connected to the solar PV cells is:

_____ (4.93)

for the solar PV power and the design voltage of 30kV, the output current at the terminal of the solar PV cells is 29.88Amps. These two values i.e. terminal voltage and terminal current of the PV cells help to determine the minimum number of PV cells in series and the minimum number of PV cells in parallel. For a PV cell ON voltage of 0.5V number of cells in series is

.

And for the PV current of 29.88Amps

Number of cells in parallel

.

Using equation 4.84 for the PV dc-dc converter and defining a ripple factor of 2%,

In order to be able to perform the analysis, some assumptions have been made. For instance a design voltage of 30kV was used for the PV cells. However in actual effect, the PV cells are operated at point of maximum power and the voltage for maximum power used. Table 4.1 gives a summary of the actual system parameters used for the studies.

Table 4.1 System Parameters

R_2	4mΩ	R_f	4mΩ
L_2	0.1246H	L_f	4mH
R_1	4mΩ	C_f	60μF
L_1	0.1246H	R_s	1.6976Ω
R_o	4mΩ	L_s	14.3mH
L_o	0.09H	n_s	44000
		n_p	1800

4.6.6 Simulation Equations

The equations for simulation have been obtained by manipulating equations 4.1 to 4.28 in Section 4.2. They are as follows:

For the Inverter:

— – (4.94)

— – (4.95)

— – (4.96)

Where,

— (4.98)

— (4.99)

— (4.100)

Also,

— (4.101)

— (4.102)

— (4.103)

(4.104)

For the Rectifier:

—— (4.105)

—— (4.106)

—— (4.107)

Where,

— (4.108)

— (4.109)

— (4.110)

For Battery DC-DC Converter:

— (4.111)

— (4.112)

4.7 Conclusion

The model derivation and some design considerations have been presented in this Chapter. A compact model of the system was achieved by first transforming the models developed in the physical reference frame to the q-d-o reference frame to remove time varying variables. The transformed models are then put in their complex forms to reduce the number of equations. Each of the forms of the derived model will be used for various analyses in Chapter Five. Also in this Chapter, some design criteria were used and certain assumptions made to determine parameters of the system.

CHAPTER FIVE

RESULTS AND ANALYSIS

5.1 Introduction

The steady state analysis of the system under different operating conditions and the Open-Loop, Large-Signal Simulation study is carried out in this chapter. The developed model and system parameters have been employed in this Chapter. The simulation studies have been done using the full order model (involving the PWM generated switching functions).

5.2 Steady State Analysis

A sinusoidal function is said to be in steady state when the amplitude, frequency and phase angle are constant. Steady state therefore is the state of the system in which all transient and disturbances have been cleared. The beauty of the reference frame transformation which has been used to derive the system model is that sinusoidal time varying voltages and currents become constant dc quantities whose values depend on the amplitude and initial angle alone of the original a-b-c reference frame signals. At steady state, the differential equations become algebraic equations (since —). The equations are then solved simultaneously rather than embarking on the cumbersome process of solving several differential equations.

From the hourly demand on the 11kV Gaskiya feeder, the least apparent power demand is 1100kVA (at I=100A) while the maximum apparent power demanded is 1870kVA (at I=170A). These two limits form the boundaries of the study.

Where is the rated supply voltage.

is varied from 0.4 of its nominal value to 1.4 of this value, specifying 60% sag to a 40% swell condition. This initial range of variation is chosen to ensure that the series inverter does not go into over modulation pending when the critical dc link capacitor voltage is determined. It is important to note however that the aim is to compensate for interruption in the interconnected mode which will imply that a range with minimum boundary value of $\gamma = 0.1$ will be used.

Hence (5.1)

Where

Also,

Now solving equations 4.40 to 4.47 the following equations are obtained:

(5.2)

— (5.3)

(5.4)

— (5.5)

(5.6)

(5.7)

Also, let

(5.8)

(5.9)

(5.10)

(5.11)

(5.12)

A MATLAB script was written for the solution of this problem according to the flow charts shown under the respective sub-sections for different studies carried out.

5.2.1 UPQC on Distribution Network

This section shows the results of installing the UPQC alone on the distribution network. Figure 5.1 shows the flow chart for these studies. A program listing has been attached in Appendix F

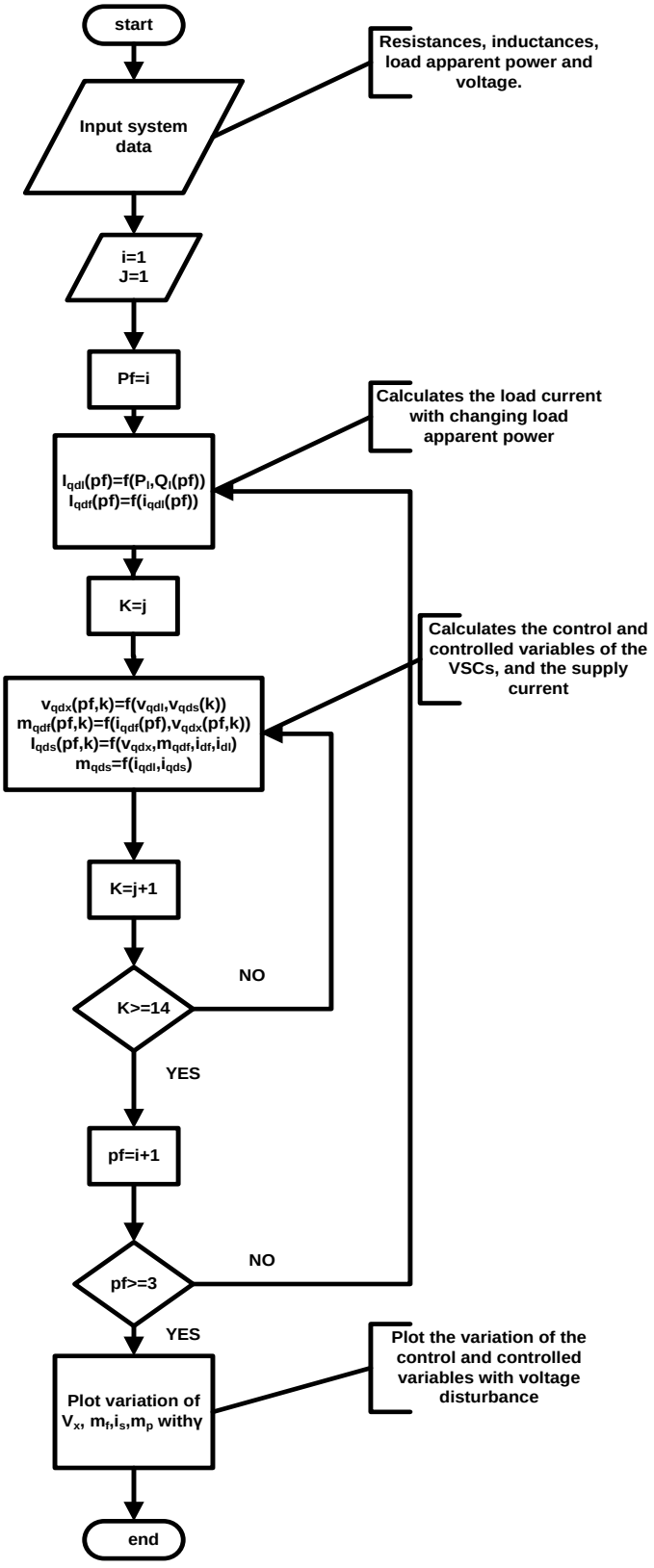


Figure 5.1: Flow Chart for UPQC with no Limitation

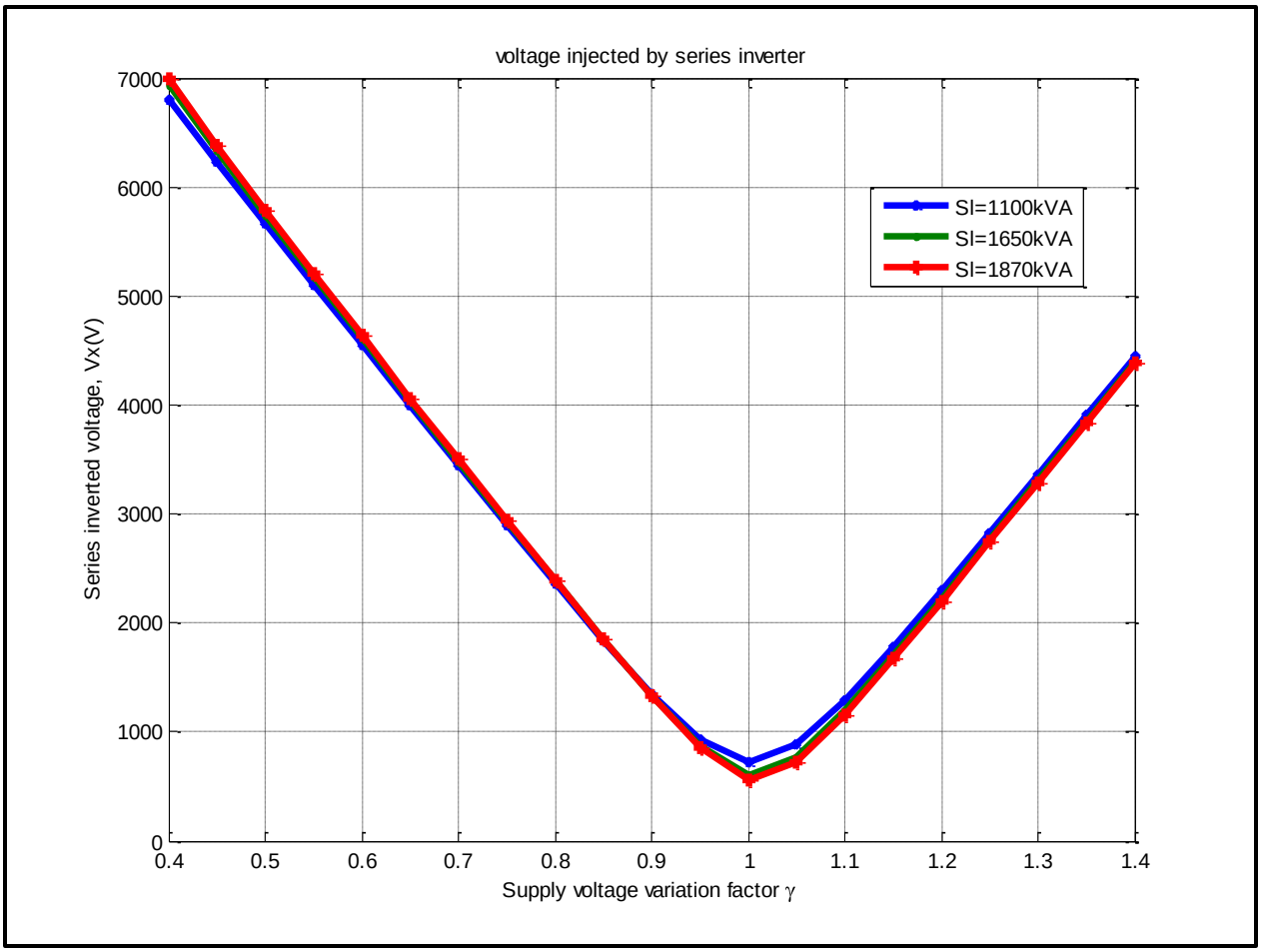


Figure 5.2 Voltage Injected by Series Inverter to Regulate Load Voltage

Figure 5.2 is obtained from equation (5.2) and equation (5.8). It shows the peak value of the voltage injected by the series inverter to maintain the load voltage constant as the supply voltage varies from 0.4 of its value to 1.4 of its value. The change in direction at $\gamma>1$ shows voltage injected in the opposite direction. Hence a voltage is injected during voltage sag such that the sum of the supply voltage and the injected voltage of the series inverter regulates the load voltage at rated value. The values of V_x from $\gamma>1$ shows the peak value of voltage injected by the series transformer when there is a swell at the supply side. These injected voltages subtract from the supply voltage also keeping the load voltage at rated value. The injected voltage at $\gamma=1$, has to do with the difference in angle between the supply and the load voltages. In other words, when

there is voltage sag, the UPQC supplies the extra power needed by the load and when there is swell, the UPQC absorbs the extra power from the source through the series inverter and feeds it back to the source through the shunt inverter. It is important to note that the voltage values shown occur at the secondary of the series transformer connected to the series inverter. This pattern is also observed in the current drawn by the series inverter shown in Figure 5.3.

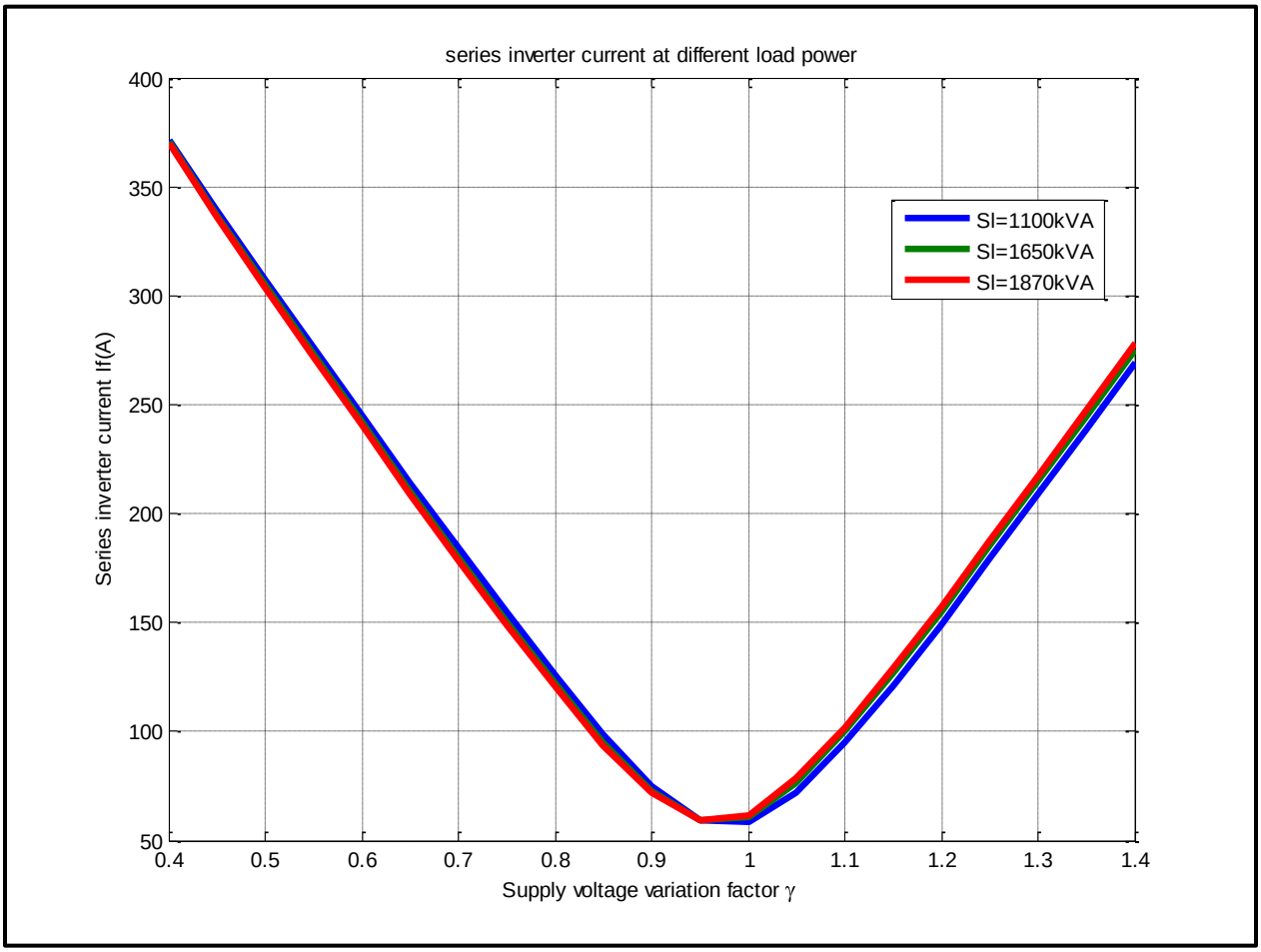


Figure 5.3 Series Inverter Current at Different Load Power.

Figure 5.3 is obtained from equation (5.4) and equation (5.10). It shows the peak value of current flowing through the series inverter as the supply voltage is varied. The power supplied is maximum with the most sag and reduces gradually as the extent of sag reduces. For the period of

voltage swell,$\gamma > 1$, the inverter absorbs the excess power from the supply and feeds it back through the shunt rectifier.

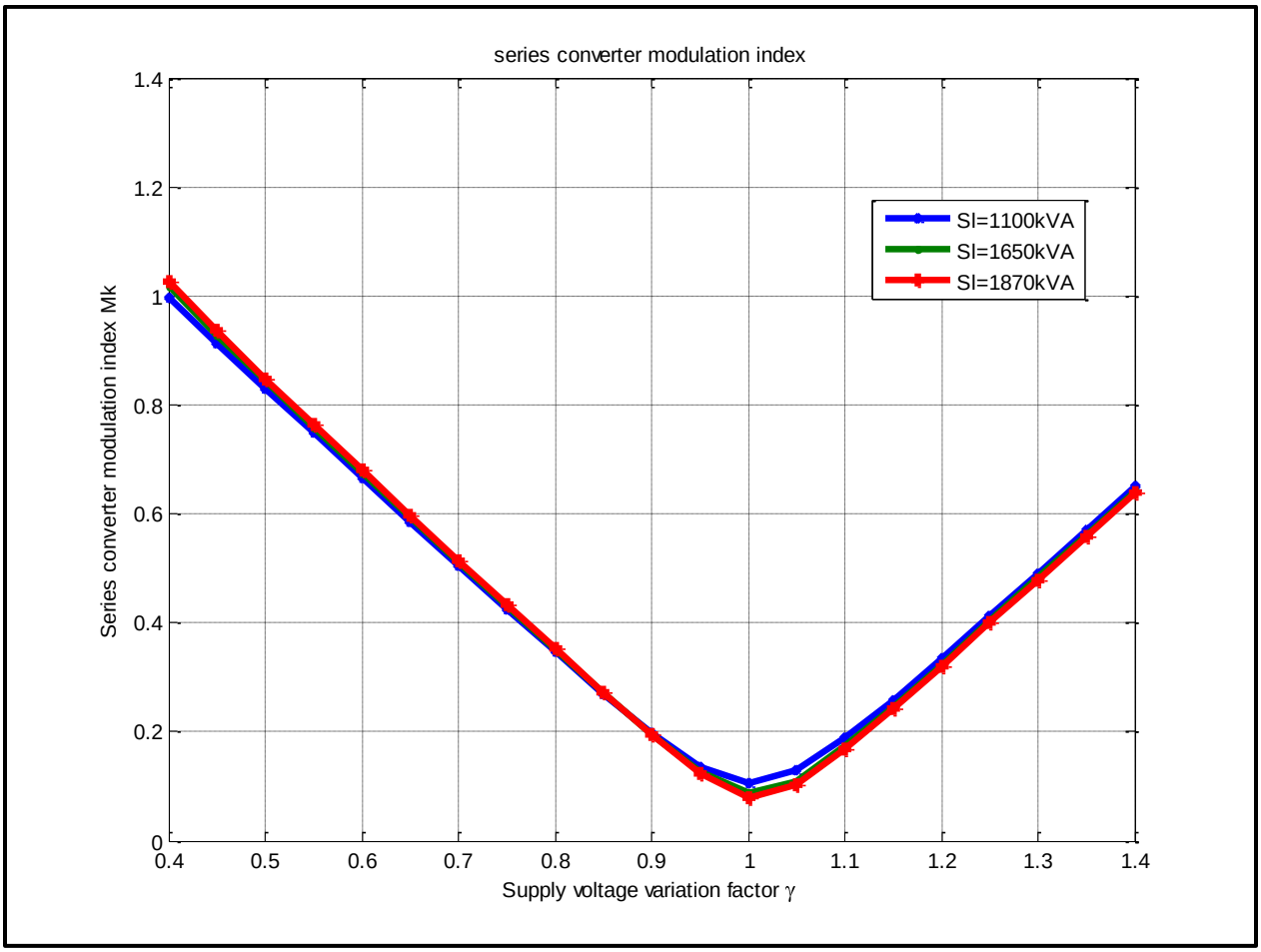


Figure 5.4 Series Inverter Modulation Index with Variation in Supply Voltage at different Load Power

Figure 5.4 shows the modulation index of the series inverter for the stated conditions. It has been obtained from equation (5.5) and equation (5.11). The plot gives the value of the modulation indices for the stated conditions if the load voltage must remain at rated value. For instance, at sag of $\gamma = 0.9$, for the load voltage to be regulated at its rated value, the peak value of the modulation index of the series inverter should be 0.2. The little disparity in the three (3) curves

for different load apparent power has to do with the drop in the line. It shows that the voltage drop on the line due to the line impedance is not significant for the given load condition

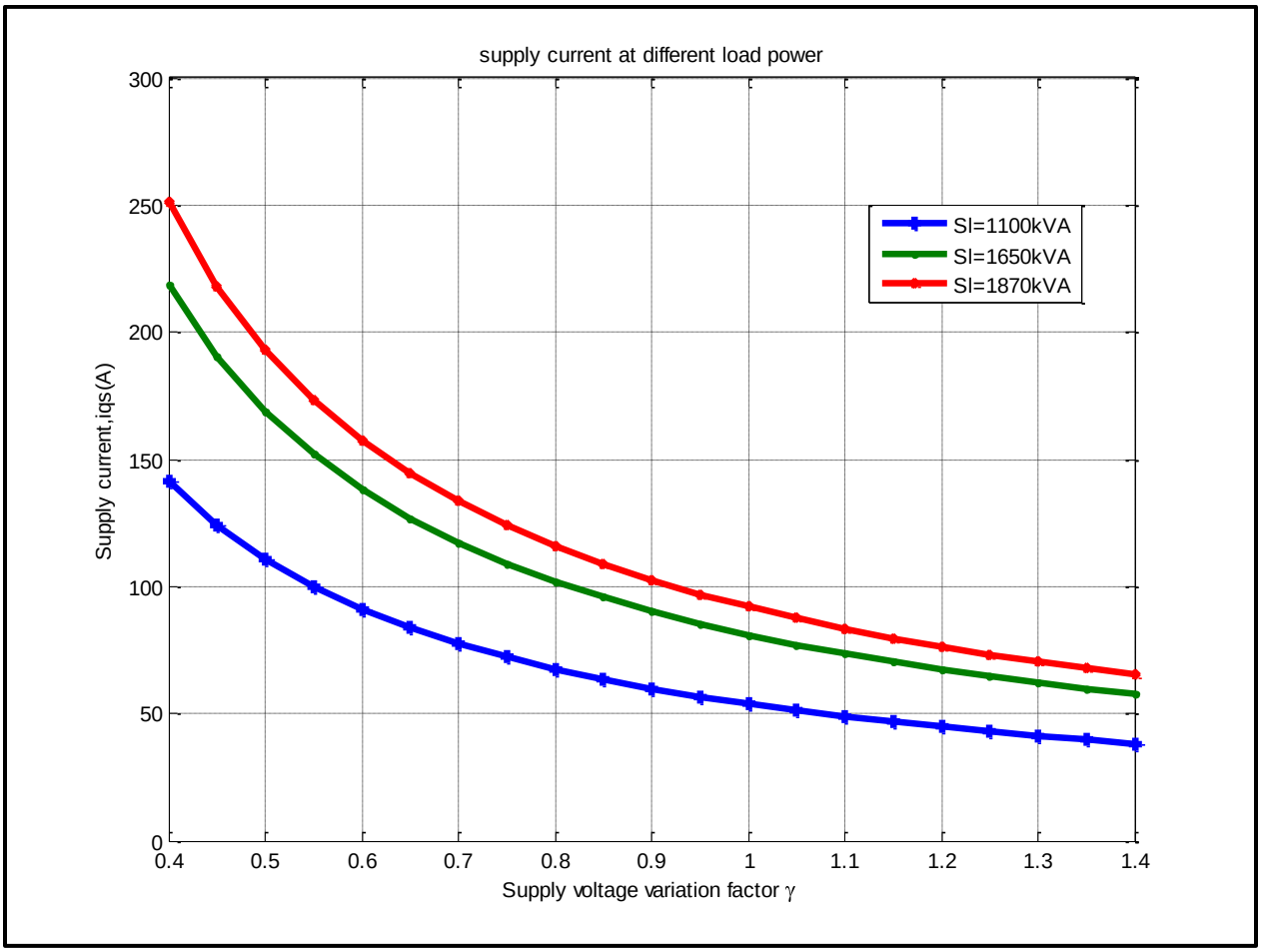


Figure 5.5 Supply Current at Three Different Apparent Power (pf = 0.8)

Figure 5.5 is obtained from equation (5.6). It shows the value of the supply current at three different loads with a power factor of 0.8. From the plots, it is observed that the supply current increases as the load apparent power increases. However, comparing these plots with the values in Table 3.1 shows that this is not connected with the total load power but only the real power of the load. For instance at S_l =1100VA and γ =1, if there was no UPQC the load current should have been about 100A from the data from PHCN. However a value of about 60A is observed in Figure 5.5. This is because the reactive power requirement of the load is supplied by the UPQC

Hence the shift in the plot of supply current at different load apparent powers is due entirely to the average power increase of the load. This condition is made even more obvious when the average power is kept constant and only the reactive power requirement of the load is varied (studied later). For each apparent power, the supply current reduces as the supply voltage increases. This is because load power is constant. The normal supply current occurs at $\gamma = 1$ for each of the load apparent power. For $\gamma < 1$, the supply power increases mildly beyond its value at $\gamma = 1$ and then more rapidly at this extra power flows through the shunt rectifier, the dc link and then through the series inverter where it is supplied to the load so that the load does not notice the decrease in supply voltage. For $\gamma > 1$ the reverse occurs.

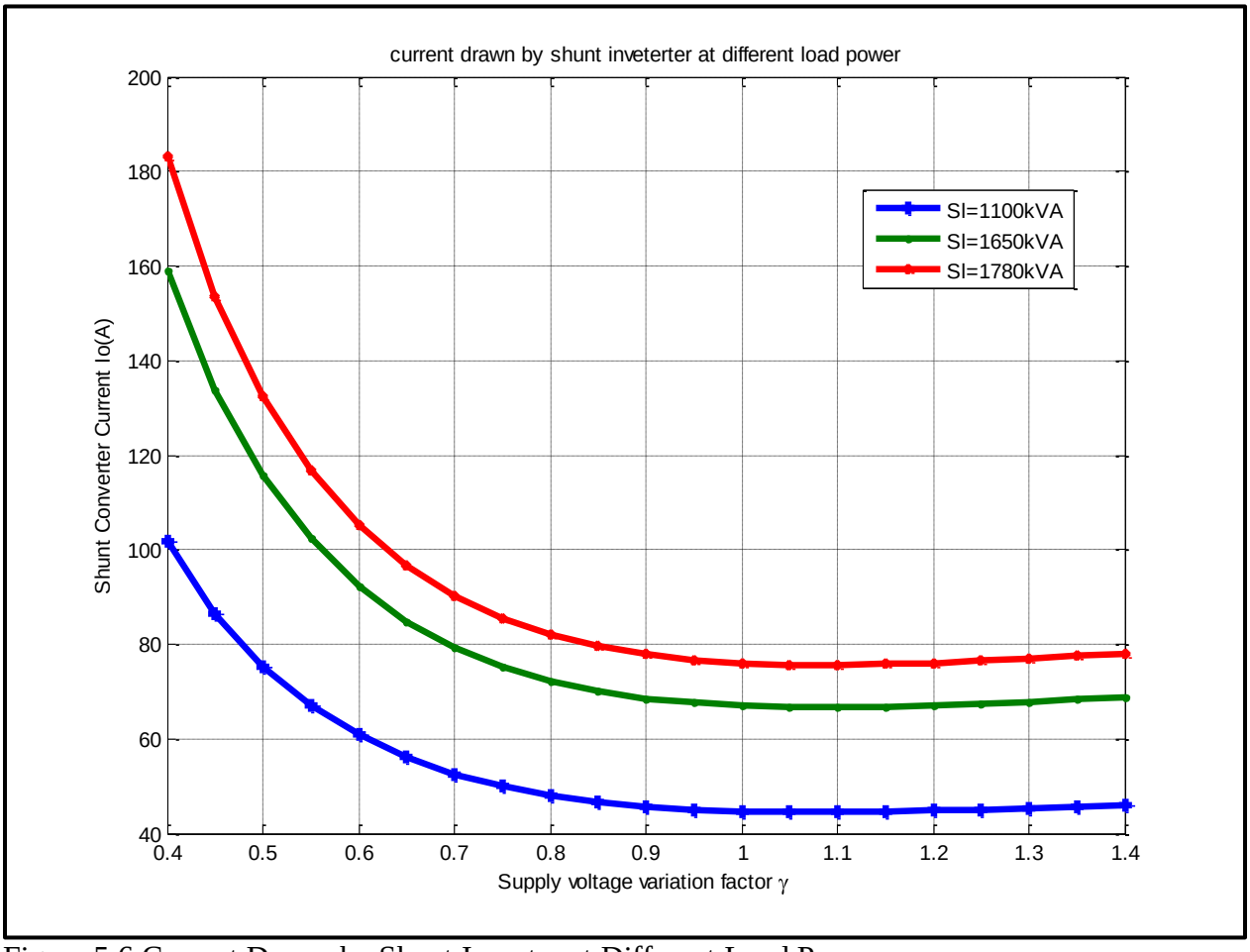


Figure 5.6 Current Drawn by Shunt Inverter at Different Load Power

Figure 5.6 shows the peak value of the current drawn by the shunt inverter for the different load conditions and variations in supply voltage. The plot has been obtained from equation (5.7) and equation (5.12). This current comprises of the component for the load reactive power requirements and that to maintain the real power balance in the system, that is, maintain the dc link voltage at its constant value. Maintaining the dc link voltage constant is necessary because the series inverter supplies real power to the system during voltage sag and absorbs real power from the system during voltage swells. As seen from the plots of Figure 5.6, current drawn increases with increase in the apparent power of the load. Also, for each load apparent power, the current drawn increases rapidly for values of $\gamma < 0.9$. This increase is due to the extra real power drawn from the source to maintain real power balance. However, for $\gamma > 1$ the current flattens and even attempts to rise in the opposite direction. For this region, real power component of the shunt rectifier flows in the opposite direction, that is, the series inverter absorbs the excess power and feed it back to the supply through the shunt rectifier.

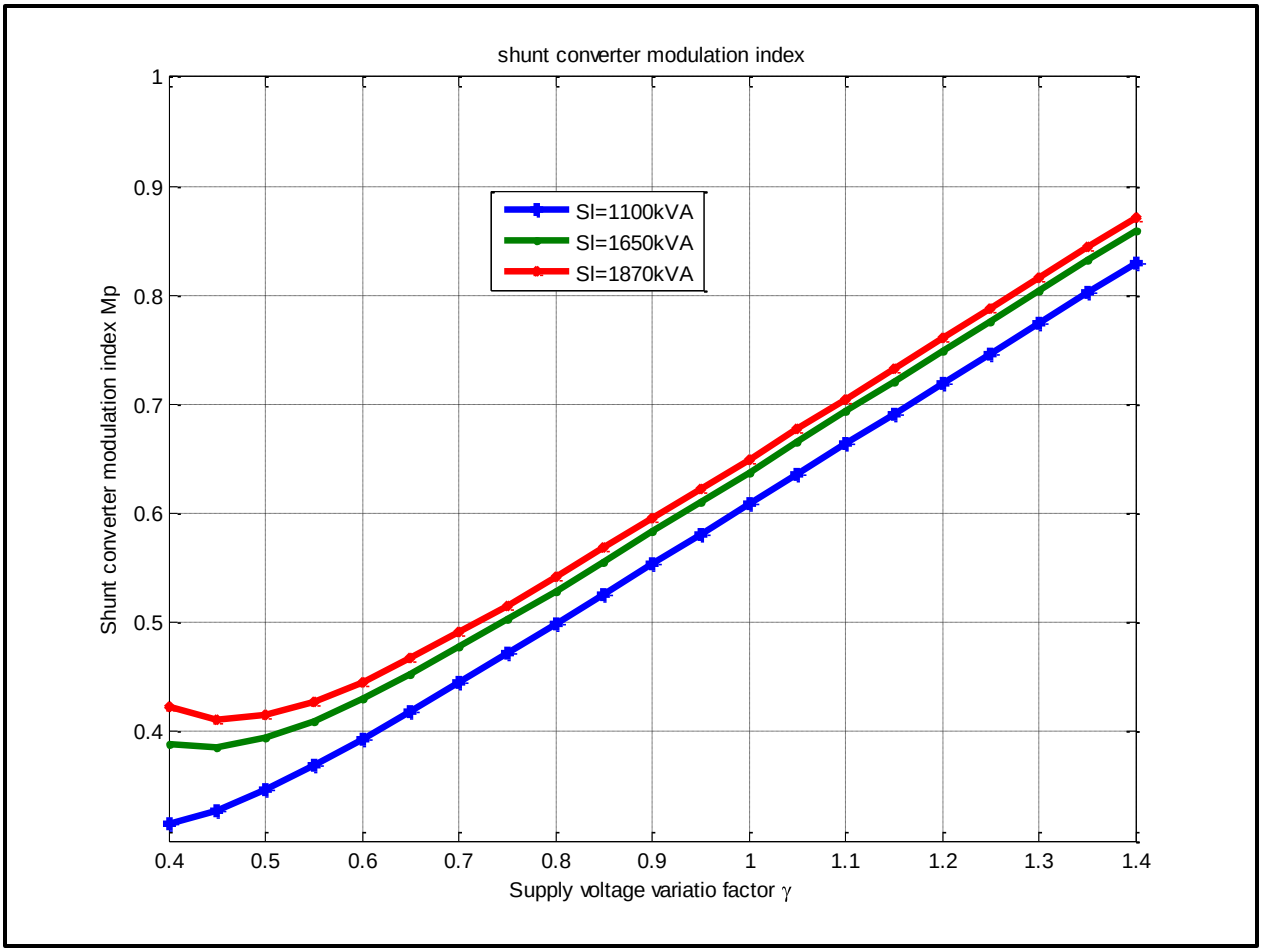


Figure 5.7 Shunt Inverter Modulation Index

Figure 5.7 shows the shunt inverter modulation index at different load power. The plot has been obtained from equation (5.3) and equation (5.9). It gives an indication of the value of the modulation index of the inverter to achieve the objective of compensating load reactive power requirement and maintaining the dc link voltage constant.

Load Reactive Power Compensation: In this study, the Load apparent power requirement is varied at a power factor of 0.8 and at constant supply voltage. The power flows in the system is studied. For these studies, is obtained from equation (4.46) from equation (5.6) and from equation (5.4). The complex powers are calculated as follows:

– (5.13)

– (5.14)

– (5.15)

The flow chart for the study is shown in Figure 5.8

Utility active power = R (S_s)

Utility Reactive power = Im (S_s)

Shunt Inverter active power = R (S_o)

Shunt Inverter reactive power = Im (S_o)

Series Rectifier active power = R (S_f)

Series Rectifier reactive power = Im (S_f)

R (a) is the real part of a

Im (a) is the imaginary part of a.

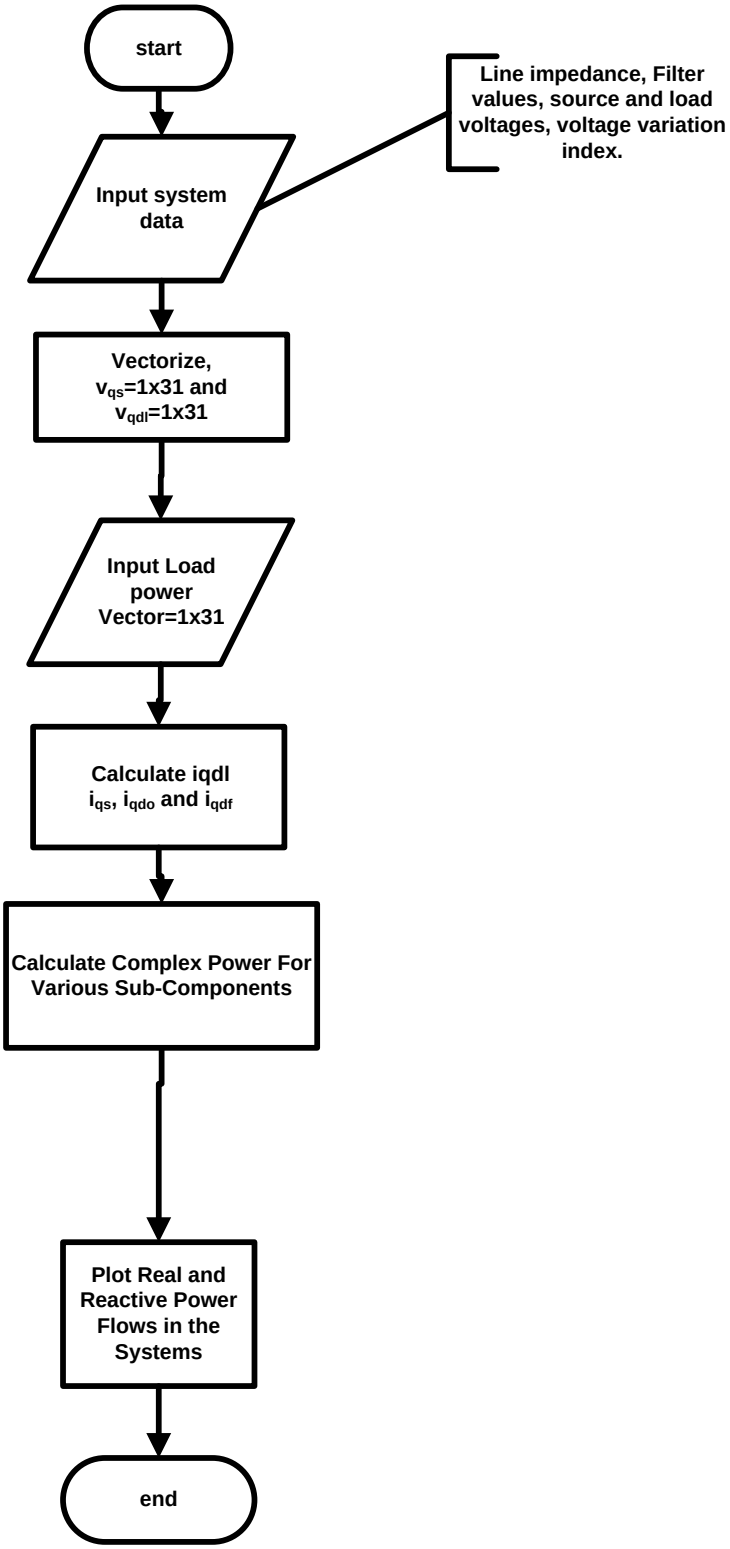


Figure: 5.8: Flow Chart for Power Flow Studies.

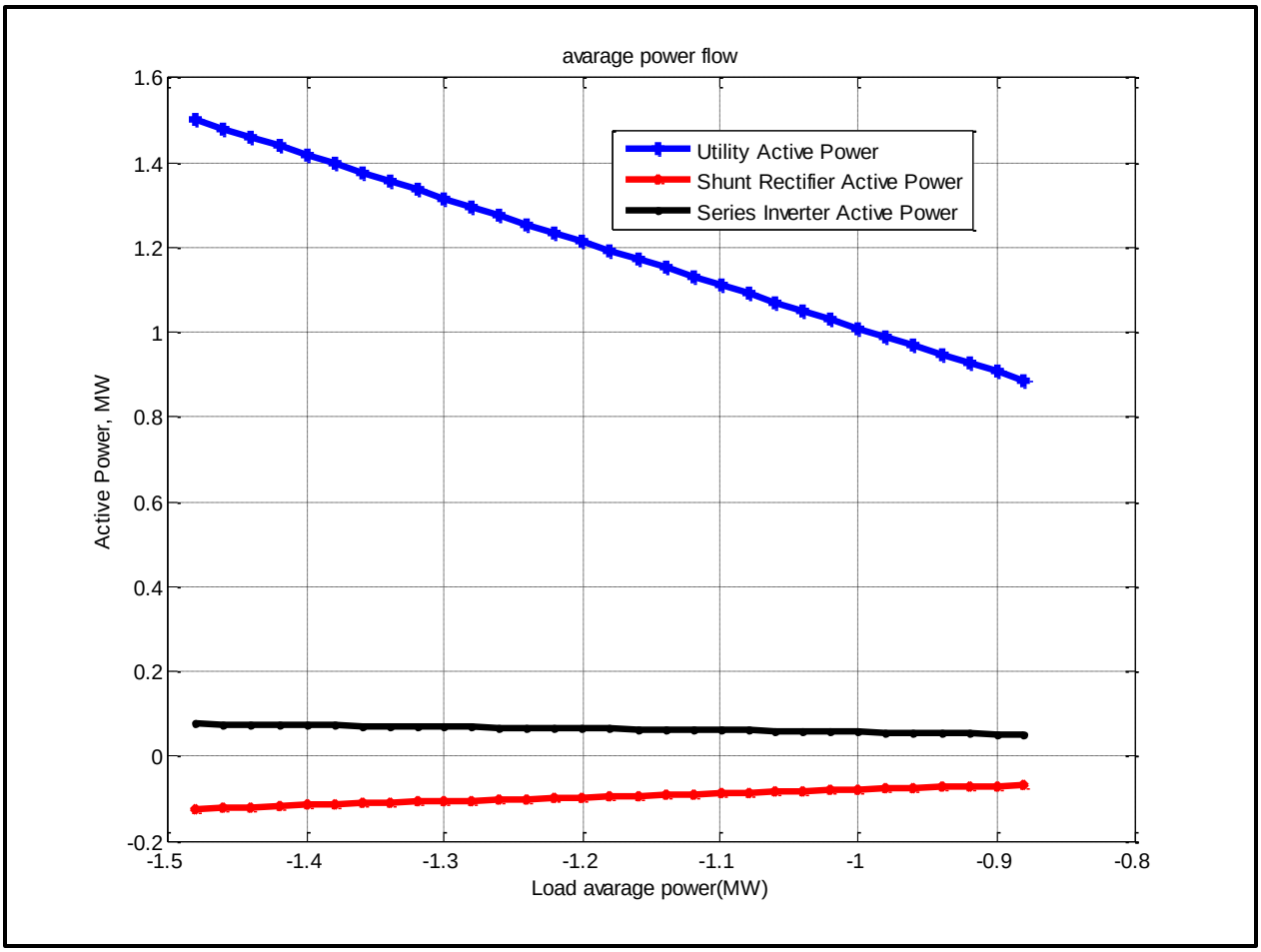


Figure 5.9: Average Power Flow through the System

Figure 5.9 shows the average power flow through the system. It is obtained from the real parts of equations (5.13), (5.14) and (5.15). As seen from the figure, the real power from the source increases as the load real power increases showing that the source supplies the load average power requirement. The exchange of real power between the shunt and series converter can be seen from Figure 5.9. The shunt inverter absorbs some real power which is fed back to the system through the series inverter. In this manner, the UPQC maintains the dc link voltage and regulates the load voltage. Since there is a difference between supply voltage angle and load voltage angle, there is some real power flow between the source bus and load bus even during

normal operation. This accounts for the flow through the two converters even when the study was carried out at rated voltage for both source and load.

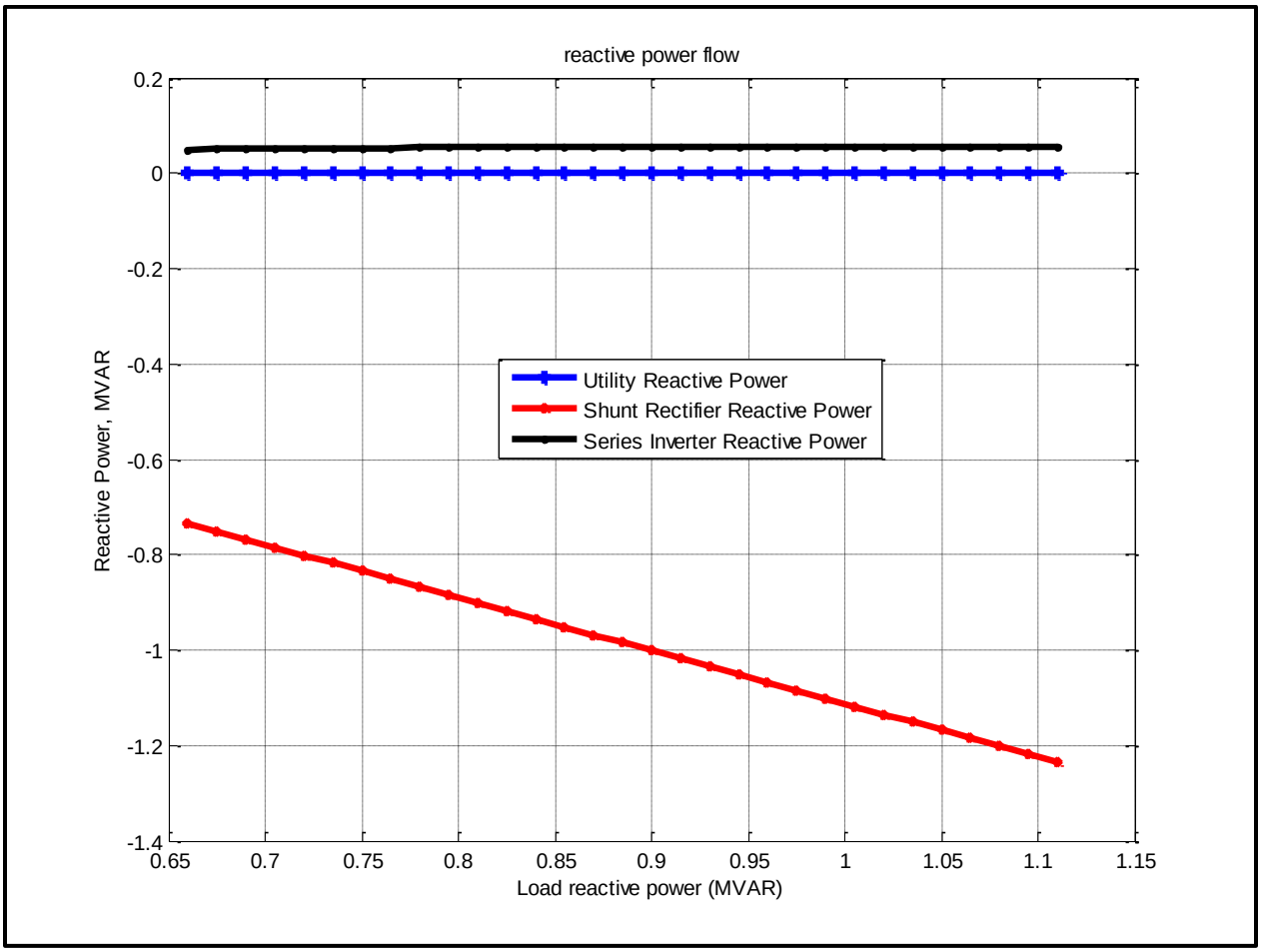


Figure 5.10: Reactive Power Flow through the System

Figure 5.10 shows the reactive power flow in the system. It has been obtained from the imaginary parts of equations (5.13), (5.14) and (5.15). As seen from Figure 5.10, the source reactive power remains constant at 0VAR while the load reactive power is varied. The source therefore does not supply the load reactive power requirement. This requirement is met by the shunt inverter as seen from Figure 5.10. The shunt inverter reactive power becomes increasingly negative (reactive power supply) as the load reactive power becomes increasingly positive

(reactive power absorbed). The reactive power absorbed by the series inverter has to do with the difference between the source voltage angle and the load voltage angle it also increases mildly as the load reactive power increases.

5.2.2 UPQC with Limitation

In this section, the determination of critical capacitor voltage is carried out. As it is desired to compensate for voltage interruption, this study becomes very relevant since it indicates whether this objective can be achieved with the system as constituted and gives an idea of what must be done to achieve it. In order to be able to control the system at its extreme points (minimum sag and maximum swell) there is a value of capacitor voltage that is critical otherwise there would be a case of over-modulation. The two necessary conditions for this study are stated in the following two equations:

(5.16)

(5.17)

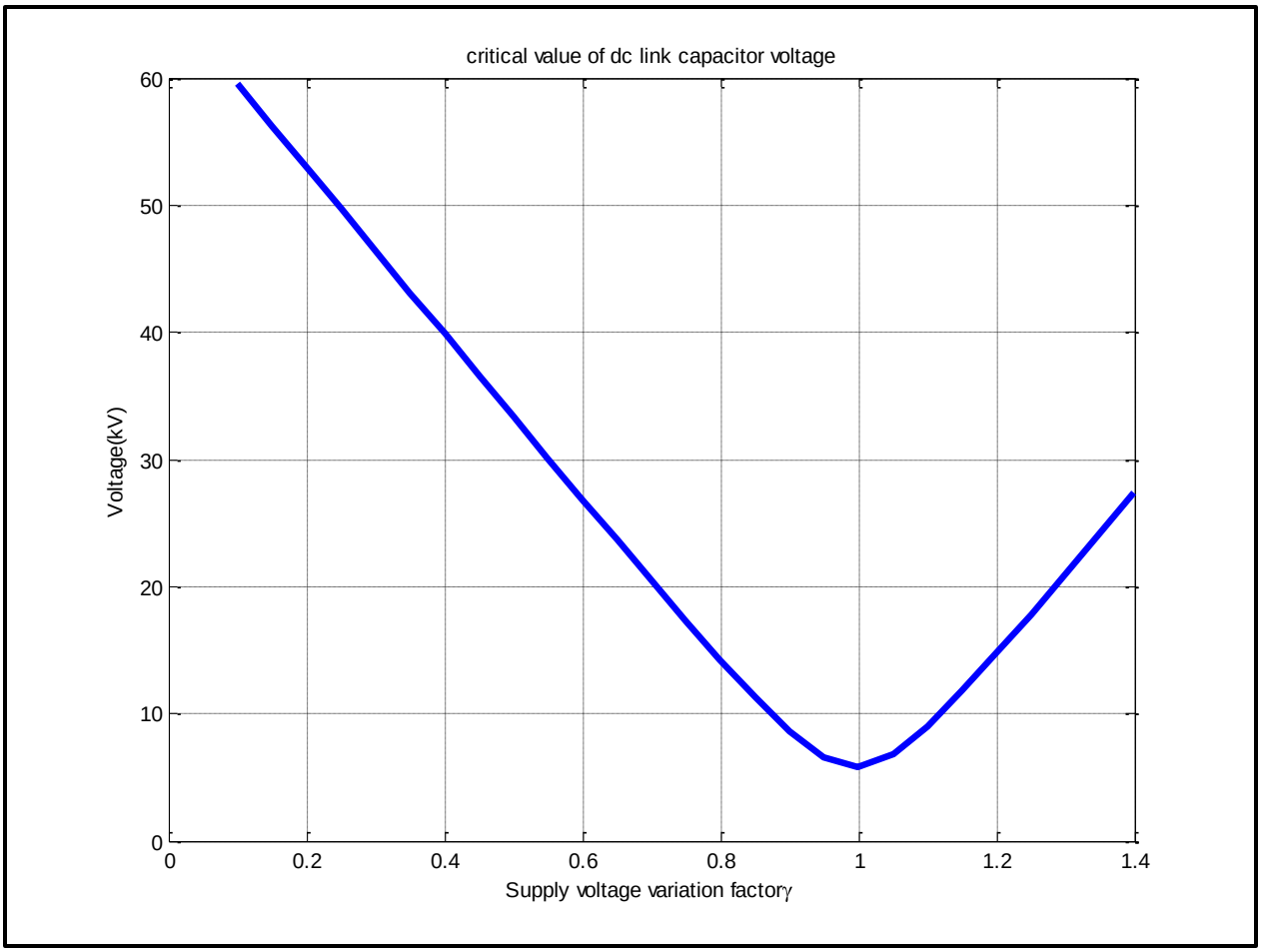


Figure 5.11 Critical Value of DC Link Capacitor Voltage

Figure 5.11 shows the critical values of dc link capacitor voltage for the range of variation proposed and for maximum load demand. It has been obtained from equation (5.17). This is a limitation in the sense that the required voltage level must be tenable. For the range of γ used in the earlier studies (i.e.), it is observed from Figure 5.11 that a 40kV capacitor is required. However, from the Figure 5.11, it can be observed also that for the system to be able to compensate for a 90% drop in supply voltage, a 60kV capacitor with is required. This will ensure that a case of over-modulation does not occur and that the system remains controllable. The capacitor voltage at is again necessary due to the difference in angle between the supply voltage and the load voltage. To carry out this study, the voltage injected by the series inverter is

taken to be simply the difference between the supply voltage and the load voltage. In order words the little line drop is neglected. This is because the supply current is not known a priori (i.e. before the load is applied); this assumption could also have added to the value of the dc link capacitor voltage at . However, generally, it is observed from the plot that how deep or how high the supply voltage can go and the system remains controllable are determined by the value of the dc link capacitor voltage. Taking the upper value of 60kV for the dc link voltage, the system will most definitely be able to compensate for voltage interruption and remain controllable.

5.2.3 Unified Power Quality Conditioner (UPQC) with Photovoltaic and Battery Energy Storage System

In this section, the entire study system is looked at. This is done by returning to equation (4.45) which was earlier removed to study the UPQC alone without the PV/BESS as in Section 5.2.1. Hence the same set of equations have been used as in Section 5.2.1 except that now, has been included in equation (4.45). The idea is to observe the improvement or otherwise offered by the inclusion of the PV/BESS sub system to the UPQC in the interconnected mode and also to study the performance of the system during the islanding mode. For this study, the supply voltage is taken at four discrete points including the entire range studied earlier in section 5.2.1. That is, from . The chosen points are for voltage interruption, to study any other sag condition apart from interruption, looking at normal operation and for a 20% swell condition. For all these values of supply voltage, the load average power is varied from a value of 1.4MW representing the power requirement from the PV and BESS (Section 4.6.5), through to a value of 1.87MW to include and exceed the maximum value of 1.66MW. The study is carried out at three solar radiations in Zaria. S= 0.85 representing

[redacted] p

the highest insolation, S = 0.45 representing the most prevalent insolation apart from the lowest insolation and S = 0.07 representing the lowest insolation level.

In order to see clearly the response of the battery to these changes, the load reactive power requirement is kept constant at 0.858MVAR determined from the steady state calculation Section 4.6.5. Only the average power is varied covering the entire range of demand as shown in the measurement obtained from PHCN.

The non-linear model of the solar PV cell has been presented in equation (4.25) and (4.26). The maximum power point for each solar radiation can be determined using the power equation of the solar PV cell given as:

(5.18)

Substituting equation (4.25) into equation (5.18),

——— (5.19)

The optimal power point is found by differentiating equation (5.19) with respect to and equating to zero to obtain the voltage at optimal power. Figure 5.14 gives the calculated optimal voltage at maximum power point in different irradiation level

v

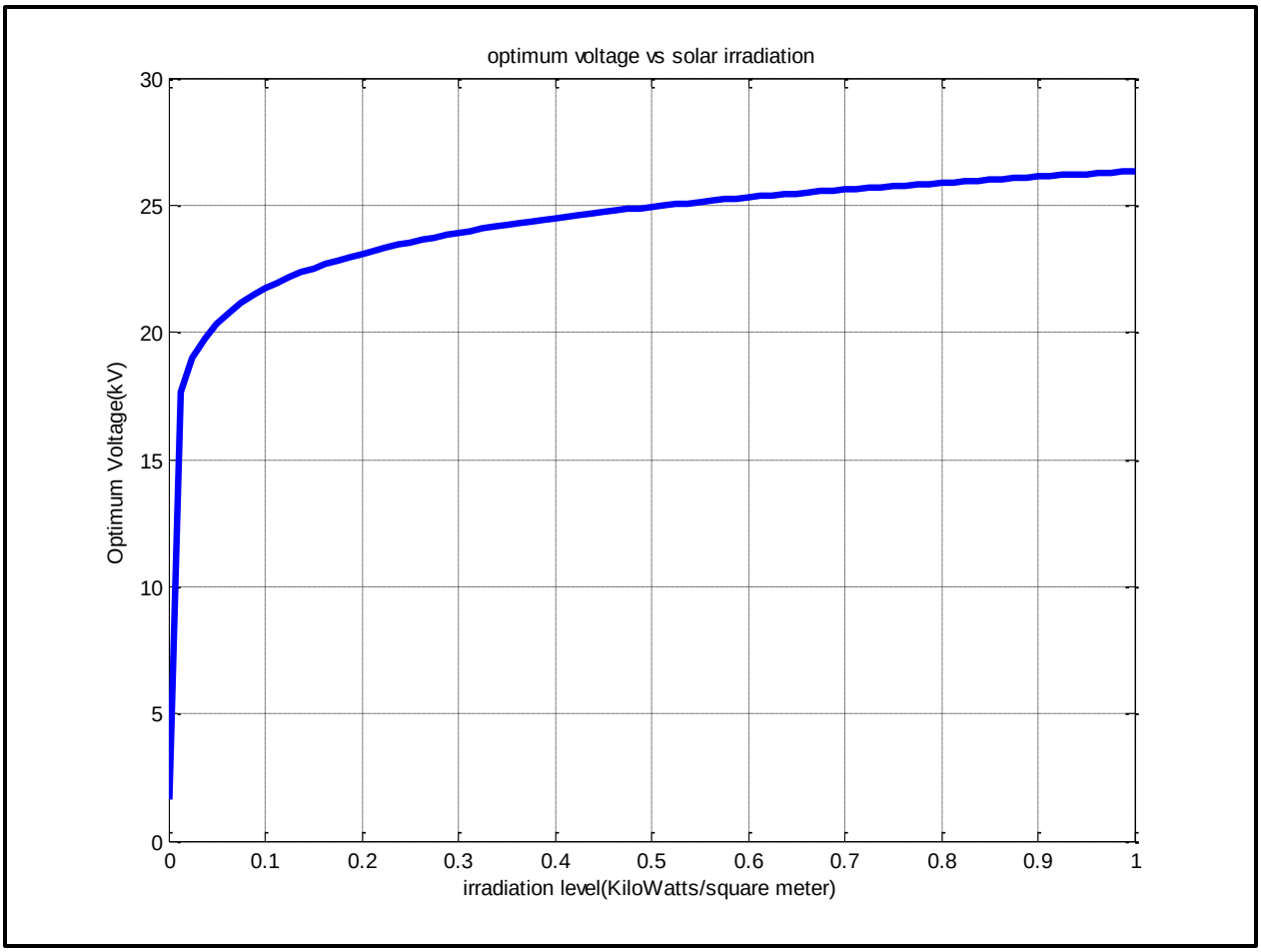


Figure 5.12 Optimum Voltage at Maximum Power for different Insolation Level.

From the plot in Figure 5.12, which has been obtained from equation 5.35 by setting the derivative with respect to equal to zero, it is seen that for maximum power at an insolation of S = 0.45 the voltage for optimal power is 24kV. For S = 0.85 the voltage for optimal power is 26kV. For S = 0.07, voltage for optimum power is 20kV. The parameters of the solar PV cells are given in Table 5.1.

Table 5.1 Parameters of PV System

I_{rs}		θ_r	300°K
q		I_{src}	8.03A
k		k_θ	0.0017
	298°K	n_s	44000
A	1.92	n_p	1800

A MATLAB script was written for this study according to the flow chart presented in Figure 5.13.

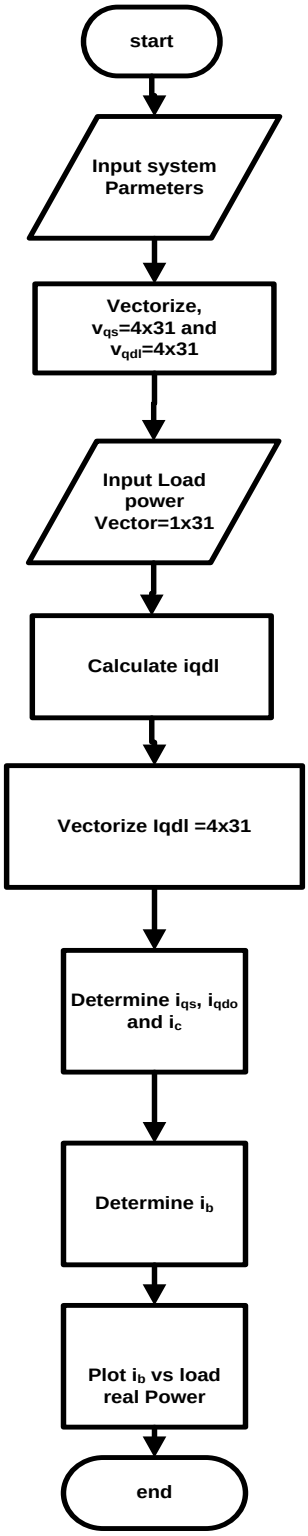


Figure: 5.13: Flow Chart for UPQC with PV and BESS

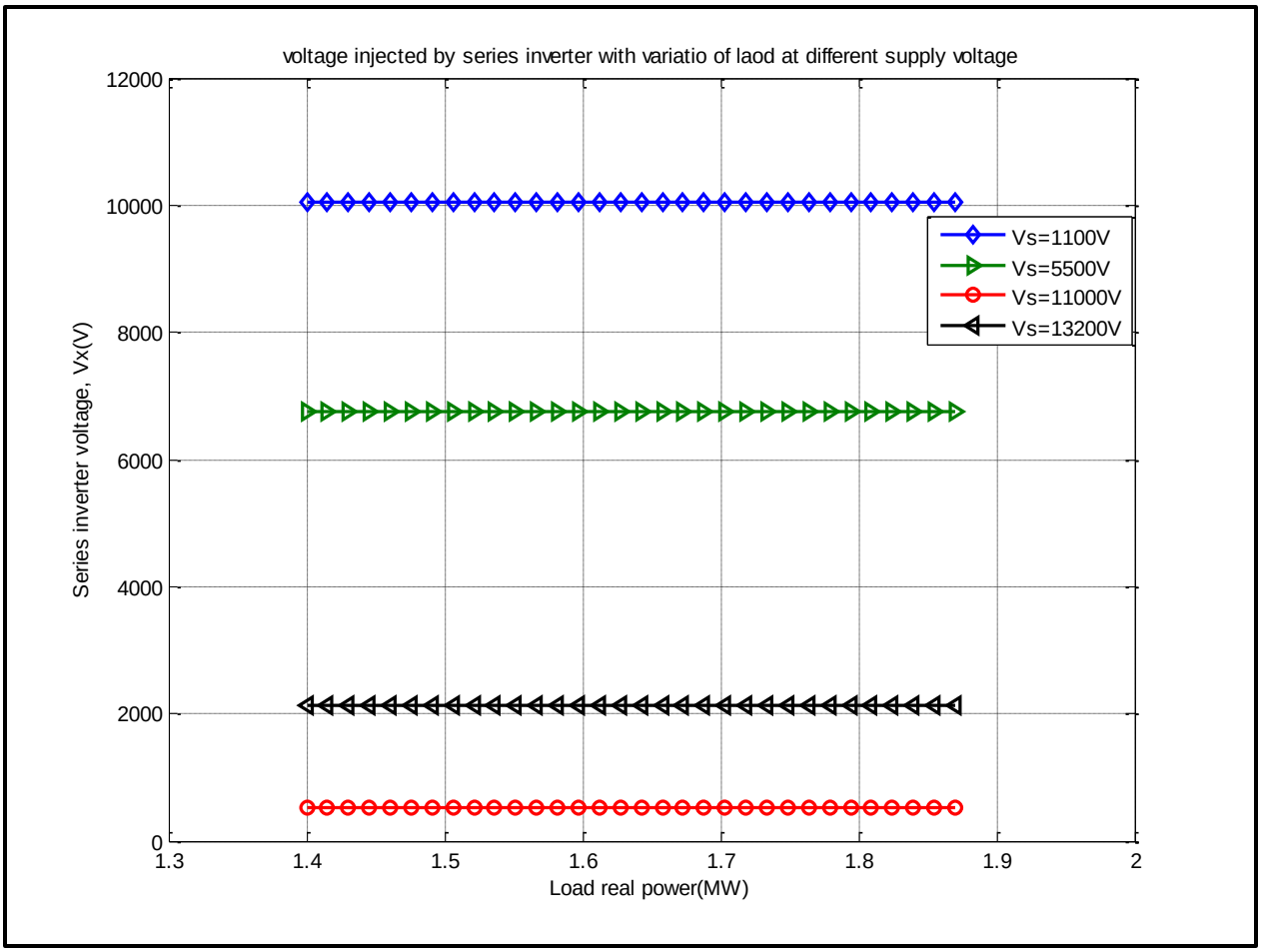


Figure 5.14: Voltage Injected by Series Inverter with Variation of Load at Different Supply Voltage (S = 0.85).

Figure 5.14 shows the peak values of the voltages injected by the series inverter for the four (4) voltage levels of the supply chosen. The highest value is injected when the supply sag is the most and the least value is injected when the supply is at rated value. Again the voltage injected at normal value results from the difference between supply and load voltage angles. During supply voltage swell conditions, there is voltage injected in the opposite direction to the voltages injected during supply voltage sag. This is evident from the reversal in position between the plot for and . As injected series inverter voltage is independent of load but dependent only on the difference between supply voltage and load voltage, the values of

voltage injected for each supply voltage chosen remain constant over the range of variation of load and for the three solar insolation levels.

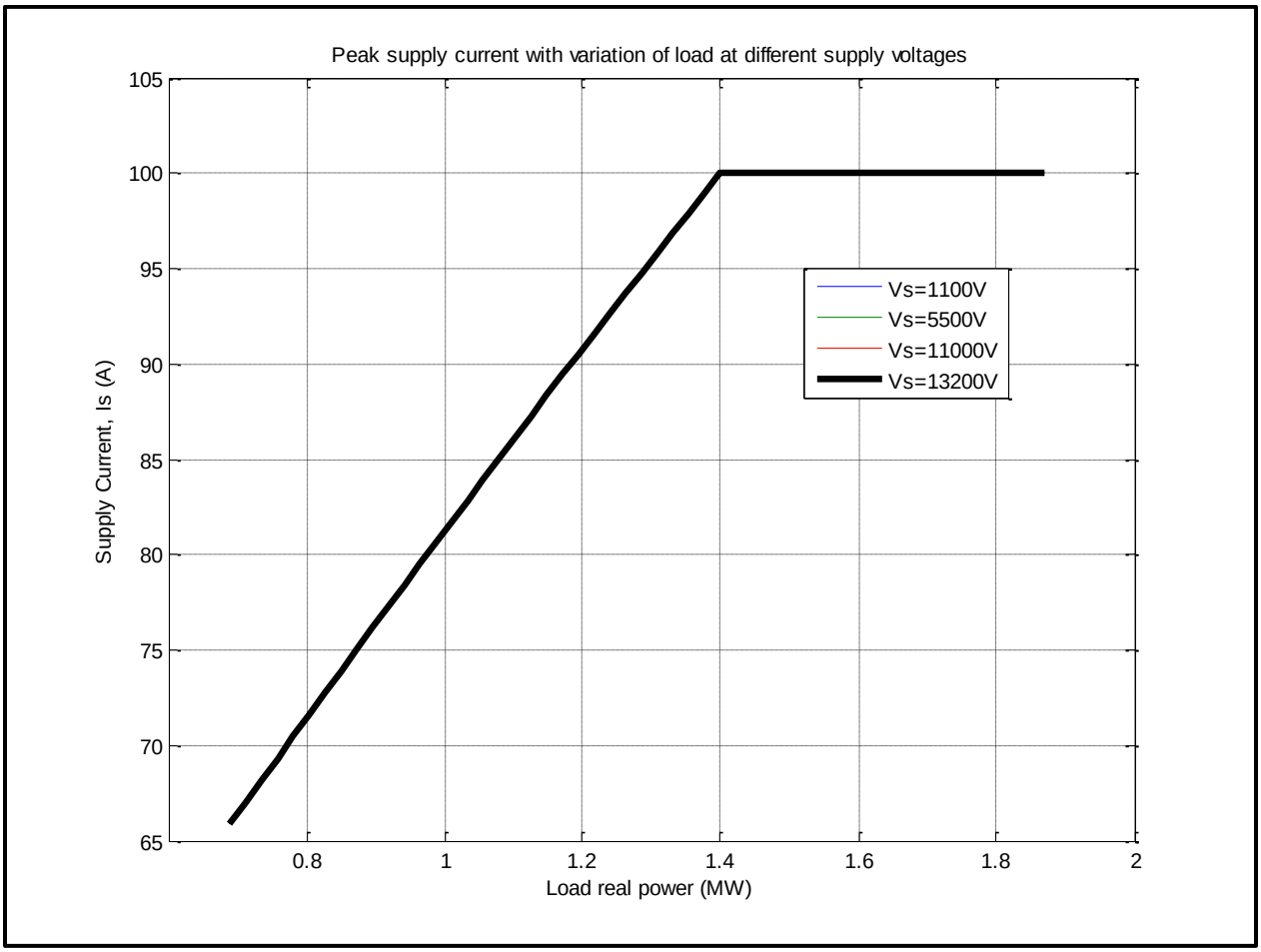


Figure 5.15 Peak Supply Current with Variation of Load at Different Supply Voltage (S = 0.85).

Figure 5.15 shows the variation in the peak value of the supply current with variation in the load average power for the four voltage supply voltage level and for solar insolation of 0.85. It is noticed that the change in the supply voltage does not affect the supply current over the range of load real power variation as all the four plots for the four supply voltage levels coincide. Figure 5.15 shows the variation of the supply current up to the maximum active power of the load. Beyond this point, the supply current remains constant at 100A. The profile of the supply current

in Figure 5.15 is due to the introduction of the PV/BESS. In an earlier study (see Figure 5.5) when the PV/BESS had not be connected, the supply current level had risen for lower supply voltage. The fact that the plots for the supply current coincided for all four (4) supply voltage levels means that the power drawn from the source has been limited to its value at normal operation for the given load conditions irrespective of supply voltage variations. The extra power that previously was supplied by the source for voltage sag conditions is now sourced from the PV/BESS.

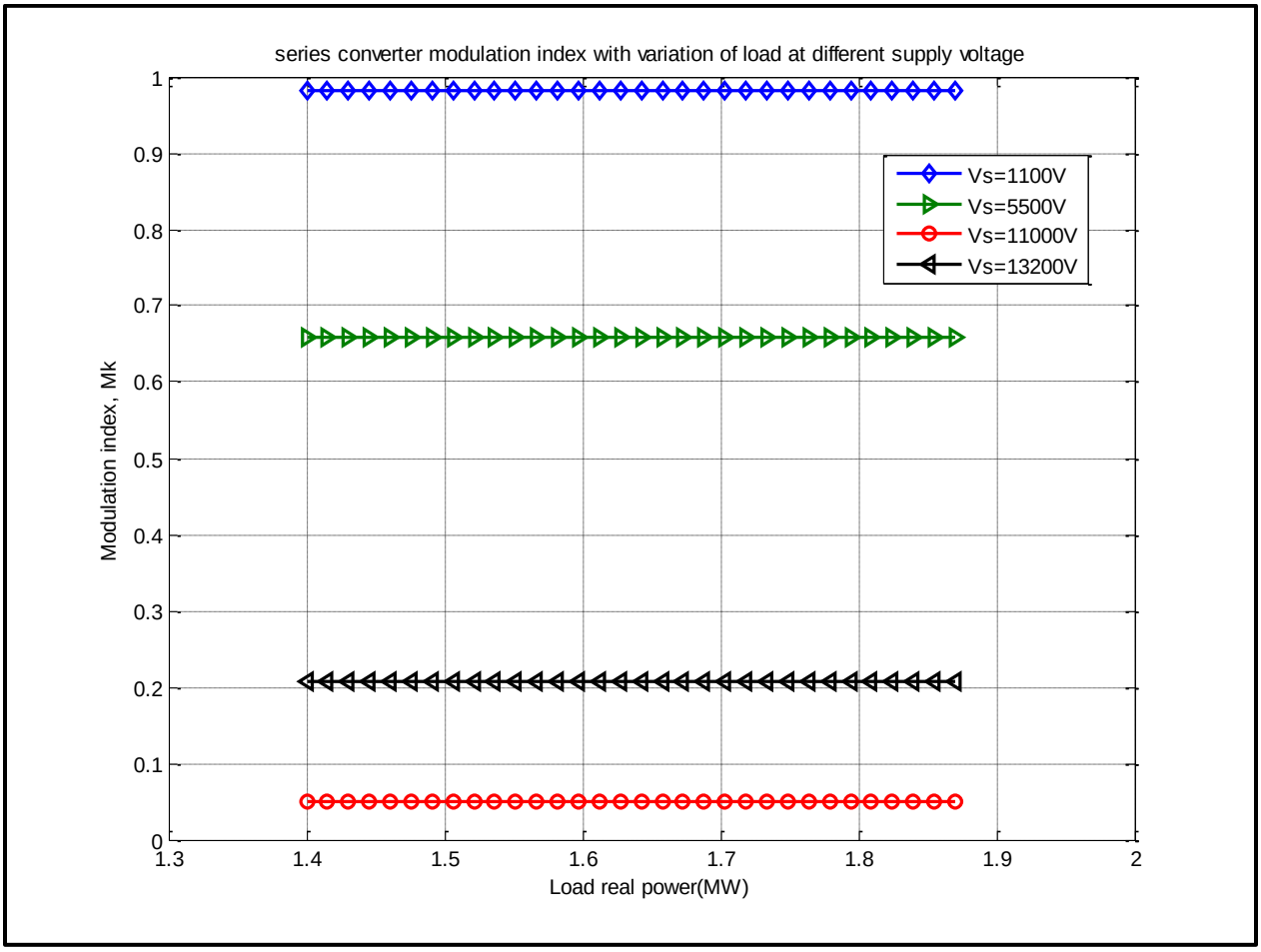


Figure 5.16 Series Converter Modulation Index with Variation of Load at Different Supply Voltage (S = 0.85).

Figure 5.16 provides the series inverter modulation index for the four supply voltage levels. Again this shows the values of the modulation index for the inverter if the load voltage must be regulated at its rated value. It is independent of load and solar insolation.

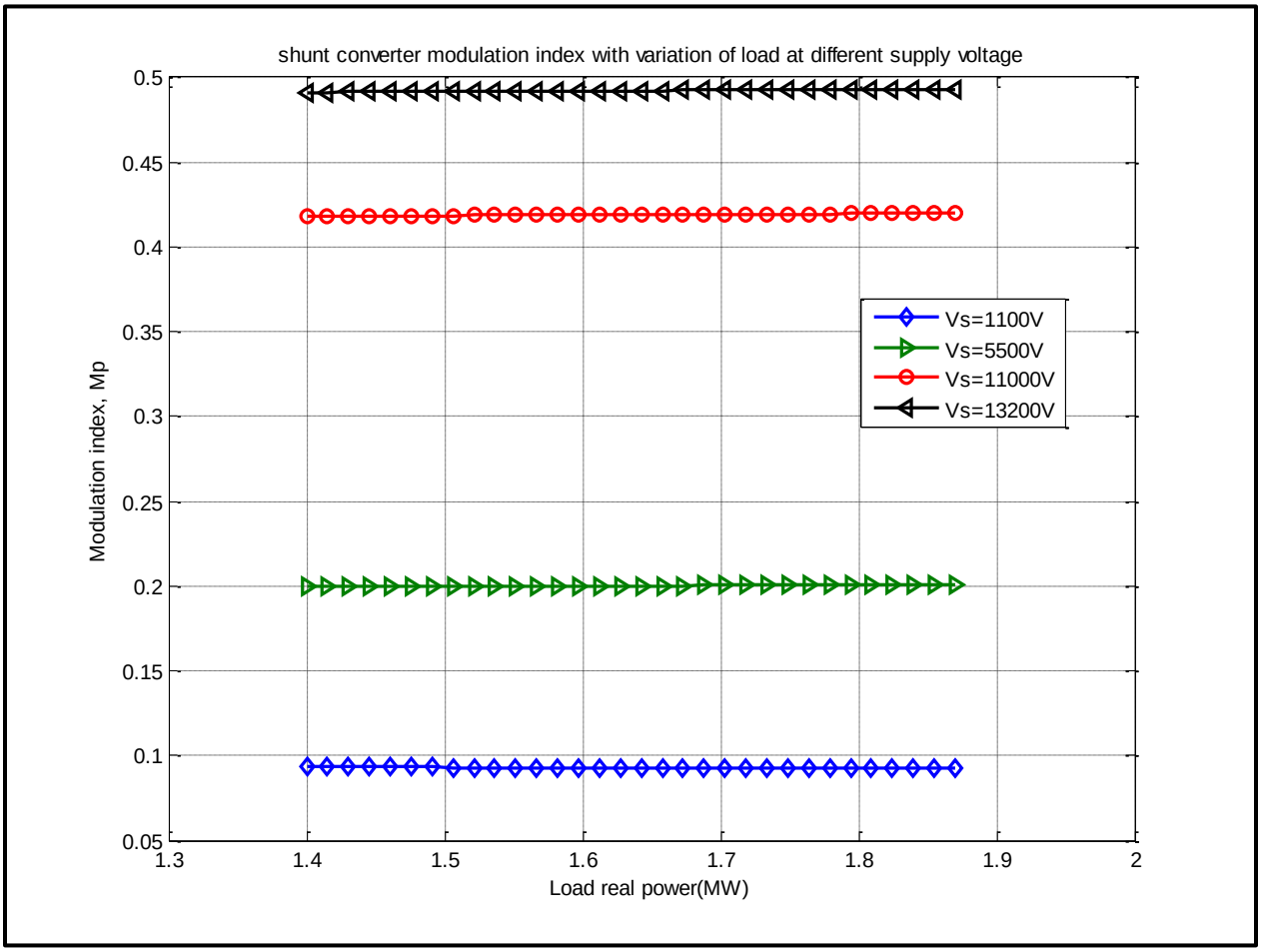


Figure 5.17 Shunt Inverter Modulation Index with Variation of Load at Different Supply Voltage(S = 0.85).

Figure 5.17 shows the shunt inverter modulation index. The shunt inverter performs the dual function of supplying the load reactive power and of maintaining the dc link voltage constant. To maintain the dc link voltage constant, the shunt inverter either absorbs some real power from the supply during periods of supply voltage sag or supplies real power to the supply during periods

of voltage swell. In order to achieve this, the modulation index must be as shown in Figure 5.17 for the supply voltage levels studied.

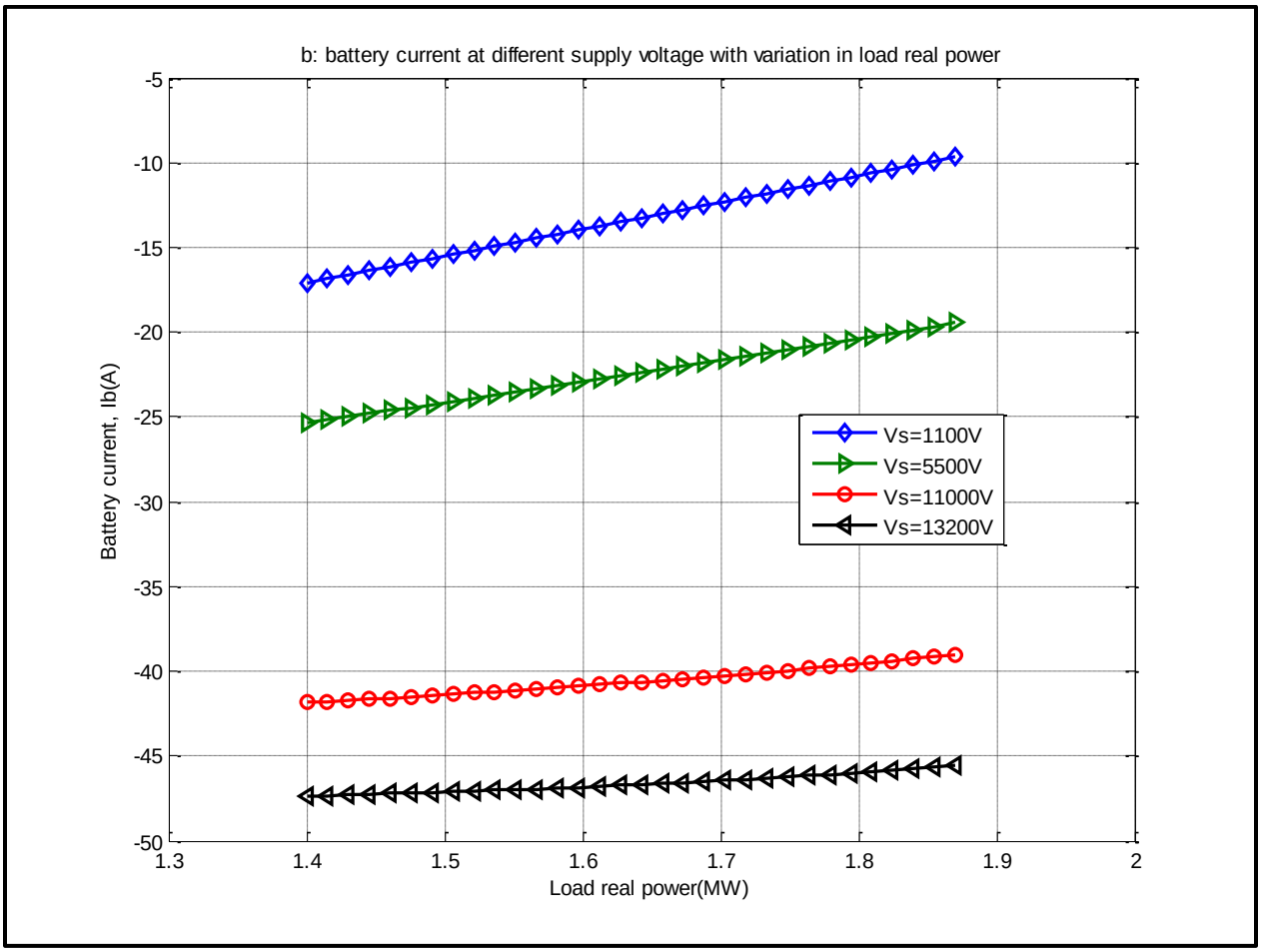


Figure 5.18 Battery Current with Variation of Load at Different Supply Voltages (S = 0.85).

Figure 5.18 shows the response of the battery to the load variation at different supply voltage level and for solar insolation of S = 0.85. It has been obtained from equations (4.21), (4.24) and (4.45). A positive battery current indicate battery is discharging or supplying power while a negative battery current indicate battery charging or absorbing power. For the supply voltage level of , that is , the battery charges with a higher charging current for lower load real power. The charging current of the battery reduces progressively as the load real

power demand increases. Although, for this case, that is S = 0.85, the battery never gets to supply power. In the case of S = 0.45 and S = 0.07 shown in Figure 5.19 and Figure 5.20 respectively, the battery discharges when the load demand exceeds what the combination of the utility and PV can supply. This shows that for S = 0.85 the power output of the combination of the utility and PV can meet load demand up to maximum load even during supply voltage interruption. For a supply voltage of which occurs for which is also a sag condition, there is a downward shift in the curve of Figure 5.18. In other words, the charging current of the battery increases. This is because at this voltage more power is available from the utility compared to what is available at $\gamma = 0.1$. This trend is observed for $\gamma = 1 (V_s = 11000V)$ and $\gamma = 1.2$ (V_s=13200V).

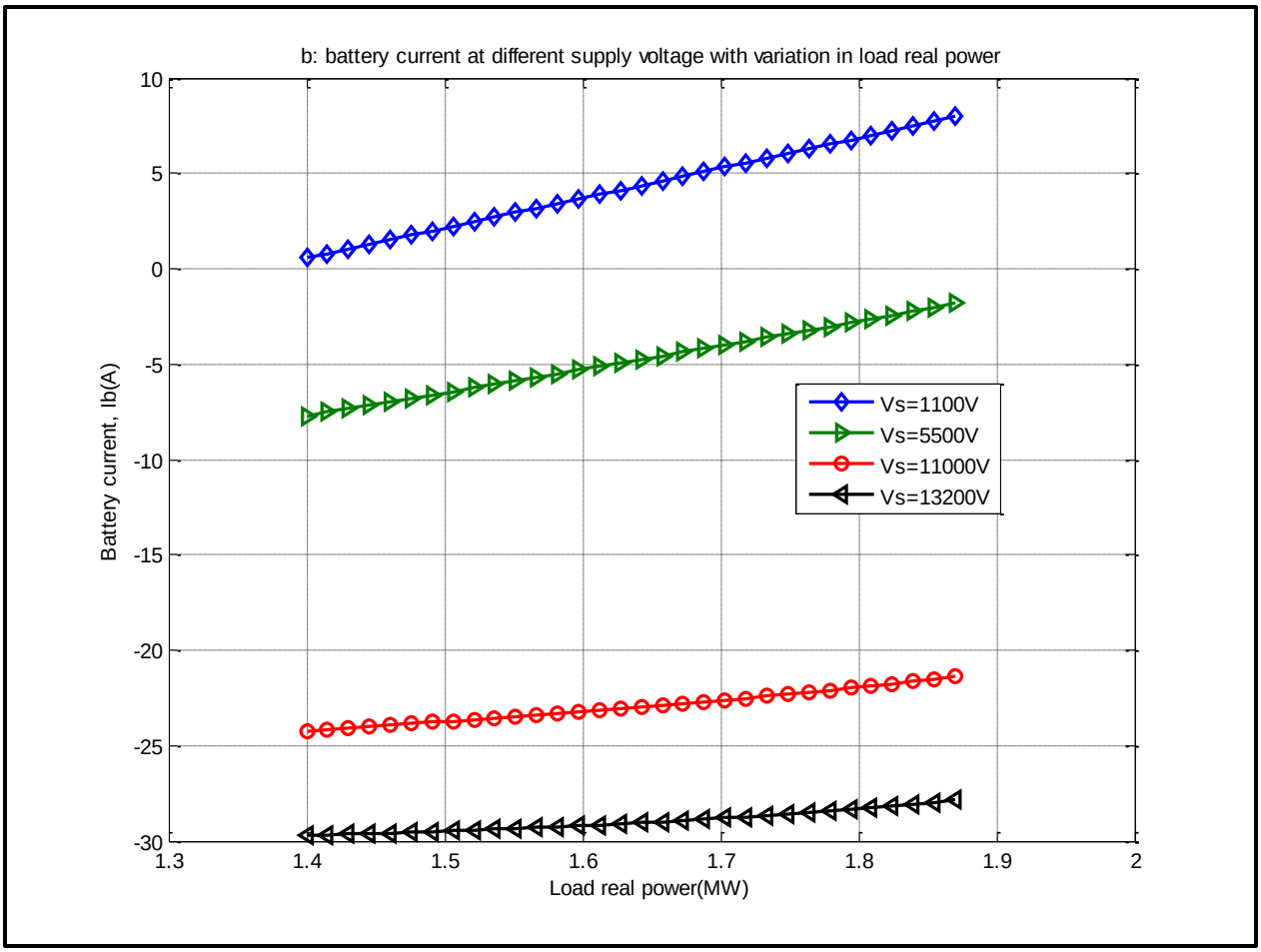


Figure 5.19 Battery Current with Variation of Load at Different Supply Voltage (S = 0.45).

Figure 5.19 (obtained from equation (4.21), (4.24) and (4.45)) shows the same result in Figure 5.18 with the exception that the solar insolation level has reduced from 0.85 to 0.45. The result of this change is that the battery is engaged faster than it was when solar insolation was 0.85. It is seen from Figure 5.19 that at , the battery is already engaged in supplying load power for a load power of 1.4MW. When , the battery charges with a much lower charging current compared to the same situation for S = 0.85 in Figure 5.18. Generally therefore, as envisioned, the battery's involvement depends on the available solar insolation and the load demand. This ensures efficient utilization of available solar energy resources.

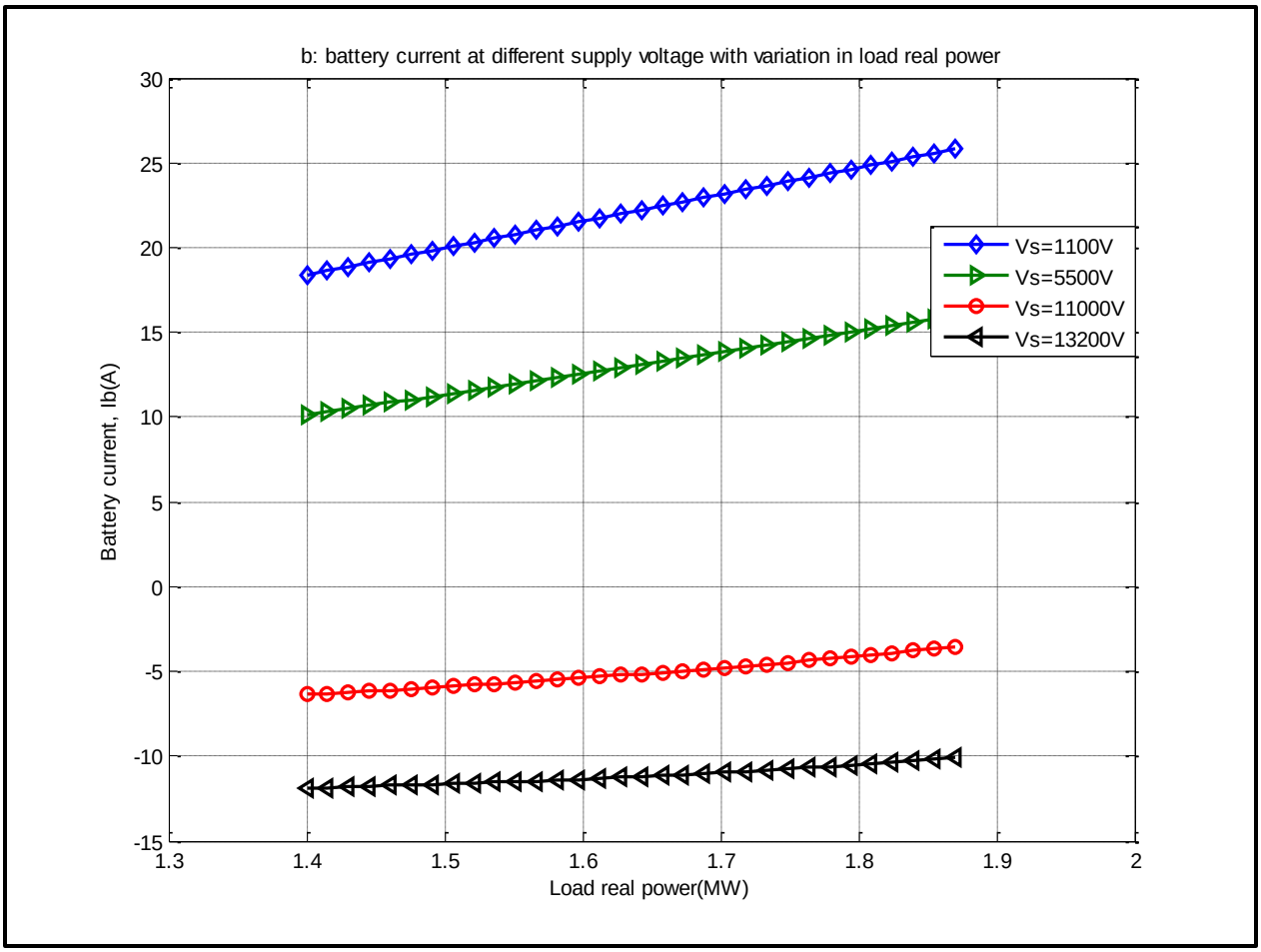


Figure 5.20 Battery Current with Variation of Load at Different Supply Voltage (S = 0.07).

S = 0.07 represents the case of lowest available solar insolation. For this situation, the battery contributes to meeting load demand both for the case of and . The power supplied to the system by the battery at this low insolation is evidently much higher than that for the same condition in Figure 5.18. It is seen also that for and the charging current of the battery is much lower compared to the same condition in Figures 5.18 and 5.19.

5.2.4 Loss of Supply Compensation

The islanding mode of operation of the system occurs when there is a loss of supply. There are two possible configurations for this mode of operation. In the first configuration, Figure 3.5, the

PV/BESS system supplies a part of the load requirement through the shunt inverter while in the second configuration Figure 3.6, the PV/BESS system supplies the same part of load power requirement through the series inverter.

Result: The total real power to be supplied by the PV/BESS system had been calculated from Section 4.6.5 to be 1.4940MW. Hence, for this study, the real power has been varied from 0-1.4940MW.

Possibility A:

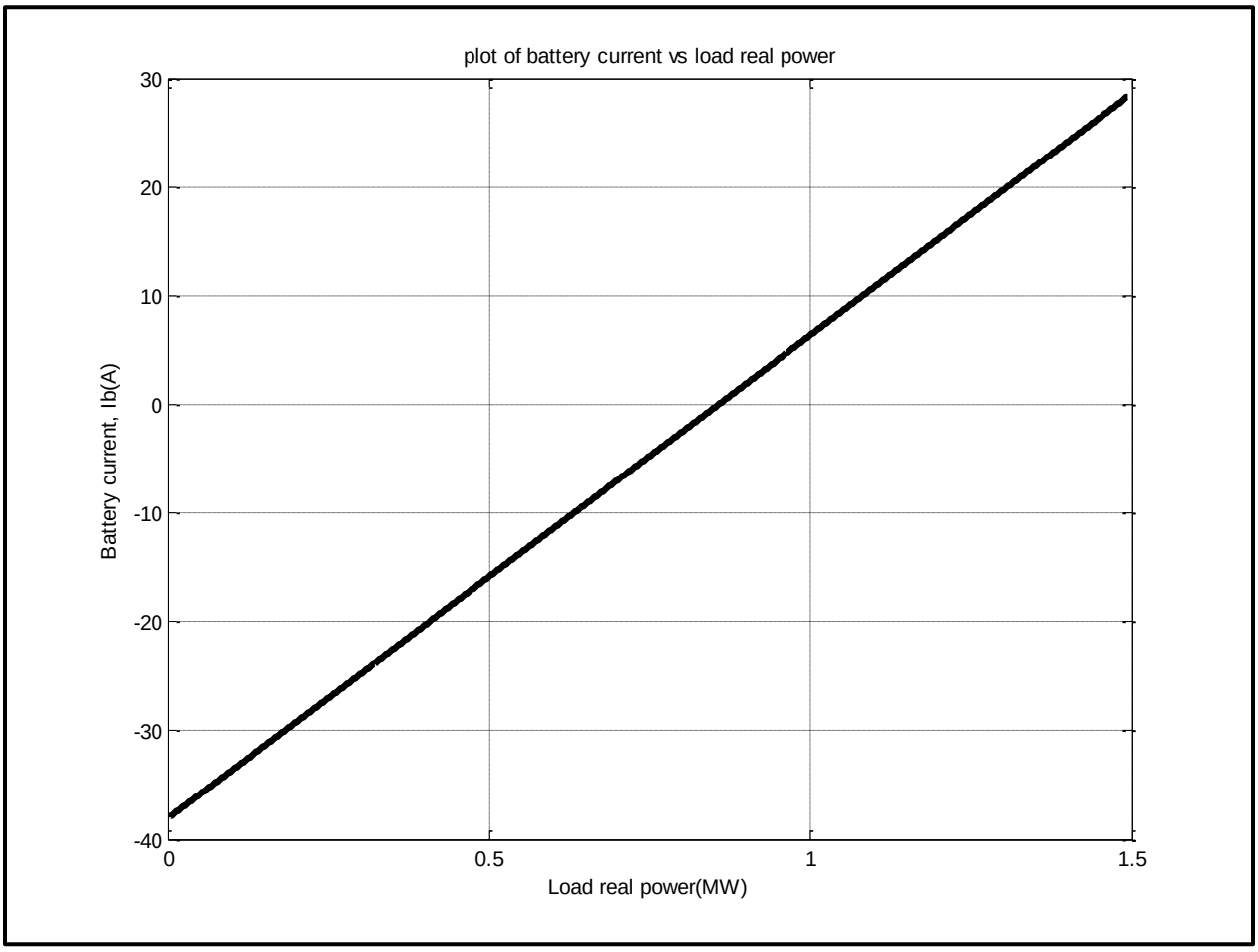


Figure 5.21 Battery Current versus Load real power in Islanding Mode Possibility A (S = 0.85)

The plot of Figure 5.21 shows the battery current with variation in load real power. As seen from the figure, the battery changes from charging to discharging, as the load power increases. For a load real power of zero all of the output power of the PV system goes into charging the battery and the battery charges at a current of about 39.84Amps. As the load real power demand increases the charging current of the battery reduces gradually until load power of about 0.8576MW. Beyond this load power which approximates a power of 0.8964MW for the PV system calculated in Section 4.6.5, the battery begins to discharge. The output power of the

battery at this point augments the output of the PV system. For lower solar insolation levels, the same result is observed except that in this case, the change from charging to discharging of the battery occurs faster since the available power from the solar cells is lower as in Figure 5.22 and 5.23.

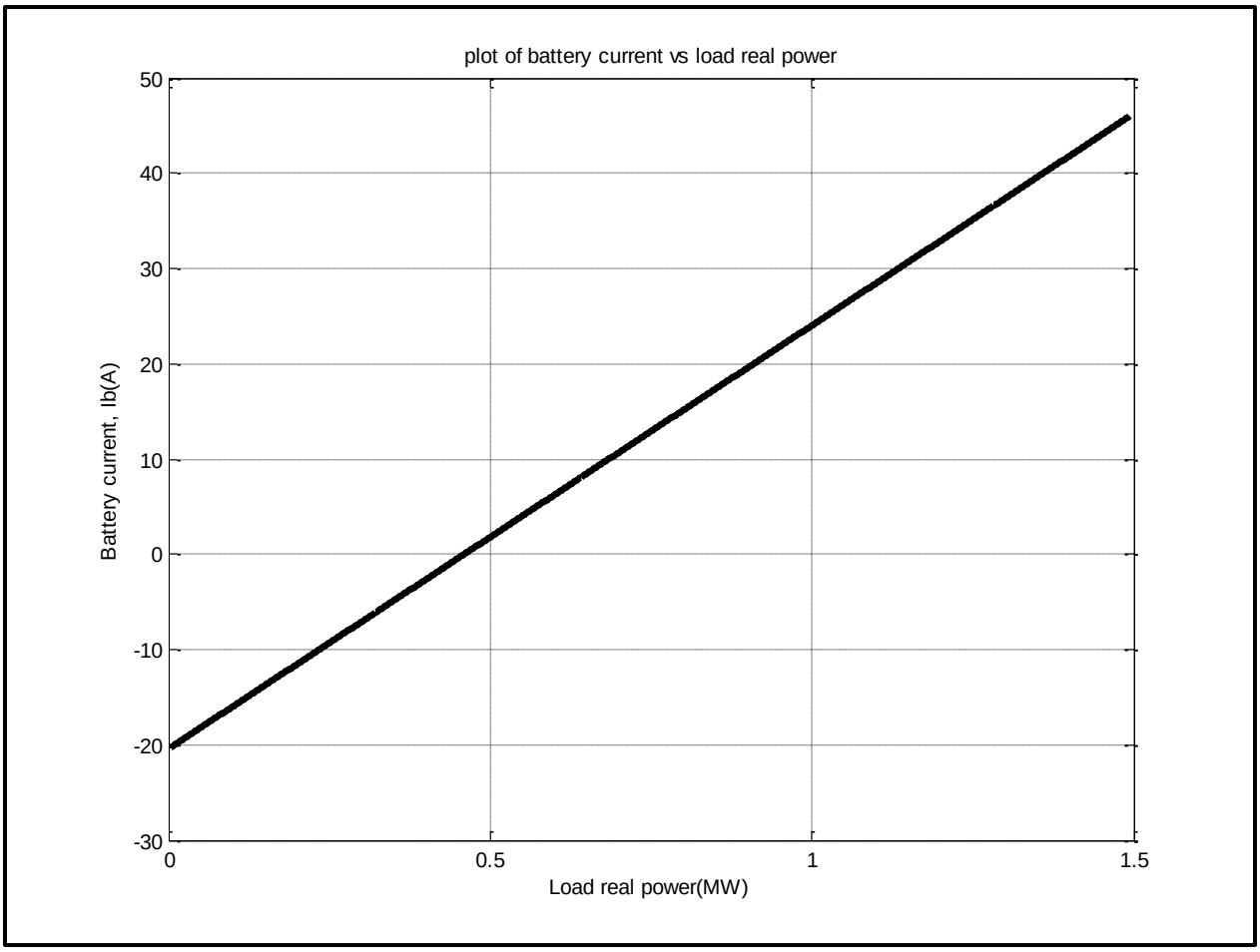


Figure 5.22 Battery Current vs Load Real Power in Islanding Mode: Possibility A (S = 0.45)

Comparing Figure 5.22 with Figure 5.21 for a load real power of zero for instance, the charging current of the battery is much lower for Figure 5.22 than for Figure 5.21. This is because for S=0.45 less power is available from the solar PV system. This is also the reason the battery changes from charging to discharging faster in this case than in the case for Figure 5.21. The trend of the two plots is however similar and for the same reason. That is, the battery absorbs

power when the output of the solar PV system is greater than the load requirement and supplies power to augment the output of the PV system when load power requirement begins to exceed the output from the solar PV system.

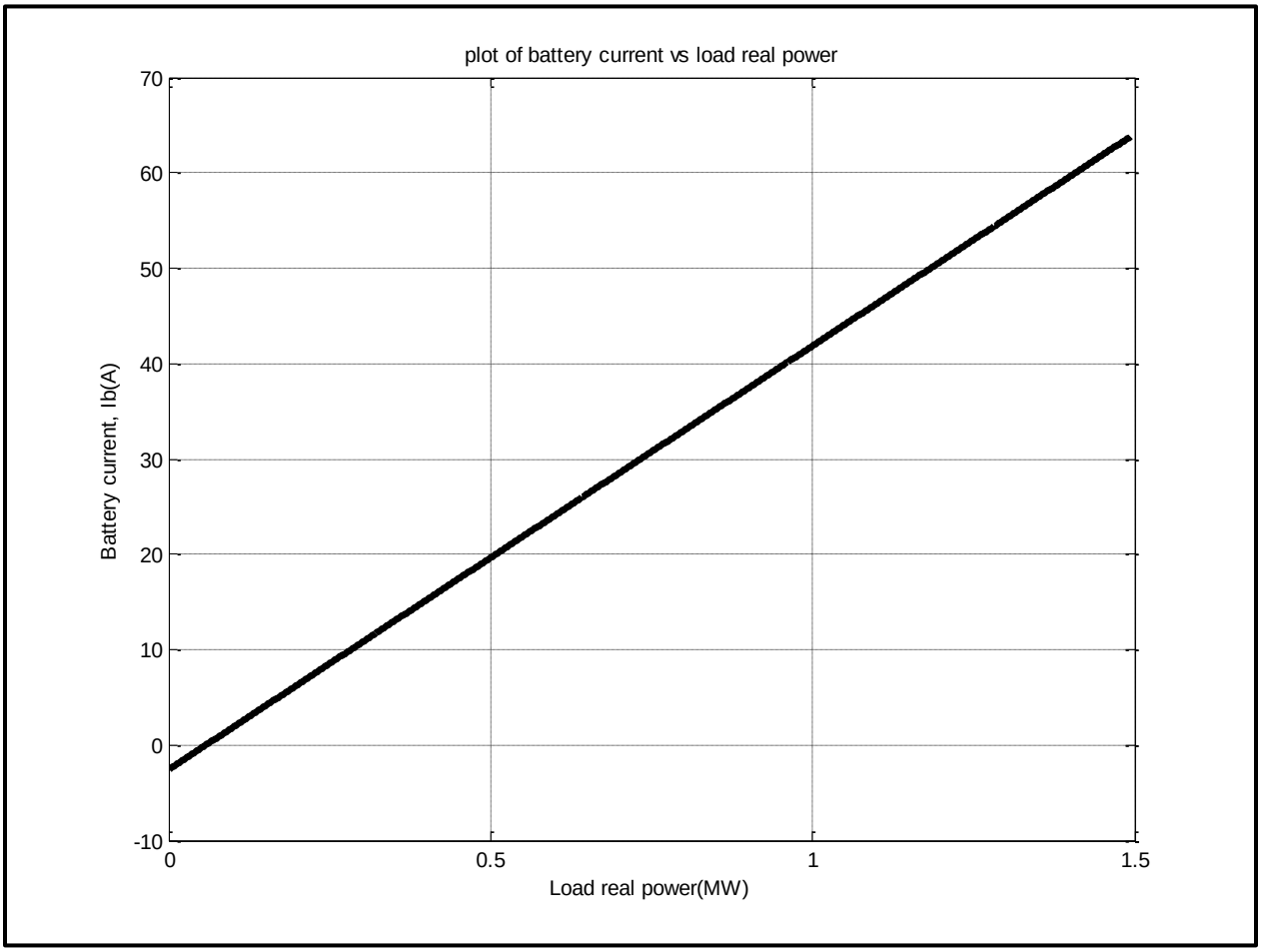


Figure 5.23 Battery Current vs Load Real Power in Islanding Mode: Possibility A (S = 0.07)

Figure 5.23 shows the response of the battery in islanding mode for the least solar insolation that is S = 0.07. For this condition, the battery for the most part supplies the load requirement since the output power from the PV system is very minimal.

It is important to note for Figures 5.21, 5.22 and 5.23 that the response of the battery rather than the capacity is shown. From the analysis on design consideration, the battery is to meet only 40 percent of the load during islanding condition. In the actual physical system therefore, as the

load exceeds the capacity of the battery and the PV system, the system should shut down. If this condition occurs, it becomes the limit of the system in the islanding mode.

Possibility B:

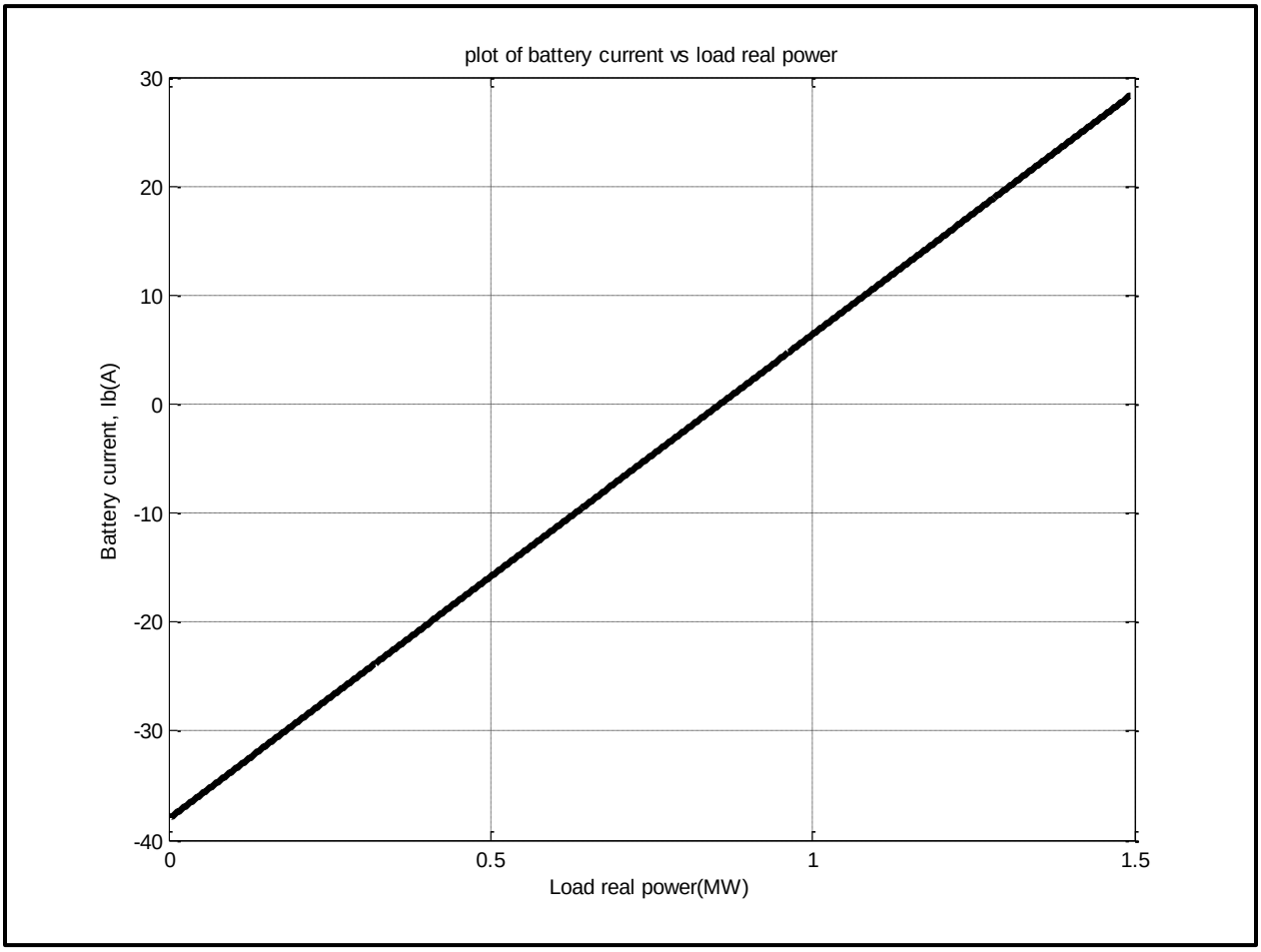


Figure 5.24 Battery Current vs Load Real Power for islanding mode: Possibility B (S = 0.85)

Figure 5.24 shows the plot of the battery current and Load real power variation for islanding mode possibility B. The result here is similar to that in Figure 5.21 and it is for the same reasons. This shows that both possibilities can be used to evacuate power to the load in the islanding or standalone mode. The particular configuration chosen would therefore depend upon some other

considerations. Figure 5.25 is for the case of S=0.45 which compares exactly with Figure 5.22 while Figure 5.26 is for S = 0.07 and again it is similar to Figure 5.23 for the same reasons.

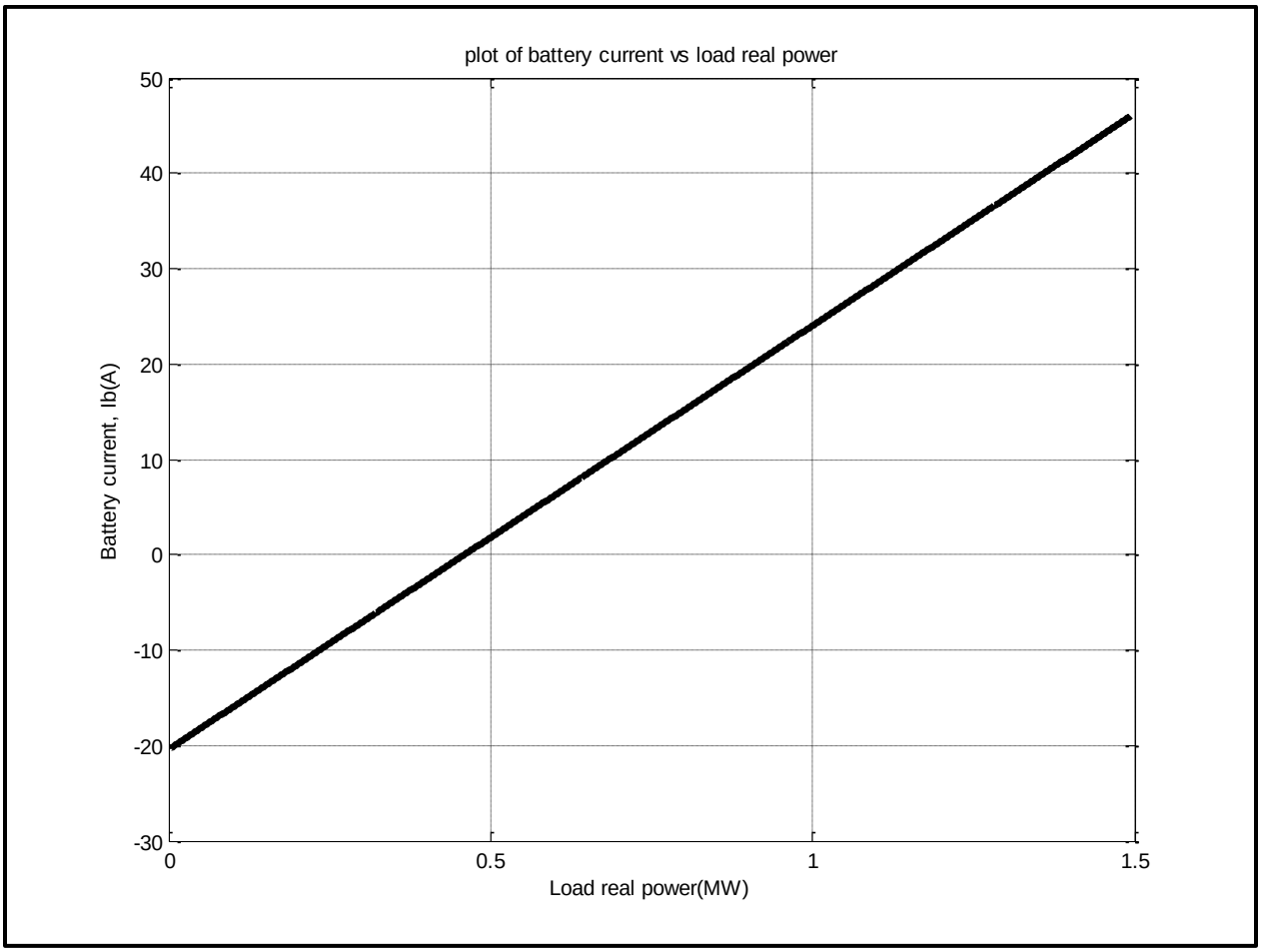


Figure 5.25 Battery Current vs Load Real Power for Islanding Mode Possibility B (S = 0.45)

The plot in Figure 5.25 is similar to that for Figure 5.22 for the same reasons. Hence, for the two possibilities in the islanding mode, the system is able to meet the load requirement for which it's been designed. As noticed earlier, other considerations such as, perhaps, ease of control, cost and so forth will have to be considered to determine which configuration is used.

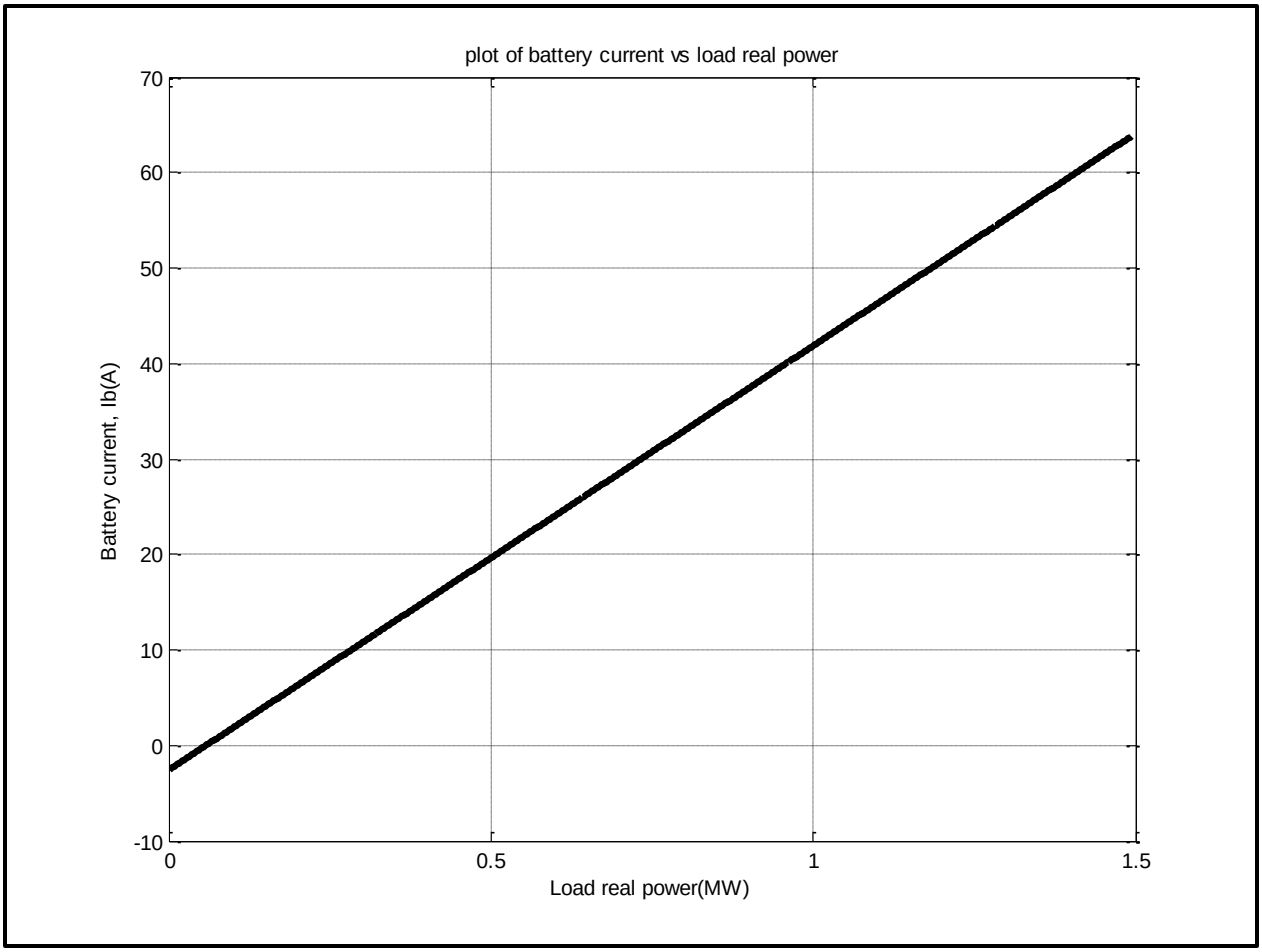


Figure 5.26 Battery Current vs Load Real Power for Islanding Mode Possibility B (S = 0.07)

5.3 Open Loop Large Signal Simulation

The open loop large signal simulation provides a better understanding of the system. The essence is to verify that the system behaved properly as predicted by the steady state analysis. Pre-specified control signals have been used. These control signals have been obtained from the steady state analysis carried out in section 5.2. They are seen from the plots of M_p and M_k for the different scenarios studied in section 5.2. The simulations have been carried out over a large number of switching cycles to reach steady state. In this section also various scenarios or

operating conditions are looked at and the results compared with the corresponding steady state analysis in section 5.2

5.3.1 UPQC without Limitation

Voltage Sag: From Figure 5.2, voltage sag of 35 percent is taken. That is $\gamma = 0.65$. From Figure 5.2 $V_{x,}$ the peak value of the voltage injected by the series inverter is about 4632.2V. For this condition, the peak value of the modulation index M_k seen in Figure 5.4 is 0.6. Using this pre-specified control value and equations 4.94 to 4.104, the following simulation results are obtained for the three phase voltages injected by the inverter.

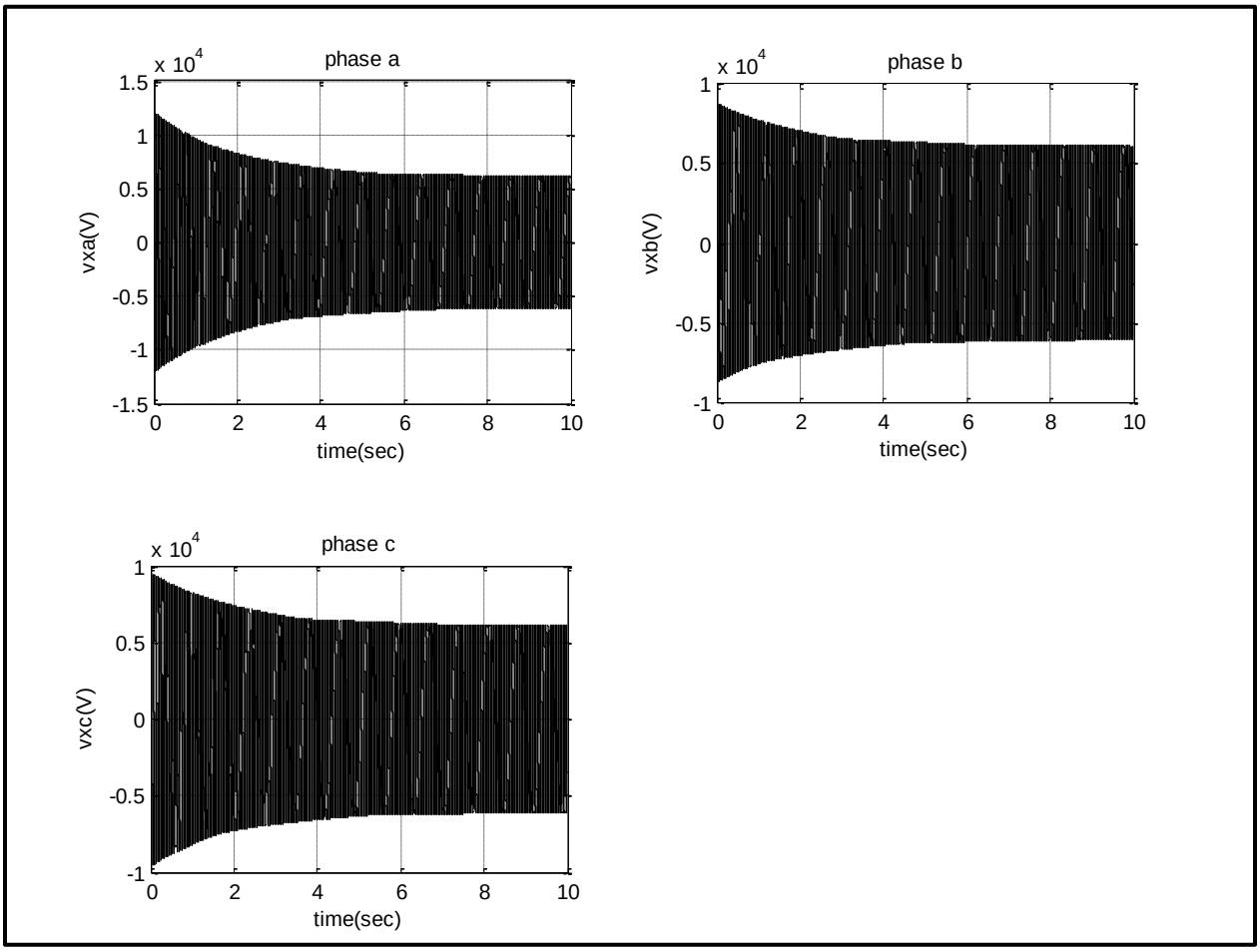


Figure 5.27: Simulation Results for Voltage Sag Condition.

Figure 5.27 shows the simulation result for a voltage sag condition. The result agrees largely with that obtained for the steady state analysis. As can be seen from the figure, the three phase voltages injected by the series inverter for this condition settles down to a value of about 5000V. This result agrees with a value of 4632.2V obtained for the steady state analysis. The difference has to do with MATLAB solver and the switching actions involved which were not there in the steady state analysis. Figure 5.28 shows the generation of the switching pulses for the SPWM used.

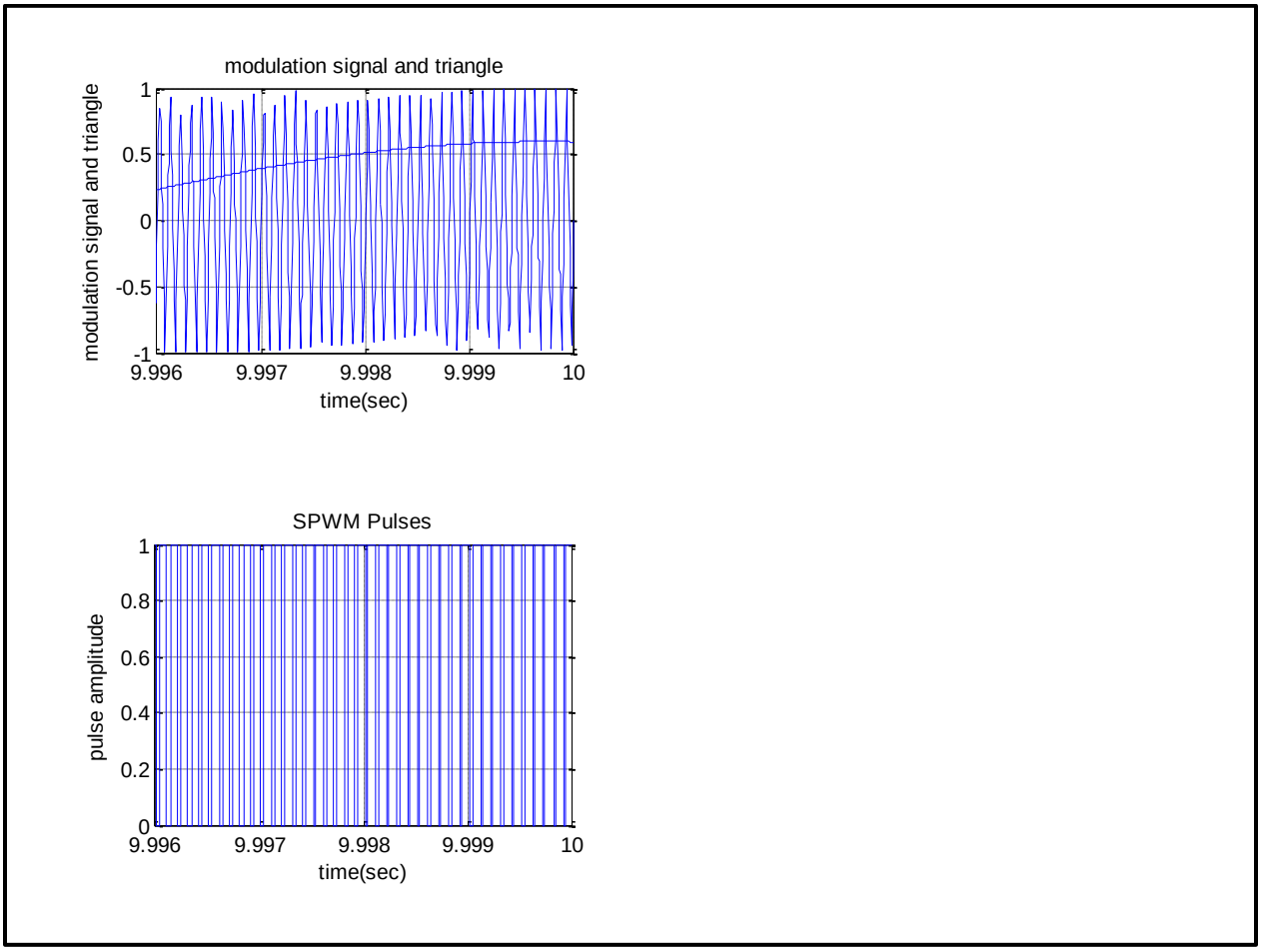


Figure 5.28: Generation of SPWM Pulses for Converter Switches (Voltage Sag Condition)

Figure 5.28 shows phase a generation of the SPWM pulses used for switching. Phase b and phase c are similar, only they are shifted by the appropriate phase angle. As explained in Section 2.2.4, the pulses are generated by comparing a sinusoidal signal with a triangular carrier signal. The magnitude and phase angle of the sinusoidal signal is related to the magnitude and phase angle of the output signal. In Simulink, the pulses are generated using a logic comparator block. The output of this block can be fixed to be high if the sinusoidal signal is equal to or greater than the carrier signal or otherwise. The former has been used in this work. The Simulink model for this result have been included in Appendix G

Normal Operation:

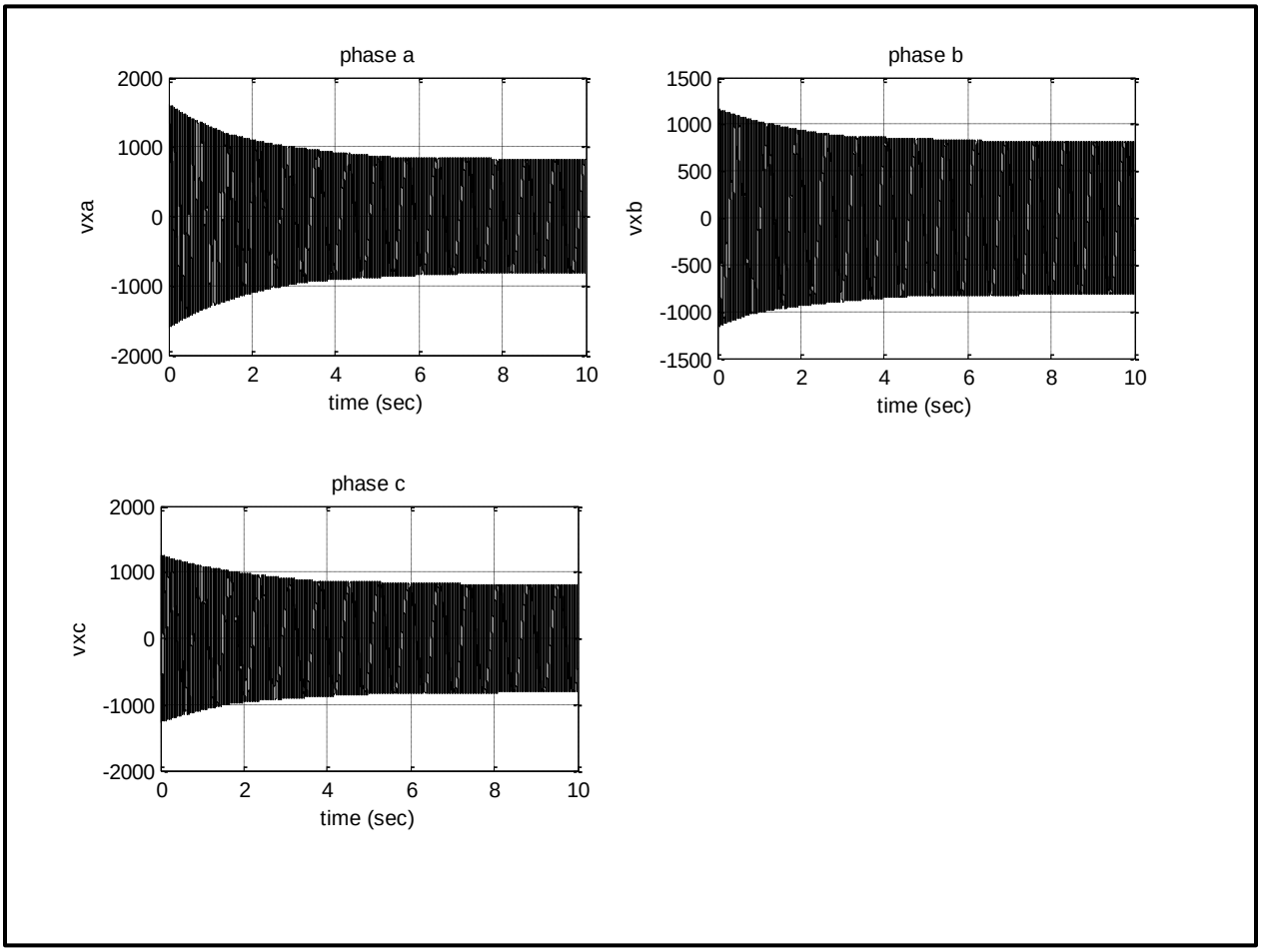


Figure 5.29: Simulation Results for Normal Operation

Figure 5.29 shows the simulation result for normal operation (i.e. $\gamma = 1$) of the voltage injected by the series inverter. For this operating point, it is seen from Figure 5.2 that the steady state voltage injected by the series inverter is about 718.8V. This value agrees with the steady state value seen in Figure 5.29. The generation of the SPWM for normal operation is shown in Figure 5.30.

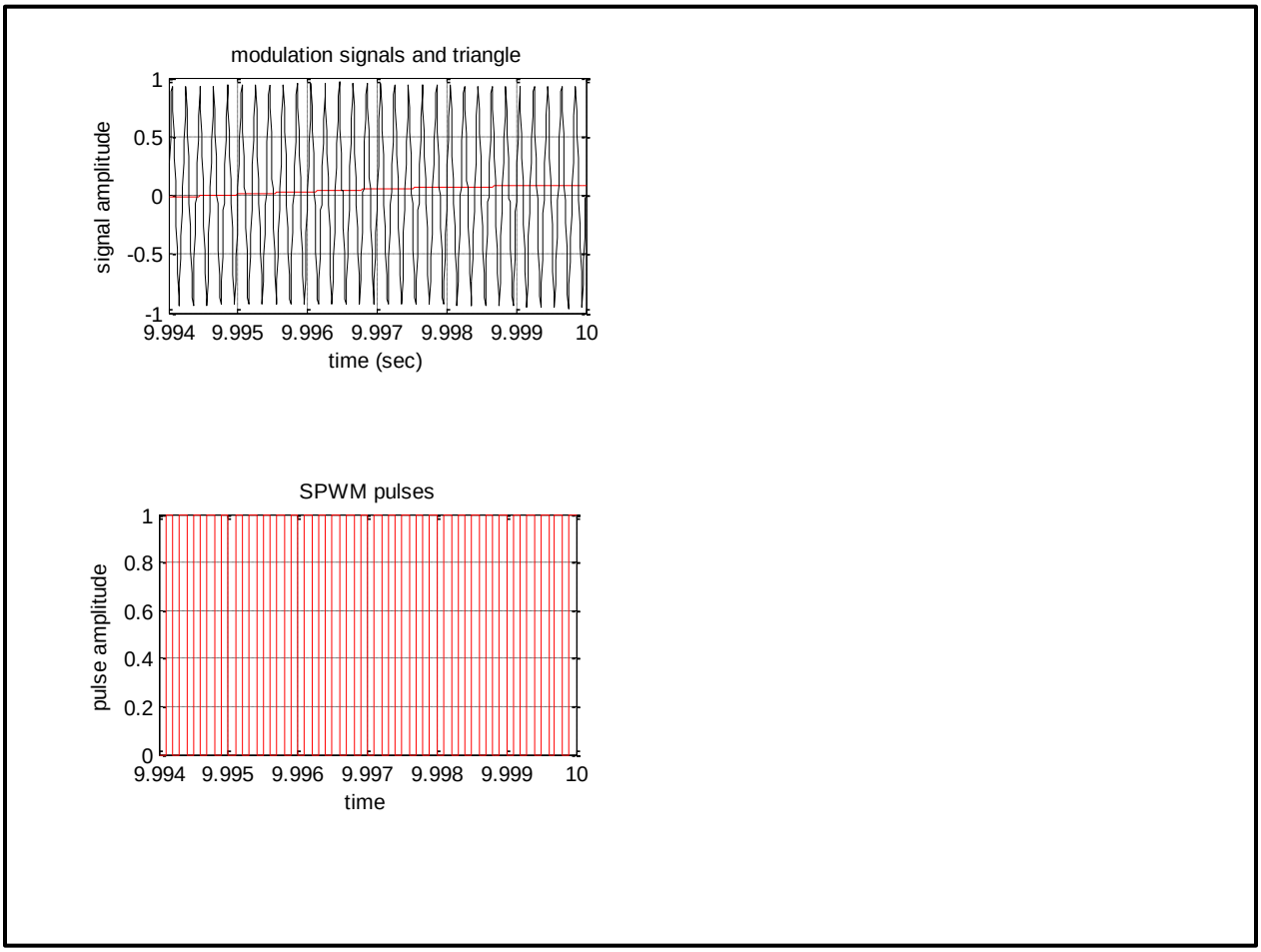


Figure 5.30: Generation of SPWM Pulses for Converter Switches (Normal Operation)

Voltage Swell:

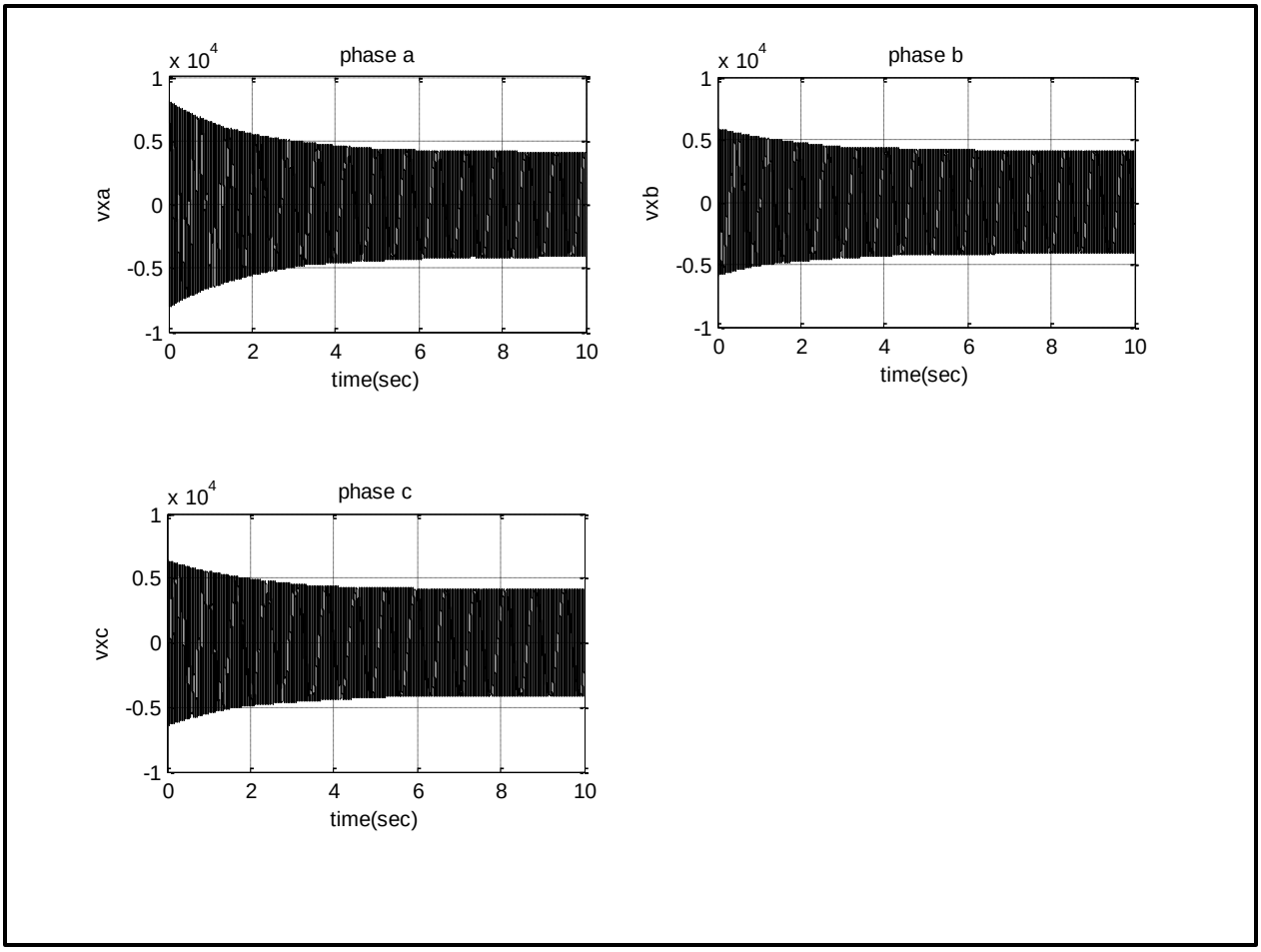


Figure 5.31: Simulation Results for Voltage Swell Condition

Figure 5.31 shows the simulation result for a voltage swell condition. Generally, voltage swell occurs for $\gamma > 1$. The result shown in Figure 5.31 is for the case of $\gamma = 1.25$ which represent a 25 percent swell condition. From Figure 5.2, the voltage injected by the series inverter for this condition is about 2741.1V. The result obtained from simulation compares well with that obtained from the steady state analysis. The little discrepancy again is due to the numerical method employed by the Simulink software and the effect of switching. The generation of the SPWM pulses for this operating point is shown in Figure 5.32

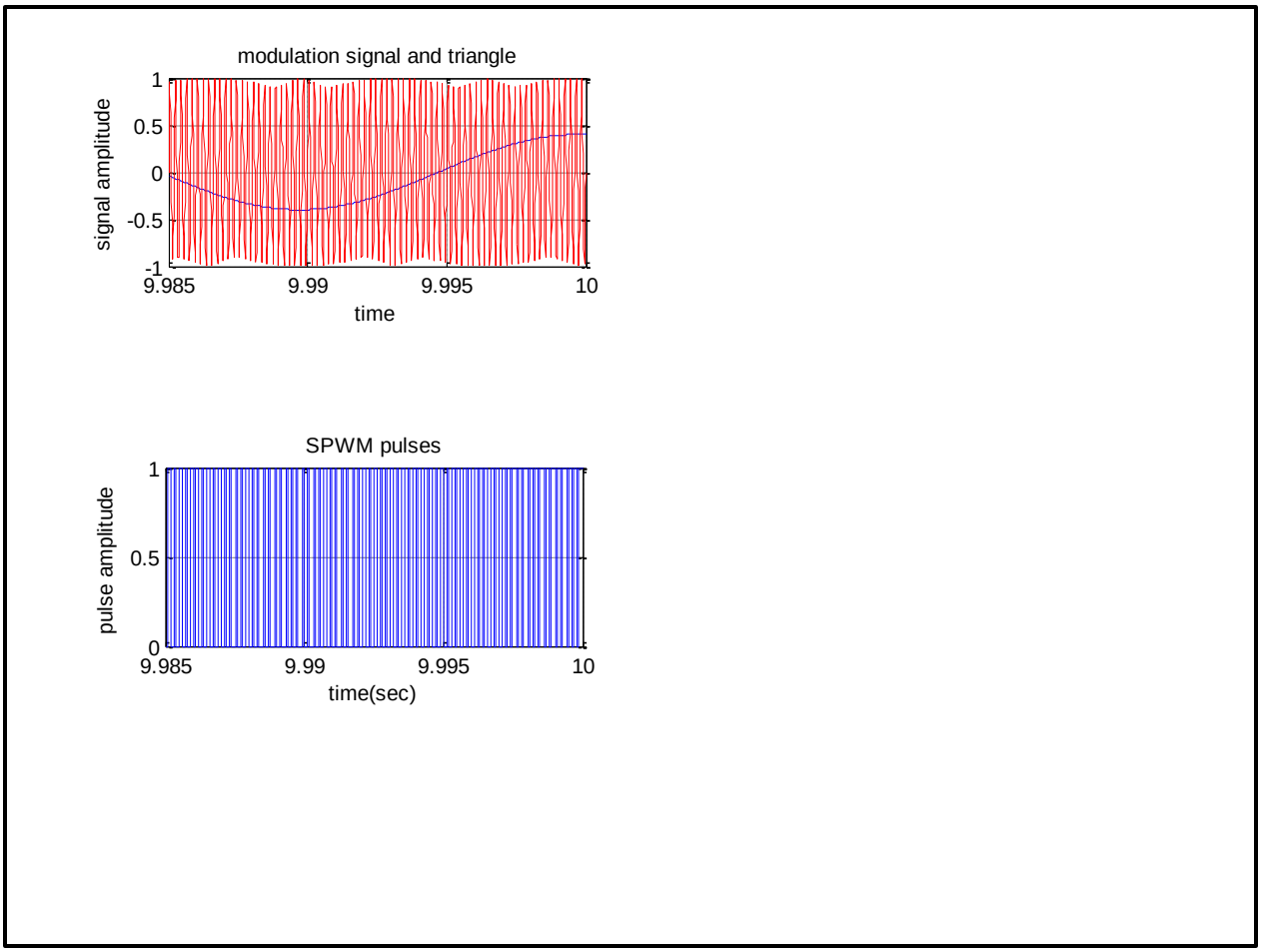


Figure 5.32: Generation of SPWM Pulses (Voltage Swell).

5.4 Conclusion

The developed model of the system in Chapter Four has been solved in this chapter. A MATLAB script has been written to obtain the response of system under different operating conditions. The power flow within the system is shown including some simulation result of certain aspects of the system.

CHAPTER SIX

CONCLUSIONAND RECOMMENDATION

This chapter presents the conclusion of the work. A summary the study is stated so also the some recommendation for further work.

6.1 Summary

In this work, the Unified Power Quality Conditioner (UPQC) has been adapted for the compensation of interruption in supply and amelioration of loss of supply. This has been made possible by the inclusion of Photo Voltaic (PV) system and Battery Energy Storage System (BESS) in the DC-link of the UPQC. The BESS is connected through a bi-directional DC-DC converter for efficient utilization of available renewable energy resource.

An in-depth analytic study of the system has been done using the system model derived from first principle, MATLAB/Simulink and the 11kV PHCN Gaskiya feeder. This study has enabled the determination of the behavior of the system under various operating conditions. The known compensating capabilities of the UPQC have been retained with the developed configuration. System shows capability to compensate for both sag and swell in utility supply voltage. Moreover, the power flow in the system shows that the reactive power requirement of the load is supplied locally by the UPQC.

Two modes of operation of the system have been defined namely: interconnected mode and islanding mode. In the interconnected mode, the load power is supplied by the utility and the combination of the PV/BESS. In this mode, the contribution of the PV/BESS depends on the

state of the utility supply and the power demand by the load. The response of the BESS depends on an additional factor which is the available solar insolation.

In the islanding mode, which occurs when there is a loss of supply, a part of the load power requirement is taken care of by the PV/BESS. The BESS acts to augment the output power of the PV. The response, therefore, depends on the solar insolation level and load power requirement.

6.2 Conclusion

This research has extended the functionality of the Unified Power Quality Conditioner (UPQC). The following significant achievements have been made:

i. The UPQC has been enhanced to compensate for voltage interruptions as well as ameliorate the effect of loss of supply at any time when these power quality events occur.

ii. The Photovoltaic system and the energy storage system collaborate real time in meeting system need thereby ensuring efficient utilization of available alternative source of energy

iii. A systematic step by step development of the system model has been carried out. This presentation in one volume of model development will serve as reference material for subsequent researchers.

6.3 Recommendation for Further Work

The following recommendations are made for the advancement of the current effort

i. The data used shows the behavior of all loads connected on the feeder. However, it would be desirable to study how the behavior of one consumer affects other consumers connected to the

same point of common coupling. So it would be an improvement of the current effort if data of the load profile of individual consumers on the network are obtained. The nature of the loads can also be ascertain and a proper load model used for a better understanding of system response.

The BESS can be sized depending on the maximum load it is to supply so that the exact behavior of the system can be observed at its extreme point.

ii. For determination of the exact duration of interruption and loss of supply that the system can compensate for, there would be need to appropriately size the PV and BESS. Factors such as ambient temperature, days of autonomy and so forth would then need to be considered. This is an area in which further work can be done.

iii. The system can be used as a Distributed Generation source. For this the PV system and the energy storage has to be properly sized. A load management strategy has to be determined either in terms of allocating time or sharing load. In the first case, it is assumed that utility power is available all the time. Hence, the user can desire, for instance, to use the PV system during peak periods and therefore avoid high cost of electricity at such periods. For the time allocation strategy, the PV system must be sized to be able to supply load maximum demand unless if some loads are non-essential.

REFERENCES

Alexander, K. and Marc, T. Thompson. (2007). *Power Quality in Electrical Systems.* McGraw-Hills Company

Akagi, H. (2006). Modern Active Filters and Traditional Passive Filters. *Bulletin of the Polish Academy of Science,* vol. 54, no. 3, pp. 255-269.

Barry, W. Williams. (Accessed 2014). *Power Electronics: Drives, Applications and Passive Components*. [Online], Available: Protect.eee.strath.ac.uk/text book

Bijoyprakash M. (2012). *Analysis of single phase SPWM Inverter*. A B.Tech Thesis Submitted to the Department of Electrical Engineering National Institute of Technology Rourkela

Byun-Moon Han, Bo-Hyung Cho, Seung-Ki Sul and Jae-Eon Kim. (2006). Unified Power Quality Conditioner for Compensation of Voltage Interruption. *Journal of Electrical Engineering and Technology,* vol. 1, no. 4, pp. 503-512.

Considine D. (1997). *Energy Technology Handbook*. McGrawhill Book Company.

Davari M., S.M. Ale-Emran., H. Yazdanpanahi and G.B. Gharehpetian. (2009). Modelling the Combination of UPQC and Photovoltaic Arrays with Mult-Input Single-Output DC-DC Converter. *IEEE Transaction on Industrial Electronics,* 978-1-4244-3811-2.

Debapriya Das, (2006). *Electric Power Systems.* New Age International (P) Limited.

El-Habrouk and Darwish M.K. (2001). Design and Implementation of a Modified Fourier Analysis Harmonic Current Computation Technique for Power Active Filters using DSPs. *IEE Proceedings on Electronics and Power Application,* vol. 148, no. 1, pp. 21-28

El-Habrouk and Darwish M.K. (2002). A New Control Technique for Active Power Filters Using a Combined Genetic Algorithm/Conventional Analysis. *IEEE Transactions on Industrial Electronics,* vol. 49, no. 1, pp. 58-28.

Fujita, H. and Akagi H. (1998). The Unified Power Quality Conditioner: The Integration of Series- and Shunt- Active Filter. *IEEE Transactions on Power Electronics,* Vol. 13, no. 2, pp. 315-322

Hossein Karimi-Davijani. (2012). *Analysis and Control of a Microgrid with Converter fed Distributed Energy Sources.* A Dissertation Presented to the Faculty of the Graduate School Tennessee Technological University.

Hossienpour M., Mohamedrezapour Y. and S. Torabzade. (2009). Combined Operation of Unified Power Quality Conditioner and Photovoltaic Array. *Journal of Applied Sciences,* vol. 9 no. 4, pp. 680-688

Ieeexplore.ieee.org/xpl/mostrecentissue.jsp?punumer=5154052. Accessed 06-05-2014.

Jayanti, N.G., Malabika Basu, Micheal F.C. and Kevin G. (2006). Rating Requirements of a Unified Power Quality Conditioner (UPQC) for Voltage Ride Through Capability Enhancement. *3rd IET International Conference on Power Electronics, Machines and Drives*, Dublin, Ireland, pp. 632-636.

Juan Manuel C.,Leopoldo Garcia F., Jan T. B., Eduardo Galvan., Ramon C. P. Guisado., Ma. Angeles Martin P., Jose Ignacio L. and Narcisco Moreno-Alfonso. (2006). Power- Electronic Systems for the Grid Integration of Renewable Energy Sources: A Survey. *IEEE Transaction on Industrial Electronics*, vol. 53, no. 4, pp. 1002-1016.

Khadem S.K.,M. Basu and M.F. Conlon. (2010). Power Quality in Grid Connected Renewable Energy Systems: Role of Custom Power Devices. *International Conference on Renewable Energies and Power Quality* Granada Spain

Khadkikar V. (2008). *Power Quality Enhancement at Distribution Level Utilizing The Unified Power Quality Conditioner(UPQC).* A PhD Thesis report presented at Ecole De Technologie Superieure University Du Quebec Canada.

Khadkikar V., Chandra A., Barry A.O. and Nguyen T.D. (2011). Power Quality Enhancement Utilising Single-Phase Unified Power Quality Conditioner: Digital Signal Processor-Based Experimental Validation. *IET Power Electronics*, vol. 4, Iss. 3, pp. 323-331.

Marcelo C. Cavalcanti., Gustavo M.S. Azevedo., Bruno A. Amaral and Fracisco A.S.Neves. (2006). Unified Power Quality Conditioner in a Grid Connected Photovoltaic System. *Electrical Power Quality and Utilization Journal* vol.12, no. 2 pp. 59-68

Maria I. M. M., Enrique R.C. and Fermin B.G. (2006). Comparison of Control Strategies for Shunt Active Power Filters in Three-Phase Four-Wire Systems. *International Conference on Renewable Energies and Power Quality*, Barcelona, Spain.

Metin Kesler and Engin Ozdemir. (2009). Simplified Control Method for Unified Power Quality Conditioner(UPQC). *International Conference on Renewable Energies and Power Quality*, Valencia Spain

Mohammad H. Rashid. (2005). *Power Electronics; Circuits, Devices and Application.* 3rd Edition, Prentice- Hall of India

Malijana Odavic, Mark Sumner, Pericle Zenehetta and John C. Clare. (2010). A Theoritical Analysis of the Harmonic Content of PWM Waveforms for Multiple Frequency Modulators. *IEEE Transaction on Power Electronics*, vol. 25, no. 1, pp. 131-141.

Ned Mohan., Tore M. Underland and Williams P. Robbins. (1995). *Power Electronics Converters Application and Design.* Second Edition Wiley and Sons Incoporated.

Paduchuri C.B. and Subhransu S.D. (2012). Design of Unified Power Quality Conditioner (UPQC) Connected to Three Phase Four Wire System. *International Journal of Computer and Electrical Engineering*, vol. 4, no. 1, pp. 60-64.

Paul C. Krause., Oleg Wasynczuk. and Scott D. Sudhoff. (2002). *Analysis of Electric Machinery and Drive Systems*. 2nd Edition IEE Press NJ USA.

Sambo A. (2005). Renewable Energy for Rural Development: The Nigerian Perspective. *ISESCO Science and Technology Vision* vol. 1, pp. 12-22

Seyed Ali Nabavi-Niaki. (1996). *Modeling and Application of Unified Power Flow Controller (UPFC) for Power Systems.* A thesis Submitted to the Graduate Department of Electrical and Computer Engineering University of Toronto.

Sheetal K. Asuri. (2010). *Modeling and Control of Sparse Converter fed Induction Motor Drives.* A thesis Submitted to the Faculty of the Graduate School Tennessee Technological University.

Woo C.L. Dong M. L. and Taeck K.L. (2010). New Control Scheme for a Unified Power Quality Compensator-Q with Minimum Active Power Injection. *IEEE Transactions on Power Delivery*, vol. 25 no. 2 pp. 1068-1076.

APPENDIX A

SYSTEM MODEL IN ABC REFERENCE FRAME

The detailed derivation of the system model is provided in this Appendix.

A.1 DISTRIBUTION SYSTEM

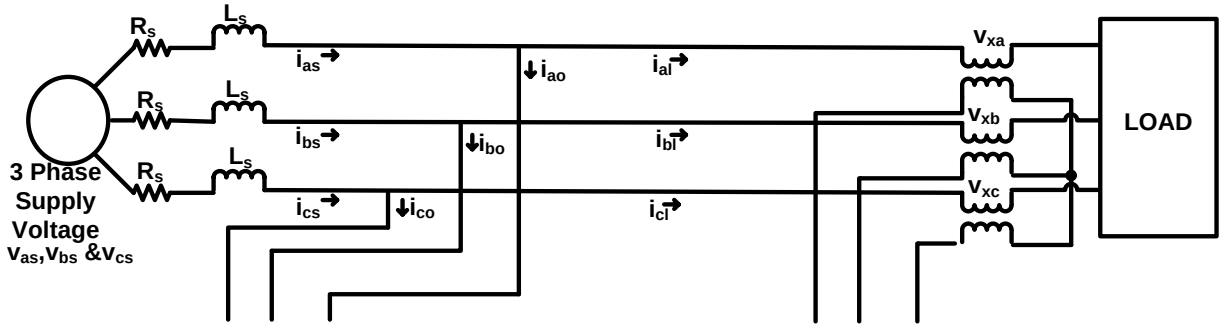


Fig. A.1 Distribution System Showing the Influence of the UPQC

Applying KVL and KCL to the network in Fig. A.1,

(A.1)

(A.2)

(A.3)

(A.4)

(A.5)

(A.6)

Where,

A.2 MODEL OF RECTIFIER

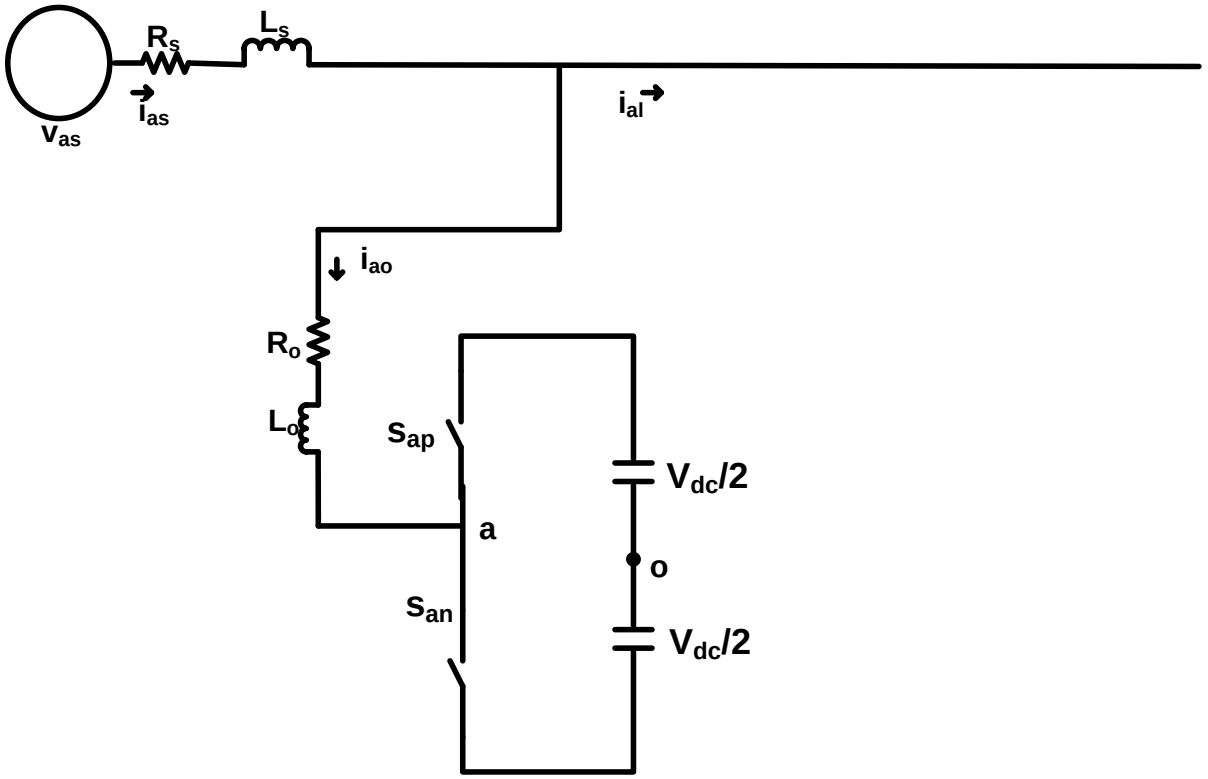


Fig. A.2: Phase A of Rectifier Connected to the Distribution Network

Consider Fig. A.2 which shows phase a of the three phases of the system. The switching devices have been replaced with ideal switches with switching functions as shown on the diagram. The rectifier operates in two modes; in mode one, In mode two,

Mode 1:

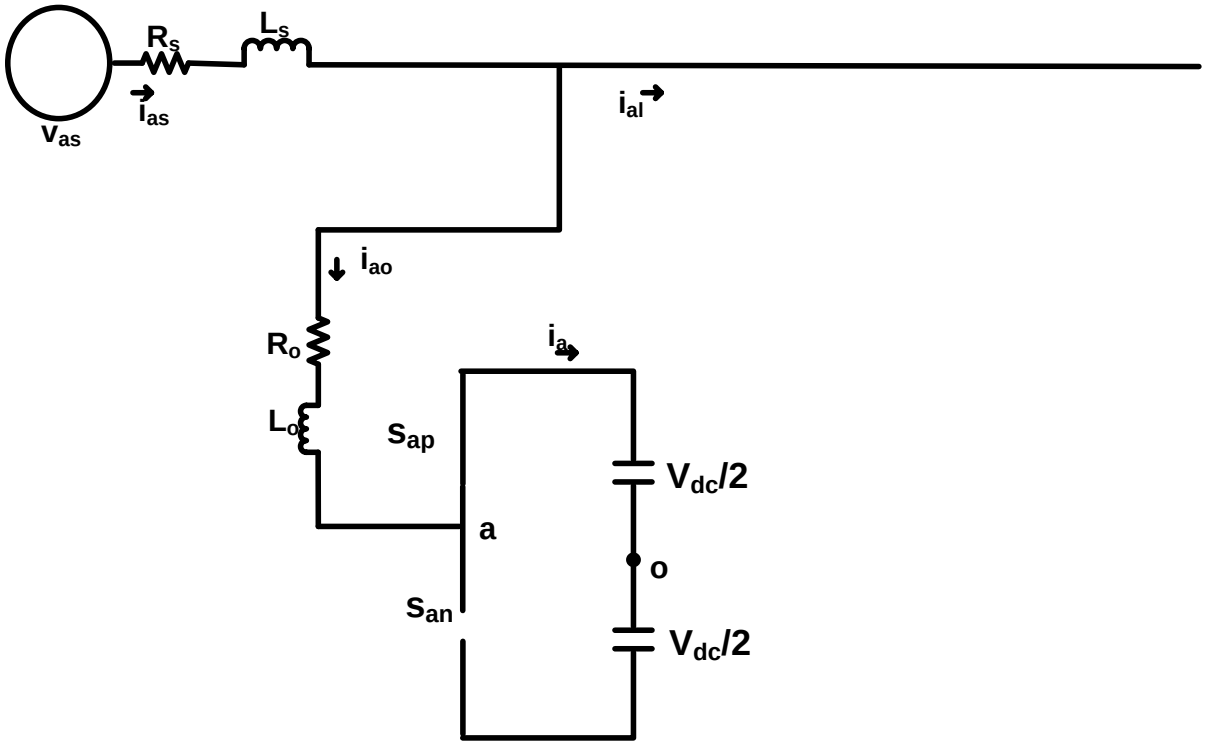


Fig. A.3: Mode One Operation of the Rectifier

Fig. A.3 shows Mode One of the operations of the Rectifier.

Applying KVL,

But, —, therefore,

— (A.7)

Mode 2:

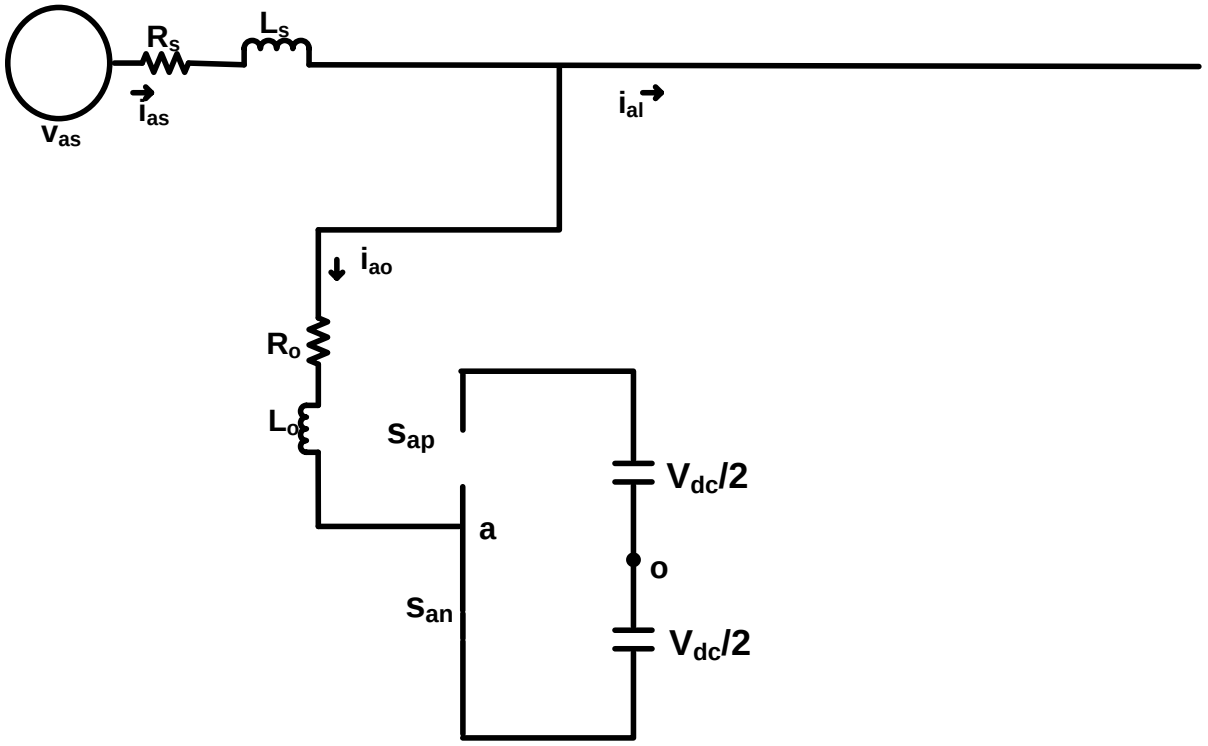


Fig. A.4: Mode Two Operation of the Rectifier

Fig. A.4 shows Mode Two of the operation of the Rectifier

Also from KVL:

But, —, therefore,

— (A.8)

Combining the two modes, i.e. multiplying equation A.7 by s_{ap} and equation A.8 by s_{an} and adding

— (A.9)

But which implies that

Hence equation A.9 becomes

— (A.10)

Substituting for equation A.10 becomes

— (A.11)

For phase b and c the equation are given below:

— (A.12)

— (A.13)

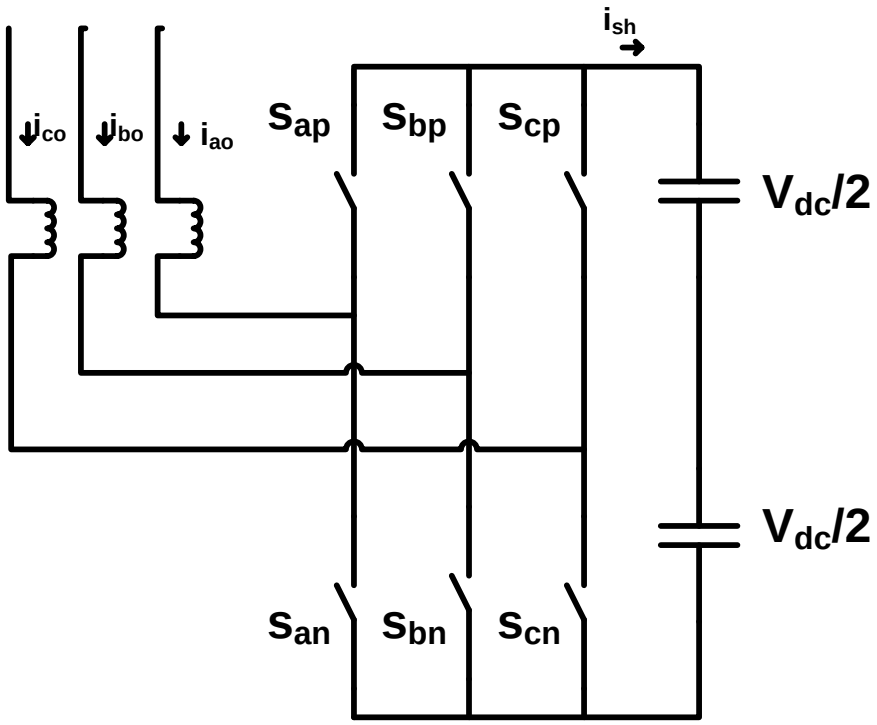


Fig. A.5 Current Flows through the Rectifier

Fig. A.5 shows the current flow in the Rectifier. From the figure,

For the three phases

(A.14)

A.3 MODEL ON INVERTER

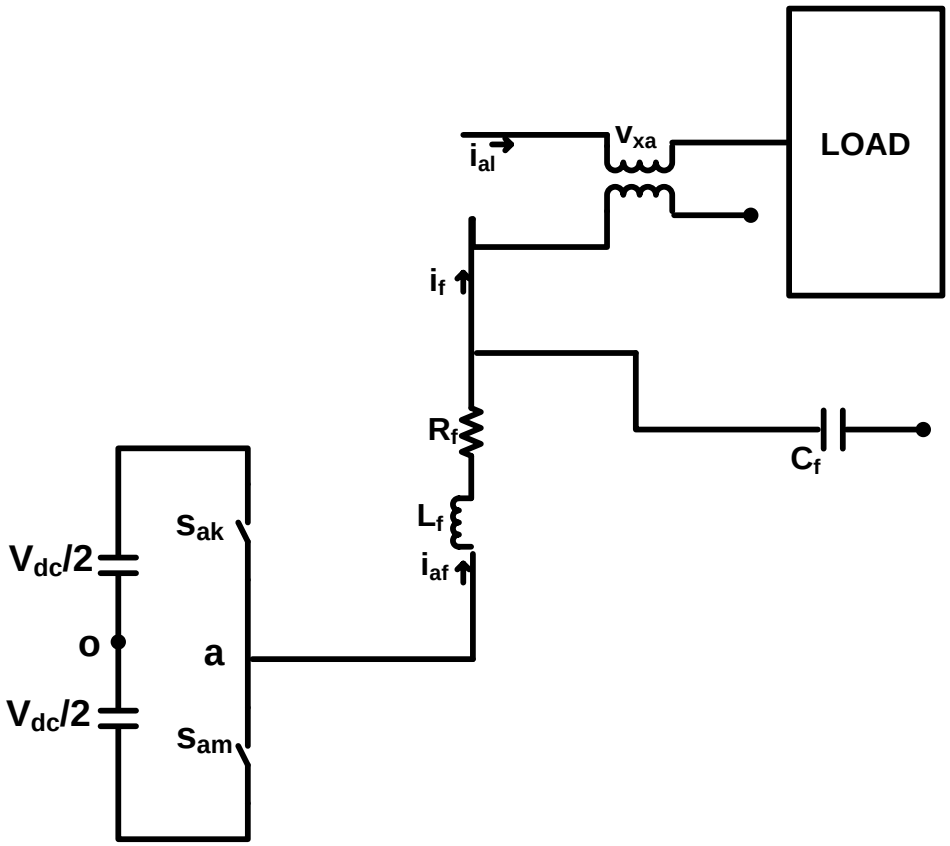


Fig. A.6 Phase a of the Inverter Connected to the Distribution Network

Consider Fig. A.6.Which shows phase (a) of the three phases of the system. The switching devices have been replaced with ideal switches with switching functions as shown on the diagram. The inverter operates in two modes; in mode one, in mode two,

Mode 1:

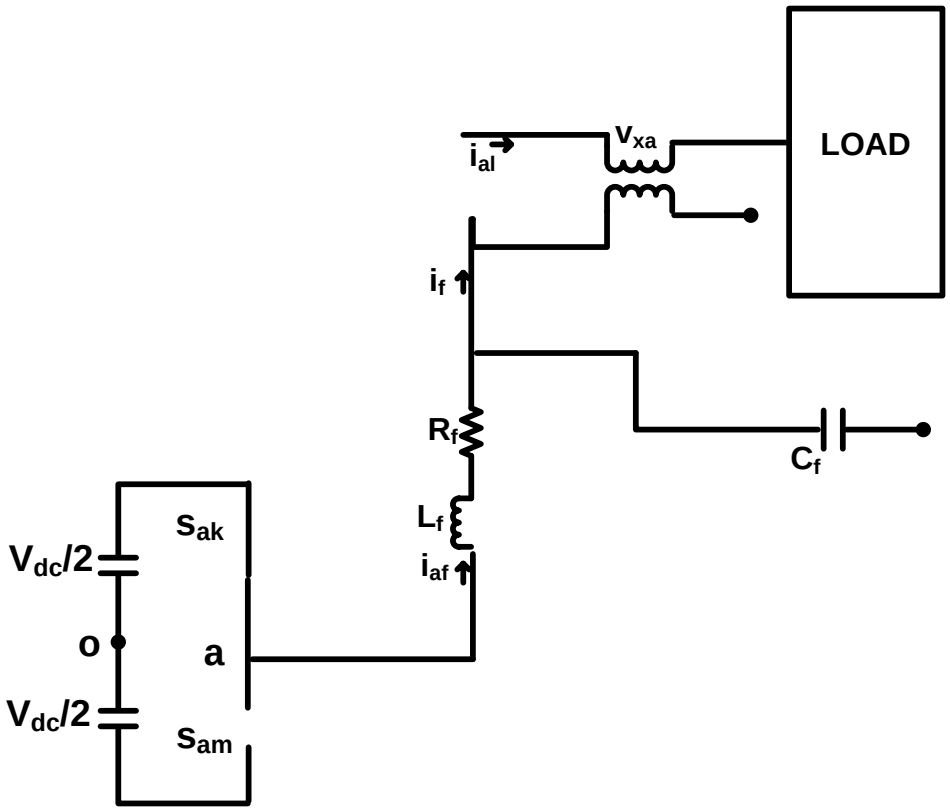


Fig. A.7: Mode One of Inverter Operation

Fig. A.7 shows the Mode One of the operation of the Inverter. Applying KVL:

–

But —, hence

— – (A.15)

From KCL:

–

But therefore,

– (A.16)

Mode 2:

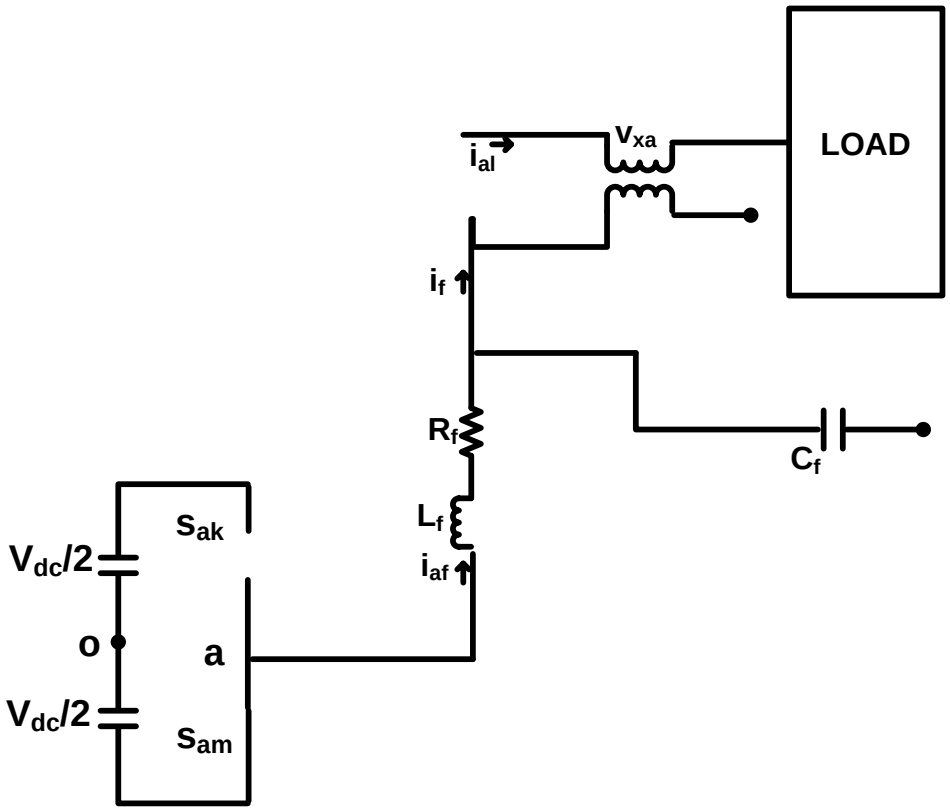


Fig. A.8 Mode Two of Inverter Operation

Fig. A.8 shows Mode Two of the operation of the Inverter from KVL:

–

But —, hence

— – (A.17)

From KCL:

– (A.18)

Combining modes 1 and 2 as in the case of the rectifier,

— – (A.19)

Now equation (A.19) becomes:

— – (A.20)

For phase (b) and (c), the equations are:

— – (A.21)

— – (A.22)

– (A.23)

– (A.24)

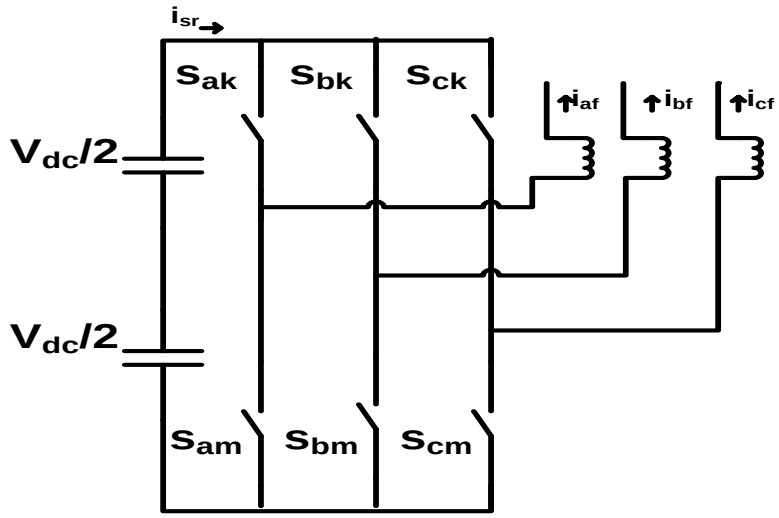


Fig. A.9: Current Flows through the Inverter

Fig. A.9 shows the current flows through the Inverter. From the figure,

(A.25)

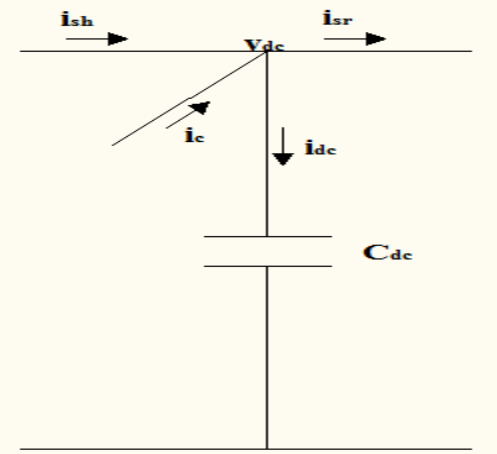


Fig. A.10: DC Link Current Flow.

Fig. A.10 shows the DC Link current flow. From the figure,

(A.26)

(A.27)

A.4 MODEL OF DC-DC CONVERTERS

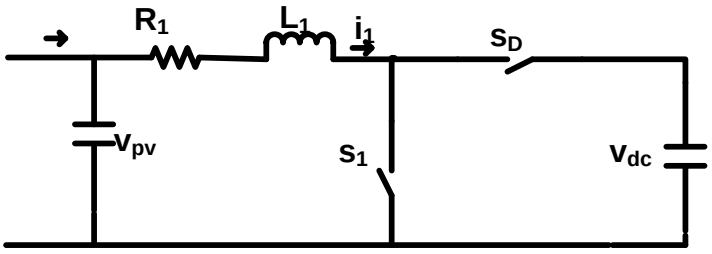


Fig. A.11: DC-DC Converter

Fig. A.11 shows a dc-dc converter in which the switching devices have been replaced by ideal switches. Like the rectifier and inverter, the dc-dc converter operates in two modes. In mode one, s_1 is ON while s_D is OFF, in mode two s_1 is OFF while s_D is ON.

Mode 1:

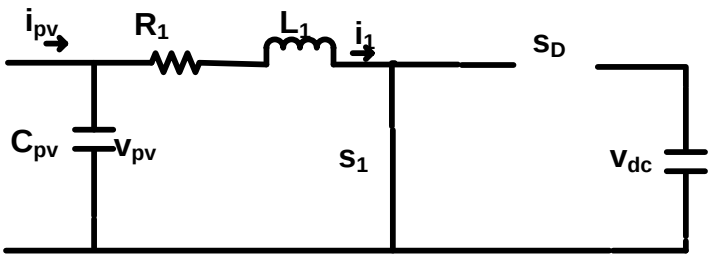


Fig. A.12: DC-DC Converter in Mode One Operation

Applying KVL to Fig. A.12;

(A.28)

From KCL:

(A.29)

Mode 2:

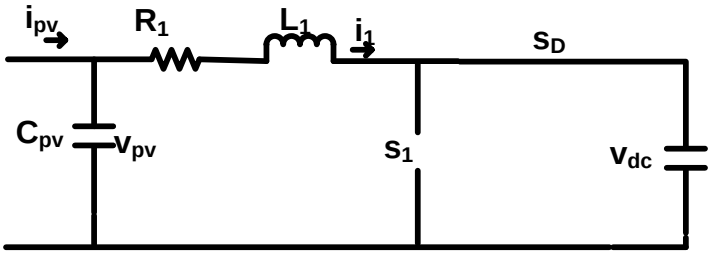


Fig. A.13 DC-DC Converter in Mode Two Operation

Applying KVL to the Circuit in figure A.12

(A.30)

(A.31)

Combining the two modes

(A.32)

But

Equation A.26 becomes,

(A.33)

(A.34)

For the DC-DC converter connected to the battery output, the derivation of the model follows the same process. Hence, we have:

(A.35)

(A.36)

APPENDIX B

MODEL OF SYSTEM IN QDO REFERENCE FRAME

The model of the system derived in appendix A is here transformed to the arbitrary reference frame. The equations are first written in compact form and then the transformation is carried out.

Let,

(B.1)

The relevant equations from appendix A are repeated below:

(A.1)

(A.2)

(A.3)

(A.4)

(A.5)

(A.6)

— (A.11)

— (A.12)

(A.13)

(A.20)

(A.21)

(A.22)

(A.18)

(A.23)

(A.24)

(A.27)

With the definitions above, equations (A.1) to (A.3) can be written in compact form as:

Note:

(B.2)

Equations (A.4) to (A.6) as:

(B.3)

(A.11) to (A.13) as:

(B.4)

(A.20) to (A.22) as:

(B.5)

(A.18), (A.23) and (A.24) as:

(B.6)

And finally (A.27) as:

(B.7)

Collecting the new equations together:

(B.2)

(B.3)

(B.4)

(B.5)

(B.6)

(B.7)

These equations will now be transformed to the arbitrary reference frame. But first the transformation will be demonstrated. Given the three phase balanced voltages below.

The arbitrary reference frame voltages are obtained as:

=

(B.8)

(B.9)

(B.10)

(B.11)

The following trigonometric identities are pertinent:

Applying these identities to equations (B.9) to (B.11) results in:

And

.

Now choosing the arbitrary reference frame such that it rotates at the same frequency with the physical reference frame, i.e. , then

And

.

The initial angle of the reference frame could also be chosen such that it is the same as the initial angle of the physical reference frame i.e. in which case:

.

Going back to equations (B.2) to (B.7), multiplying equation (B.1) by :

(B.12)

From equation (B.1) making the following substitutions

Gives:

Now for ,

(B.13)

(B.14)

Spreading this out therefore, for a three phase balanced system:

(B.15)

(B.16)

For equation (B.3)

And finally

; spreading this out for a three phase balanced system,

(B.17)

(B.18)

For equation (B.4),

Spreading this out again for a three phase balanced system:

But

(B.19)

(B.20)

For equation (B.5)

; Spreading this equation out for a three phase balanced system:

But ; hence,

(B.21)

Similarly,

(B.22)

For equation (B.6):

And spreading this out for a three phase balanced system:

(B.23)

(B.24)

And finally for equation (B.7)

From matrix algebra:

Hence:

Now

,

Relevant trigonometric identities:

Therefore;

; Therefore,

For a three phase balanced system and substituting the values of ,

(B.25)

APPENDIX C

MODEL EQUATIONS IN COMPLEX FORM

The steady state equations are obtained by setting

The steady state equations are gathered as follows:

(C.1)

(C.2)

(C.3)

(C.4)

(C.5)

(C.6)

(C.7)

(C.8)

(C.9)

(C.10)

(C.11)

The following definitions are made:

Multiplying equation (C.2) by j and adding to equation (C.1) we have:

Then;

(C.12)

Multiplying equation (C.4) by j and adding to (C.3):

(C.13)

Multiplying equation (C.6) by j and adding to (C.5)

—

;

—

— (C.14)

Multiplying equation (C.8) by j and adding to (C.7):

— –

— –

— – (C.15)

Multiplying equation (C.10) by j and adding to (C.9):

– –

–

And so,

–

– (C.16)

Finally,

– – (C.17)

Collecting the equations together:

(C.12)

(C.13)

— (C.14)

— – (C.15)

– (C.16)

– – (C.17)

APPENDIX D

DC-DC CONVERTER PARAMETER DETERMINATION

This appendix shows how the equations for the dc-dc converter discussed under the design considerations were arrived at.

D.2 DC-DC CONVERTERS

For the PV solar panel system and the connected dc-dc converter, it's been assumed that there is an internal Maximum Power Point algorithm and hence for each solar insolation used, the voltage at maximum power is determined from the figure 5.13 and used and the current calculated from equation (4.48) the duty ratio of the connected dc-dc converter is thereby fixed at two discrete values determined by the input voltage at the two prevalent solar insolation and the design voltage of the dc link. Hence for the analysis in this section, only model of the dc-dc converter connected to the battery system shall be used and the dc-dc converter connected to the solar cells is taken to be the same as that connected to the batteries. Figure (D.1) below gives a detail view of events at the output of the dc-dc converter.

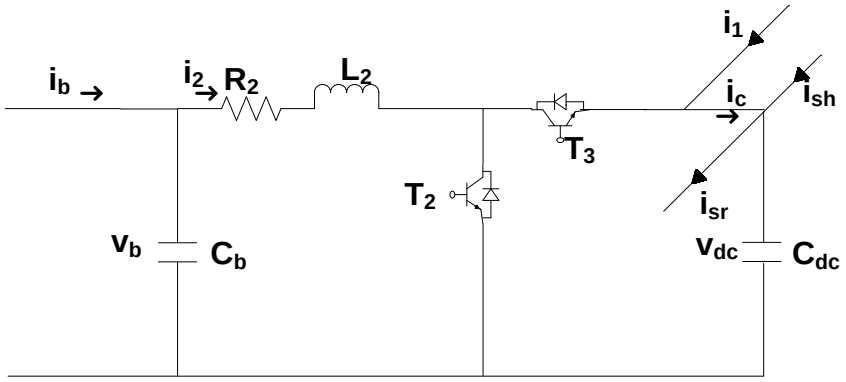


Fig. D.1 DC-DC Converter Showing Details of Interactions with other parts of the Studied System

For mode 1:

(D.1)

(D.2)

(D.3)

And for mode 2:

(D.4)

(D.5)

(D.6)

Averaging states over a period.

From equation (D.1)

(D.7)

And from equation (D.4)

(D.8)

From equations (D.7) and (D.8)

(D.9)

But;

(D.10)

Substituting (D.10) into (D.9) and simplifying

(D.11)

From (D.7) and (D.8)

(D.12)

(D.13)

Adding equations (D.12) and (D.13) and noting that ;

(D.14)

(D.15)

From equations (D.3) and (D.6)

(D.16)

(D.17)

Substituting in (D.16) and (D.17)

(D.18)

(D.19)

The capacitor can be obtained from the equation below (Muhammad H.R., 2005):

(D.20)

From figure D.1

(D.21)

(D.22)

But

(D.23)

Now from (D.12)

(D.24)

Dividing (D.24) by (D.23)

(D.25)

Hence,

(D.26)

The maximum value of occurs for the least value of and least value for . , is determined for a ripple factor of 2%.

(D.27)

(D.28)

From equations (D.28) and (D.29) we obtained

(D.29)

Note:

APPENDIX E

HOURLY SOLAR INSOLATION IN ZARIA

NASA Surface meteorology and Solar Energy - Available Tables

Latitude 11.067 / Longitude 7.7 was chosen.

Geometry Information

Elevation: **559** meters
taken from the
NASA GEOS-4
model elevation

Northern boundary
12

Western boundary
7

Center
Latitude **11.5**
Longitude **7.5**

Eastern boundary
8

Southern boundary
11

Parameters for Sizing and Pointing of Solar Panels and for Solar Thermal Applications:

Monthly Averaged Insolation Incident On A Horizontal Surface At Indicated GMT Times (kW/m^2)

Lat 11.067 Lon 7.7	Jan	Feb	Mar	Apr	May	Jun	Jul	Aug	Sep	Oct	Nov	Dec
Average@00	n/a	n/a	n/a	n/a	n/a	n/a	n/a	n/a	n/a	n/a	n/a	n/a
Average@03	n/a	n/a	n/a	n/a	n/a	n/a	n/a	n/a	n/a	n/a	n/a	n/a
Average@06	0.04	0.05	0.06	0.09	0.10	0.09	0.07	0.06	0.08	0.08	0.08	0.06
Average@09	0.52	0.56	0.63	0.65	0.63	0.56	0.50	0.47	0.56	0.62	0.62	0.55
Average@12	0.79	0.88	0.90	0.89	0.86	0.79	0.71	0.67	0.75	0.80	0.79	0.76
Average@15	0.41	0.48	0.49	0.47	0.42	0.43	0.41	0.37	0.36	0.35	0.36	0.36
Average@18	0.01	0.02	0.02	0.02	0.02	0.02	0.02	0.02	0.01	0.00	0.00	0.00
Average@21	n/a	n/a	n/a	n/a	n/a	n/a	n/a	n/a	n/a	n/a	n/a	n/a

APPENDIX F

PROGRAM LISTING

F.1 UPQC WITHOUT LIMITATION

```
clear all
Rs=1.6976;
t=(1/3);
Ls=0.0143;
Rf=0.004;
Lf=0.004;
Ro=0.004;
Lo=1;
vdc=40000;
vqs=11000;
vql=10958;
vdl=958.7;
vqdl=complex(vql,vdl);
vqdl2=repmat(vqdl,3,21);
Pl=[880000 1320000 1496000];
Ql=[-660000 -990000 -1122000];
Sl=complex(Pl,Ql);
Iqdl=(2/3)*(conj(Sl)/conj(vqdl));
% transpose of Iqdl
tIqdl=Iqdl.';
%dimensioning load current for the variations in voltage
iqdl=repmat(tIqdl,1,21);
w=2*pi*50;
Xs=-w*Ls;
Xf=-w*Lf;
Xo=-w*Lo;
Cf=34.65e-6;
Zs=complex(Rs,Xs);
Zf=complex(Rf,Xf);
Zo=complex(Ro,Xo);
n=0.4:0.05:1.4;
vs=n*vqs;
rvs=repmat(vs,3,1);
% var is (vqdl the load voltage minus the source voltage as it varies)
var=vqdl-vs;
% still var but properly dimensioned for the three different load
% conditions
VAR=repmat(var,3,1);
A=((1/t)-((w*Zf*Cf*1i)/t));
B=((-1i*w*Cf)/t);
E=Zs+Zo;
K=real((A*(abs(Zs))^2*conj(B)+E));
aa=(t*Zf*conj(B)*conj(Zs)*iqdl);
bb=(A*conj(B)*conj(Zs)*VAR);
cc=(t*A*Zs*conj(iqdl));
dd=(A*Zs*conj(B)*conj(VAR));
ee=(rvs+(Zo*iqdl)+(E*conj(iqdl)));
m=(aa+bb+cc+dd-ee);
M=real(m);s
ff=((t)^2*Zf*(abs(iqdl)).^2);
```

```
gg=(t*Zf*conj(B)*(conj(VAR).*iqdl));
hh=(t*A*(VAR.*conj(iqdl)));
ii=(A*conj(B)*(abs(VAR)).^2);
jj=(rvs.*conj(iqdl));
kk=(Zo*(abs(iqdl)).^2);
u=(ff+gg+hh+ii+jj+kk);
N=real(u);
iqs1=((-M+sqrt(M.^2-4*K*N))/(2*K));
iqs2=((-M-sqrt(M.^2-4*K*N))/(2*K));
vxqd=(Zs*iqs2+(vqdl2-rvs));
Vxqd=abs(vxqd);
iqdo=(iqs2-iqdl);
Iqdo=abs(iqdo);
iqdf=(t*iqdl+B*vxqd);
Iqdf=abs(iqdf);
mqdp=((2/vdc)*(rvs-(E*iqs2)+(Zo*iqdl)));
mqdk=((2/vdc)*((t*Zf*iqdl)+(A*Zs*iqs2)+(A*VAR)));
Mqdp=abs(mqdp);
Mqdk=abs(mqdk);
figure(1);
plot(n,Vxqd); grid on; title('voltage injected by series inverter')
ylabel('vxq(V)'); xlabel('\gamma');
figure(2);
plot(n,iqs2); grid on; title('supply current at different load power')
ylabel('iqs(A)'); xlabel('\gamma');
figure(3);
plot(n,Mqdk); grid on; title('series converter modulation index')
ylabel('Mk'); xlabel('\gamma');
figure(4);
plot(n,Mqdp); grid on; title('shunt converter modulation index')
ylabel('Mp'); xlabel('\gamma')
figure(5);
plot(n,Iqdo); grid on; title('current drawn by shunt inveterter at different
load power')
ylabel('Io(A)'); xlabel('\gamma')
figure(6);
plot(n,Iqdf); grid on; title('series iverter current at different load
power')
ylabel('If(A)'); xlabel('\gamma')
```

F.2 POWER FLOW STUDIES

```
clear all
% determining power flows.
Rs=1.6976;
t=(1/3);
Ls=0.0143;
Rf=0.004;
Lf=0.004;
Ro=0.004;
Lo=1;
vdc=60000;
vqs=11000; %1100;
vql=10958;
vdl=958.7;
```

```
vqdl=complex(vql,vdl);
vqdl2=repmat(vqdl,1,31);
vqs2=repmat(vqs,1,31);
S=1100000:25000:1870000;
Pl=0.8*S;%[10000 10000 10000];
Ql=-0.6*S;%[-6000 -8000 -10000];
Sl=complex(Pl,Ql);
iqdl=(2/3)*(conj(Sl)/conj(vqdl));
w=2*pi*50;
Xs=-w*Ls;
Xf=-w*Lf;
Xo=-w*Lo;
Cf=34.65e-6;
Zs=complex(Rs,Xs);
Zf=complex(Rf,Xf);
Zo=complex(Ro,Xo);
n=0.4:0.05:1.4;
vs=vqs;
vs1=repmat(vs,1,31);
% var is (vqdl the load voltage minus the source voltage as it varies)
var=vqdl-vs1;
Pl1=-(1/1e6)*Pl;
Ql1=-(1/1e6)*Ql;
A=((1/t)-((w*Zf*Cf*1i)/t));
B=((-1i*w*Cf)/t);
E=Zs+Zo;
K=real((A*(abs(Zs))^2*conj(B)+E));
aa=(t*Zf*conj(B)*conj(Zs)*iqdl);
bb=(A*conj(B)*conj(Zs)*var);
cc=(t*A*Zs*conj(iqdl));
dd=(A*Zs*conj(B)*conj(var));
ee=(vs1+(Zo*iqdl)+(E*conj(iqdl)));
m=(aa+bb+cc+dd-ee);
M=real(m);
ff=((t)^2*Zf*(abs(iqdl)).^2);
gg=(t*Zf*conj(B)*(conj(var).*iqdl));
hh=(t*A*(var.*conj(iqdl)));
ii=(A*conj(B)*(abs(var)).^2);
jj=(vs*conj(iqdl));
kk=(Zo*(abs(iqdl)).^2);
u=(ff+gg+hh+ii+jj+kk);
N=real(u);
iqs1=((-M+sqrt(M.^2-4*K*N))/(2*K));
iqs2=((-M-sqrt(M.^2-4*K*N))/(2*K));
vxqd=(Zs*iqs2+(vqdl2-vs1));
iqdo=(iqs2-iqdl);
iqdf=(t*iqdl+B*vxqd);
Ss=(1/1e6)*(3/2)*(vs*conj(iqs2));
So=-(1/1e6)*(3/2)*(vs*conj(iqdo));
Sf=(3/2)*(1/1e6)*(vxqd.*conj(iqdl));
Ps=real(Ss);
Qs=imag(Ss);
Po=real(So);
Qo=imag(So);
Pf=real(Sf);
Qf=imag(Sf);
VA_load=(1/1e6)*abs(Sl);
```

```
VA_supply=(1/1e6)*(vqs2.*iqs2);
VA_shunt=(1/1e6)*(vqs2.*abs(iqdo));
%VA_series=(1/1e6)*(abs(vxqd).*abs(iqdf));
figure(1);
plot(Pl1,Ps,'-b'); grid on;
hold on
plot(Pl1,Po,'-r');
plot(Pl1,Pf,'-g')
title('avarage power flow');
ylabel('MW'); xlabel('Load avarage power(MW)')
hold off
figure(2);
plot(Ql1,Qs,'-b'); grid on;
hold on
plot(Ql1,Qo,'-r');
plot(Ql1,Qf,'-g')
title('reactive power flow')
ylabel('MVAR'); xlabel('Load reactive power (MVAR)');
hold off
figure(3);
plot(VA_load,VA_supply, '-b'); grid on;
hold on
plot(VA_load,VA_shunt, '-r')
%plot(VA_load,VA_series, '-g')
title('apparent power flow')
ylabel('MVA'); xlabel('Load Apparent Power (MVA)')
```

F.3 LIMITATION STUDIES

```
clear all
Rs=1.6976;
t=(1/3);
Ls=0.0143;
Ro=0.004;
Lo=1;
w=2*pi*50;
Xs=-w*Ls;
Xo=-w*Lo;
Zs=complex(Rs,Xs);
Zo=complex(Ro,Xo);
E=Zs+Zo;
vdc=6000;
vs=11000;
vql=10958;
vdl=958.7;
vqdl=complex(vql,vdl);
S=1870000;
Pl=0.8*S;
Ql=-0.6*S;
Sl=complex(Pl,Ql);
iqdl=(2/3)*(conj(Sl)/conj(vqdl));
IQDL=abs(iqdl);
I_qdl=-IQDL:8:IQDL;
A=[111.6652 113.3348];
i_qdl=[I_qdl,A];
iqdo=-75:5:75;
```

```
n=(1/vs)*((vdc/2)+(abs(E)*iqdo)+(abs(Zs)*i_qdl));
plot(n,iqdo); grid on; title('limits of variation of supply voltage with peak
rating of shunt inverter')
ylabel('shunt inverter current'); xlabel('\gamma')
```

F.4 UPQC WITH PV/BESS

```
clear all
Rs=1.6976;%0.1;
t=(1/3);
I=100;
Ls=14.3e-3;%4e-3;
Rf=0.004;%0.01;
Lf=4e-3;
Ro=0.004;%0.01;
Lo=0.09;%4e-3;
R2=0.004;%0.096;
w=2*pi*50;
Xs=-w*Ls;
Xf=-w*Lf;
Xo=-w*Lo;
Cf=60e-6;
Zs=complex(Rs,Xs);
Zf=complex(Rf,Xf);
Zo=complex(Ro,Xo);
vdc=60000;
v_b=20000;%35000;
vqs=[1100;4400;11000;13200];
vs=repmat(vqs,1,32);
vql=10958;
vdl=958.7;
vqdl=complex(vql,vdl);
%S=1100000:25000:1870000;
Pl=1.4e6:15161:1.87e6;
Ql=-858000;
Q_L=repmat(Ql,1,32);
Sl=complex(Pl,Ql);
iqdl=(2/3)*(conj(Sl)/conj(vqdl));
i_qdl=repmat(iqdl,4,1);
i_do=-imag(iqdl);
Io=62.4869;%70;%77;
i_qo=sqrt(Io.^2-i_do.^2);
iqdo=complex(i_qo,i_do);
i_qdo=repmat(iqdo,4,1);
i_qs=repmat(I,4,32);%i_qdl+i_qdo;
B=-(1/t)*(w*Cf*1i);
vxqd=(Zs*i_qs-vs)+vqdl;
Vx=abs(vxqd);
Io=abs(i_qdo);
Is=abs(i_qs);
i_qdf=t*i_qdl+B*vxqd;
If=abs(i_qdf);
m_qdp=(2/vdc)*(vs-(Zs*i_qs)-(Zo*i_qdo));
m_qdk=(2/vdc)*(Zf*i_qdf+((1/t)*vxqd));
Mp=abs(m_qdp);
Mk=abs(m_qdk);
Ib=15.726;
```

```
I_B= repmat(Ib,4,32);
i_c=(3/4)*(real(m_qdk.*conj(i_qdf))- real(m_qdp.*conj(i_qdo)));
Ipv=2.6399;%20.475;%38.118;%20.475;%38.118;%2.6399%18;
i_pv=repmat(Ipv,4,32);
i_b=(i_c-i_pv);
S_L=(1/1e6)*Pl;
k_b=(I_B-abs(i_b))./15.726;
figure(1);
plot(S_L,Vx); grid on; title('voltage injected by series inverter with
variatio of laod at different supply voltage')
ylabel('Vx(V)'); xlabel('Load real power(MW)');
figure(2);
plot(S_L,Is); grid on; title('peak supply current with varaition of load at
different supply voltage')
ylabel('Is(A)'); xlabel('Load real power(MW)');
figure(3);
plot(S_L,Mp); grid on; title('shunt converter modulation index with variation
of load at different supply voltage')
ylabel('Mp'); xlabel('Load real power(MW)');
figure(4);
plot(S_L,Mk); grid on; title('series converter modulation index with
variation of load at different supply voltage')
ylabel('Mk'); xlabel('Load real power(MW)')
figure(5);
plot(S_L,If); grid on; title('series inverter current with variation of load
at different supply voltage')
ylabel('If(A)'); xlabel('Load real power(MW)')
figure(6);
plot(S_L,i_b); grid on; title('b: battery current at different supply voltage
with variation in load real power')
ylabel('Ib(A)'); xlabel('Load real power(MW)')
figure(7);
plot(S_L,k_b); grid on; title('battery duty ratio')
ylabel('kb'); xlabel('Load real power(MW)')
```

F.5 ISLANDING MODE POSSIBILITIES A AND B

POSSIBILITY A

```
clear all
Rs=1.6976;%0.1;
t=(1/3);
Ls=14.3e-3;%4e-3;
Rf=0.004;%0.01;
Lf=4e-3;
Ro=0.004;%0.01;
Lo=0.09;%4e-3;
w=2*pi*50;
vdc=22500;%40000;
vqs=11000;
vql=10958;
vdl=958.7;
vqdl=complex(vql,vdl);
Pl=0:100:1494000;
Ql=-858000;
Sl=complex(Pl,Ql);
i_qdl=(2/3)*(conj(Sl)/conj(vqdl));
i_ql=real(i_qdl);
```

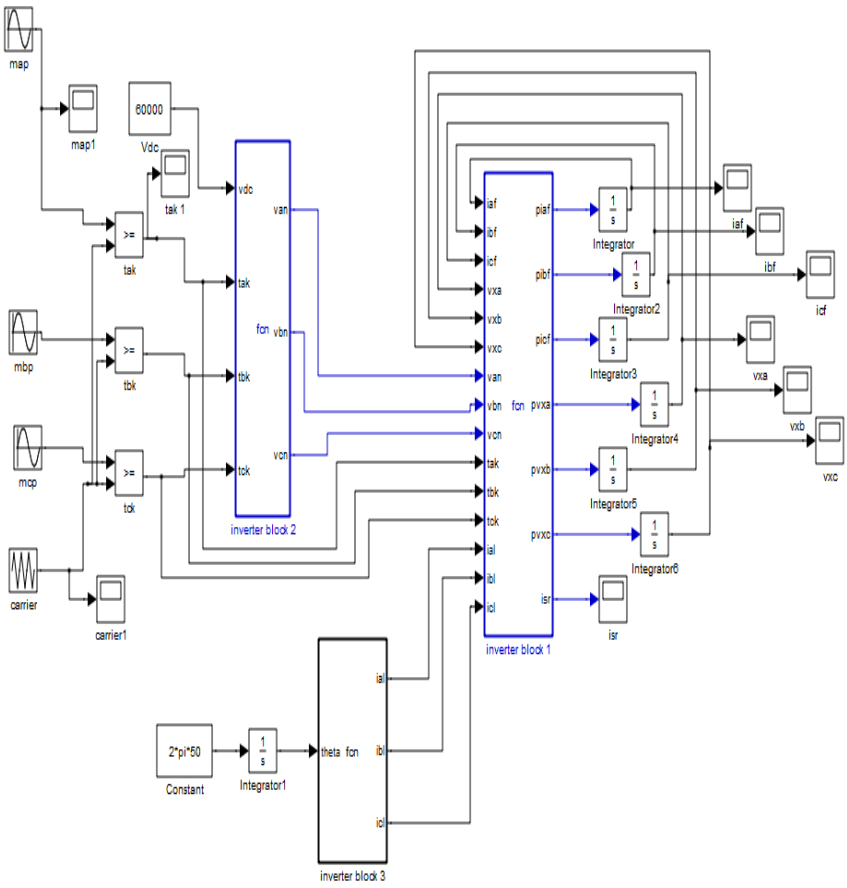
```
i_dl=imag(i_qdl);
m_qp=(2/vdc)*((Ro*i_ql)+(w*Lo*i_dl)+vql);
m_dp=(2/vdc)*((Ro*i_dl)-(w*Lo*i_ql)+vdl);
i_c=(3/4)*(m_qp.*i_ql+m_dp.*i_dl);
i_pv=2.6399;%2.6399;%20.475;%2.6399;38.118;
i_b=(i_c-i_pv);
Pln=(1/1e6)*Pl;
plot(Pln,i_b); grid on; title('plot of battery current vs load real power')
ylabel('Ib(A)'); xlabel('Load real power(MW)')
```

POSSIBILITY B

```
clear all
Rs=1.6976;%0.1;
t=(1/3);
Ls=14.3e-3;%4e-3;
Rf=0.004;%0.01;
Lf=4e-3;
Ro=0.004;%0.01;
Cf=60e-6;
Lo=0.09;%4e-3;
w=2*pi*50;
vdc=22500;%40000;
vqx=10958;
vdx=958.7;
vqdl=complex(vqx,vdx);
Pl=0:100:1494000;
Ql=-858000;
Sl=complex(Pl,Ql);
i_qdl=(2/3)*(conj(Sl)/conj(vqdl));
i_ql=real(i_qdl);
i_dl=imag(i_qdl);
i_qf=(Cf/t)*w*vdx+t*i_ql;
i_df=t*i_dl-(Cf/t)*w*vqx;
m_qk=(2/vdc)*(Rf*i_qf+w*Lf*i_df+(1/t)*vqx);
m_dk=(2/vdc)*(Rf*i_df-w*Lf*i_qf+(1/t)*vdx);
i_c=(3/4)*(m_qk.*i_qf+m_dk.*i_df);
i_pv=2.6399;%20.475;%38.118;%20.475;2.6399;
Pln=(1/1e6)*Pl;
i_b=(i_c-i_pv);
plot(Pln,i_b); grid on; title('plot of battery current vs load real power')
ylabel('Ib(A)'); xlabel('Load real power(MW)')
```

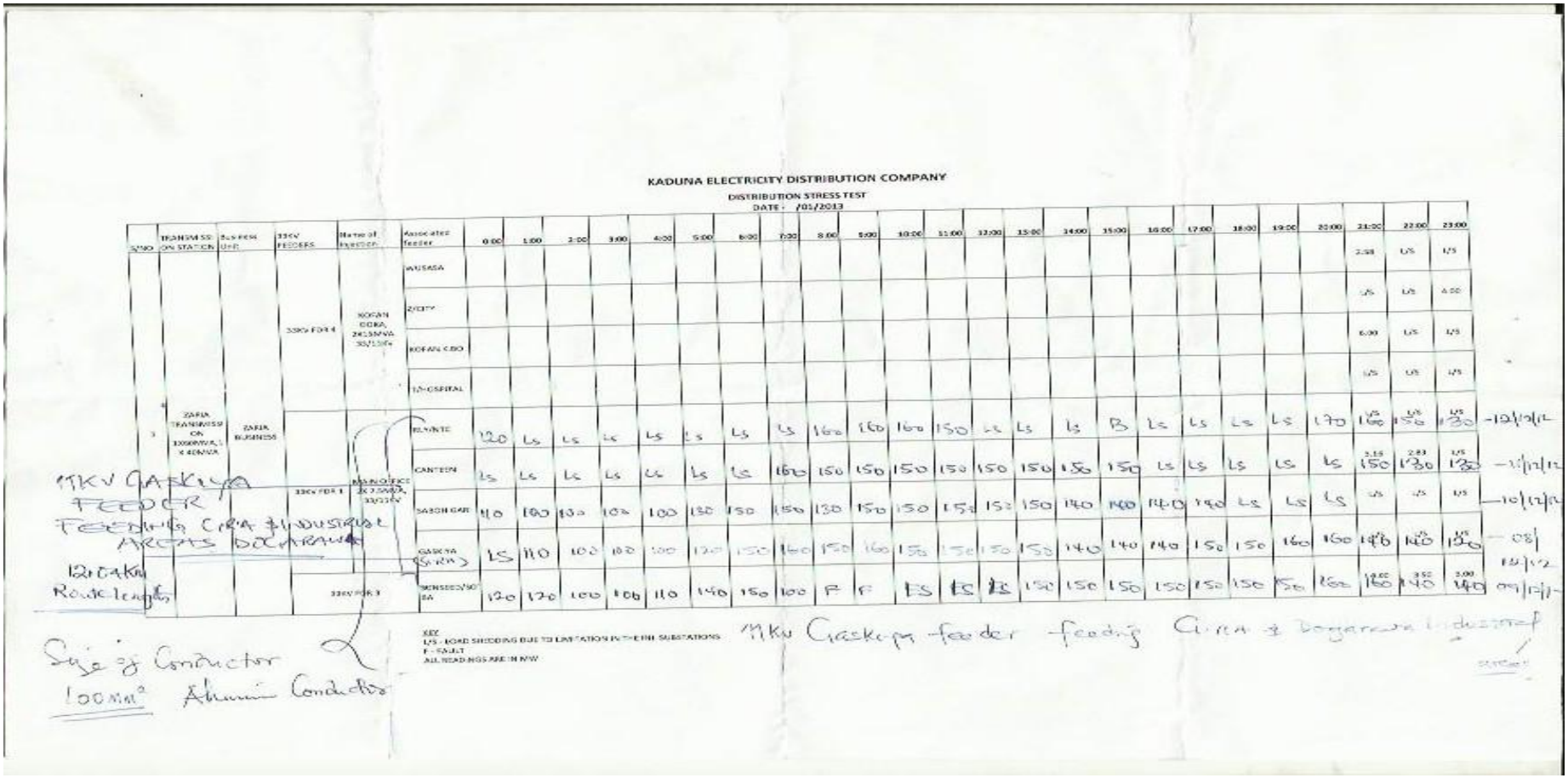
APPENDIX G

SIMULINK MODEL FOR SIMULATION STUDIES



APPENDIX H

DATA FOR HOURLY DEMAND ON THE 11KV GASKIYA FEEDER PHCN, ZARIA



KADUNA ELECTRICITY DISTRIBUTION COMPANY

DISTRIBUTION STRESS TEST

DATE: /01/2013

S/NO	TRANSMISSION STATION	5+5 FDRS U/G	33KV FEEDERS	Name of Injection	Associated Feeder	0:00	1:00	2:00	3:00	4:00	5:00	6:00	7:00	8:00	9:00	10:00	11:00	12:00	13:00	14:00	15:00	16:00	17:00	18:00	19:00	20:00	21:00	22:00	23:00	
			33KV FDR 4	KOFAN GORA 2X15MVA 33/11KV	WUSASA																						2.58	US	US	
					ZOO																						US	US	4.00	
					KOFAN GOO																						6.00	US	US	
					HOSPITAL																						US	US	US	
	ZARIA TRANSMISSION 330MVA, 1 X 60MVA	ZARIA BUSINESS			BUSINESS	120	LS	LS	LS	LS	LS	LS	LS	160	160	160	150	LS	LS	LS	B	LS	LS	LS	LS	170	160	150	130	-12/12/12
			33KV FDR 5	MAIN OFFICE 2X7.5MVA, 33/11KV	CANTEEN	LS	LS	LS	LS	LS	LS	LS	160	150	150	150	150	150	150	150	150	LS	LS	LS	LS	LS	3.15 150	2.83 130	US 130	-11/12/12
					SABON GARI	110	100	100	100	100	130	150	150	130	150	150	150	150	150	140	NEO	140	140	LS	LS	LS	US	US	US	-10/12/12
					GASKIYA (SHIRA)	LS	110	100	100	100	120	150	160	150	160	150	150	150	150	140	140	140	150	150	160	160	140	NEO	130	-08/12/12
			33KV FDR 3		SENSEDEVSOFA	120	120	100	100	110	140	150	100	F	F	FS	FS	FS	150	150	150	150	150	150	150	160	2.60 160	2.30 140	2.00 140	-09/12/12

KEY
LS - LOAD SHEDDING DUE TO LIMITATION IN THERM SUBSTATIONS
F - FAULT
ALL READINGS ARE IN MW

11KV GASKIYA FEEDER FEEDING CRIA & INDUSTRIAL AREAS DOCARAWA

120.04KM Route length

Size of Conductor 100MM² Aluminium Conductor

11Kv Gaskiya feeder feeding Cria & Dogarawa Industrial